[File 2] **INSPEC** 1898-2009/Apr W1

[File 6] **NTIS** 1964-2009/Apr W3

[File 8] **Ei Compendex(R)** 1884-2009/Apr W2

[File 34] **SciSearch(R) Cited Ref Sci** 1990-2009/Apr W2

[File 35] **Dissertation Abs Online** 1861-2009/Mar

[File 56] **Computer and Information Systems Abstracts** 1966-2009/Apr

[File 57] **Electronics & Communications Abstracts** 1966-2009/Mar

[File 60] **ANTE: Abstracts in New Tech & Engineer** 1966-2009/Mar

[File 62] **SPIN(R)** 1975-2009/Mar W4

[File 65] **Inside Conferences** 1993-2009/Apr 23

[File 95] **TEME-Technology & Management** 1989-2009/Mar W4

[File 98] **General Sci Abs** 1984-2009/Apr

[File 553] **Wilson Bus. Abs.** 1982-2009/Apr

[File 99] **Wilson Appl. Sci & Tech Abs** 1983-2009/Feb

[File 108] **Aerospace and High Technology Database** 1962-2009/Apr

[File 144] **Pascal** 1973-2009/Apr W3

[File 239] **Mathsci** 1940-2009/May

[File 256] **TecInfoSource** 82-2009/Jan

[File 434] **SciSearch(R) Cited Ref Sci** 1974-1989/Dec

[File 583] **Gale Group Globalbase(TM)** 1986-2002/Dec 13

```
Set      Items    Description
S1      3200307   S TRANSCEIVER?? OR TRANSMIT? OR TRANSMISSION?? OR
MODEM??
S2      6182811   S CHANNEL?? OR FREQUENC???
S3        17825   S COMMON(3N)S2
S4          592   S (ESTIMAT??? OR CALCULAT??? OR DETERMIN? OR
APPROXIMAT? OR INTERPOLAT? OR PROBABILITY??? OR STATISTIC??)(3N)S3
S5      3464468   S INTERFER? OR CROSS()TALK??? OR NOISE?? OR ALIASING OR
DISTORTION?? OR ARTIFACT??
S6       280199   S (REDUC? OR ATTENUAT??? OR MITIGAT??? OR RID OR
PREVENT??? OR MINIMI??? OR LESSEN? OR DIMINISH??? OR CANCEL? OR
STOP?)(3N)S5
S7           34   S AU=(SUTSKOVER, I? OR SUTSKOVER I? OR BEN()ELI, D? OR
BEN()ELI D?)
S8        20310   S S1 AND (S5 OR S6) AND (SUBTRACT? OR MINUS OR
DIFFERENCE?? OR PERCENT?)
S9           78   S S8 AND S3
S10           1   S S9 AND DEDICATED
S11           0   S S9 AND MODULO
S12           1   S S9 AND LATTICE
S13           1   S S12 NOT S10
S14           0   S S9 AND (SIGNAL()GENERAT???)
S15          23   S S8 AND MODULO
S16           0   S S15 AND LATTICE
S17          21   S S15 NOT (S10 OR S13 OR PY>2003)
S18          11   RD  (unique items)
S19           0   S S18 AND DEDICATED
S20           4   S S18 NOT (ENCRYPTION OR IMAGE OR CHAOTIC OR SPACECRAFT
OR AUDIO OR INTERFEROMETER)
S21          90   S S8 AND DEDICATED
S22          40   S S21 AND S2
S23          23   S S22 AND (ESTIMAT??? OR CALCULAT??? OR DETERMIN? OR
APPROXIMAT? OR INTERPOLAT? OR PROBABILITY??? OR STATISTIC??)
S24          12   S S23 NOT (S10 OR S13 OR S20 OR PY>2003)
S25           9   RD  (unique items)
S26           3   S S25 NOT POWER
S27           0   S S7 AND S9
S28           0   S S7 AND S8
```

10/3,K/1 (Item 1 from file: 35) <u>Links</u>
Dissertation Abs Online
02057900 ORDER NO: AADAA-I3159371
On the investigation of physical layer multiple path connections in a wireless network

...quality of service, the system requires efficient resource allocation. In the system based on a code division multiple access technique, every user contributes to the **interference** characteristics of the system. This **interference** power is proportional to the **transmitter** power. It is clear that power control is the most important factor which allows more efficient resource sharing by balancing received signal quality and **interference** power.

The multiple path connections idea is well-studied in the network layer of a wired infrastructure. Here we investigate a similar idea in the physical layer of a wireless access network. There is a major **difference** in the sense of channel existence. In the wired network, where the channels always exist, algorithms are based on smart queues and routings. In the... ...connections scheme for resource sharing.

The proposed scheme is studied under two different types of channels based on wideband code division multiple access standard, the **dedicated channel** and the **common** packet **channel**. The **dedicated** channel represents real-time traffic, while the **common** packet **channel** represents non-real-time traffic. Wideband code division multiple access technology is chosen because it has emerged as the most widely adopted third generation interface..

^13/3,K/1 (Item 1 from file: 57) Links
   Fulltext available through: STIC Full Text Retrieval Options
Electronics & Communications Abstracts

0000492341   IP Accession No: 200609-50-154451
Reduction of NTSC co-channel interference by referencing carrier frequencies to the LORAN-C signal

Rhodes, C W

Reduction of NTSC co-channel interference by referencing carrier frequencies to the LORAN-C signal

Abstract:
Co-channel **interference** may be noticed when the desired signal at the receiver is 60 dB stronger than the undesired signal. The spacing distances between **transmitters** which would be required to avoid this **interference** are prohibitive. Because FCC rules require much smaller minimum spacings, frequency offset is specified for each station to **reduce** co-channel **interference**. The offsets used in the U.S. are +/-10 kHz while the carrier frequency tolerance is +/-1 KHz. **Differences** between carriers can be 8-12 kHz.

Interference minima occur every 59.94 Hz within this range with **interference** maxima in between these minima. By referencing the visual carrier frequency of each **transmitter** to a **common frequency**, the **difference frequency** can be maintained at one of those frequencies at which the **interference** is minimum. This paper explains how the LORAN-C signal can be used as the frequency reference for television **transmitters** and how the ideal **difference** frequency can be maintained to minimize the visibility of co-channel **interference**. Equipment required is commercially available, and no rule changes are required to employ LORAN-C referenced carrier operation

Descriptors: Interference; Loran-C; **Transmitters**; Carriers; Offsets; Carrier frequencies; Minima; Referencing; Visibility; Receivers; Maxima; Television; Reduction; Stations; Tolerances; Broadcasting; Visual; Cobalt; Face centered cubic **lattice**; **Noise** levels
Identifiers:

20/3,K/1 (Item 1 from file: 2) Links
INSPEC
07209872   **INSPEC Abstract Number:** B1999-05-6320-028
Title: Three-dimensional imaging using ambiguity-free interferometry
Author Schmitt, K.; Wiesbeck, W.
Author Affiliation: Inst. fur Hochstfrequenztech. und Elektron., Karlsruhe Univ., Germany
Conference Title: AMTA '97. 19th Meeting and Symposium   p. 445-9
Publisher: Antenna Meas. Tech. Assoc , Boston, MA, USA
Publication Date: 1997 **Country of Publication:** USA   xxii+574 pp.
   Material Identity Number: XX-1999-00546
Conference Title: AMTA '97. 19th Meeting and Symposium
Conference Date: 17-21 Nov. 1997   **Conference Location:** Boston, MA, USA
Language: English
 Subfile: B
 Copyright 1999, IEE
Title: Three-dimensional imaging using ambiguity-free interferometry
Abstract: One of the key problems in SAR **interferometry** is the determination of the absolute phase of a scatterer by unwrapping the calculated phase **difference** of two SAR images. Since the phase **difference** is a function **modulo** 2 pi , software algorithms are used to perform a phase unwrapping to obtain an unambiguous phase and thus the corresponding height information. This paper presents a procedure using two different **transmit** frequencies to enlarge the unambiguous range for height determination. Measurements performed in an anechoic chamber are used to test the processing. Using this procedure it...
Descriptors: ...radiowave **interferometry**;
Identifiers: ...ambiguity-free **interferometry**; ... ...phase **difference**; ... ...**transmit** frequencies

 20/3,K/2 (Item 2 from file: 2) Links
INSPEC
06773897   **INSPEC Abstract Number:** A9802-9385-086, B9801-7710-034
Title: An interferometric SAR processor avoiding phase ambiguities
Author Schmitt, K.; Wiesbeck, W.
Author Affiliation: Inst. fur Hochstfrequenztech. und Elektronik, Karlsruhe Univ., Germany
Conference Title: IGARSS'97. 1997 International Geoscience and Remote Sensing Symposium. Remote Sensing - A Scientific Vision for Sustainable Development (Cat. No.97CH36042)   **Part** vol.4   p. 1713-15 vol.4
Editor(s): Stein, T.I.
Publisher: IEEE , New York, NY, USA
Publication Date: 1997 **Country of Publication:** USA   4 vol. lxxi+2105 pp.
ISBN: 0 7803 3836 7   **Material Identity Number:** XX97-02132

Title: An interferometric SAR processor avoiding phase ambiguities
Abstract: One of the key problems in SAR **interferometry** is the determination of the absolute phase of a
scatterer by unwrapping the calculated phase **difference** of two SAR images. Since the phase **difference** is
a function **modulo** 2 pi software algorithm are used to perform a phase unwrapping to obtain an
unambiguous phase and thus the corresponding height information. This paper presents a procedure using
two different **transmit** frequencies to enlarge the unambiguous range for height determination.
Measurements performed in an anechoic chamber are used to test the processing. Using this procedure it...
Identifiers: ...**interferometric** SAR processor... ...SAR **interferometry**; ... ...phase **difference**;
Astronomical Objects:

^^20/3,K/3 (Item 1 from file: 60) <u>Links</u>
ANTE: Abstracts in New Tech & Engineer
0000574107 IP Accession No: 2008249119
**Apparatus and method for reducing multiplicative gain variation distortions in data recording and
transmission channels**

Price, Robert; Craig, John W
, USA
Publisher Url: http://patft.uspto.gov/netacgi/nph-Parser?Sect1=PTO2&Sect2=HITOFF&u=/netaht
ml/PTO/search-adv.htm&r=1&p=1&f=G&l=50&d=PTXT&S1=3940694.PN.&OS=pn/39406 94&
RS=PN/3940694

Document Type: Patent
Record Type: Abstract
Language: English
File Segment: ANTE: Abstracts in New Technologies and Engineering
**Apparatus and method for reducing multiplicative gain variation distortions in data recording and
transmission channels**

Abstract:
Data channel gain-variation **distortions** are **reduced** by the following combination of operations.
Successively occurring data items are cumulatively added in **modulo** fashion thereby providing a sequence
of partial sums. An exponentiating circuit is introduced to provide an exponential function of the partial
sums. The exponentiated partial sums are then recorded or **transmitted** on a data channel wherein the
signals are distorted by relatively slow gain variations thereof. The received distorted signals are applied to
a logarithmic circuit wherein the multiplicative gain variation **distortions** are converted to additive
distortions. The logarithmically converted signals are applied to a **subtractor** that sequentially provides
the **differences** in **modulo** fashion between successively occurring signals from the logarithmic circuit
thereby yielding the data items with the **distortions** substantially **reduced**.

Descriptors: Distortion; Circuits; Sums; Channels; Additives; Exponential functions; Data recording
Identifiers:

20/3,K/4 (Item 1 from file: 144) Links
Pascal

12926676   PASCAL No.: 97-0196145

Modeling and experimental verification of the interconnected mesh power system (IMPS) MCM topology

LOW Y L; SCHAPER L W; ANG S S
 Bell Laboratories, Lucent Technologies, Murray Hill, NJ 07974, United States; High Density
Electronics Center (HiDEC) and Department of Electrical Engineering, University of Arkansas,
Fayetteville, AR 72701, United States

... by half. To provide a complete MCM on only two metal layers, the IMPS topology provides a
unique and complex power distribution system and signal **transmission** environment. This paper
reports on models of the IMPS structure based on finite-**difference**/partial-inductance methods
and PSpice simulation. The models can easily be constructed using a commercial three-dimensional
(3-D) field solver and the circuit models...

English Descriptors: Network analysis; Integrated circuit; Multichip module; Modeling;
 Interconnection; **Transmission** line; **Noise**; Characteristic impedance; Meshed network;
 Finite **difference** method; Distribution system

French Descriptors: Analyse circuit; Circuit integre; Module multipuce; Modelisation; Interconnexion
 ; Ligne **transmission**; Bruit; Impedance caracteristique; Reseau maille; Methode
 difference finie; Systeme distribution

Spanish Descriptors: Analisis circuito; Circuito integrado; **Modulo** multipulga; Modelizacion;
 Interconexion; Linea transmision; Ruido; Impedancia caracteristica; Red mallada cerrada; Metodo
 diferencia finita; Sistema distribucion

^26/3,K/1 (Item 1 from file: 2) Links
INSPEC
08238577   **INSPEC Abstract Number:** B2002-05-6150D-011
Title: Blind ISI mitigation
Author Mostofi, Y.; Cox, D.C.
Author Affiliation: Stanford Univ., CA, USA
Conference Title: IEEE 54th Vehicular Technology Conference. VTC Fall 2001. Proceedings (Cat.
No.01CH37211)   **Part** vol.3   p. 1903-7 vol.3
Publisher: IEEE , Piscataway, NJ, USA
Publication Date: 2001 **Country of Publication:** USA   4 vol.(lxxiii+xii+2777) pp.
ISBN: 0 7803 7005 8   **Material Identity Number:** XX-2001-02309
U.S. Copyright Clearance Center Code: 0-7803-7005-8/01/$10.00
Conference Title: IEEE 54th Vehicular Technology Conference. VTC Fall 2001. Proceedings
Conference Date: 7-11 Oct. 2001   **Conference Location:** Atlantic City, NJ, USA

Language: English
Subfile: B
Abstract: In an outdoor communication environment, a **percentage** of bandwidth is wasted sending a training sequence for **channel estimation** and equalization. For instance in GSM, 17.93% of bandwidth is **dedicated** to the **transmission** of such a known sequence. Therefore, if a blind algorithm, using only the knowledge of input constellation and/or correlation, can achieve an acceptable performance...
Descriptors: ...adaptive **estimation;** ... ...**interference** suppression... ...intersymbol **interference;** ...
...parameter **estimation;**
Identifiers: ...**channel estimation; channel** equalization... ...intersymbol **interference;**

^ 26/3,K/2 (Item 1 from file: 8) <u>Links</u>
   Fulltext available through: <u>STIC Full Text Retrieval Options</u>
Ei Compendex(R)
0015484074   **E.I. COMPENDEX No:** 2003217475898
The COMPASS RICH-1 read-out system

Baum, G.; Birsa, R.; Bradamante, F.; Bressan, A.; Chapiro, A.; Cicuttin, A.; Ciliberti, P.; Colavita, A.; Costa, S.; Crespo, M.; Cristaudo, P.; Dalla Torre, S.; Diaz, V.; Fauland, P.; Fratnik, F.; Giorgi, M.; Gobbo, B.; Ijaduola, R.; Kalinnikov, V.; Lamanna, M.; Martin, A.; Menon, G.; Pagano, P.; Schiavon, P.; Tessarotto, F.; Zanetti, A.
 Corresp. Author/Affil: Crespo, M.: INFN, Sezione di Trieste, ICTP, Via Beirut 31, 34100 Trieste, Italy
 Corresp. Author email: mcrespo@ictp.trieste.it
 Editor(s): Ekelof, T; Resvanis, L.K.; Sequinot, J
 Conference Title: RICH 2002
 Conference Location: Nestor, Pylos Greece   **Conference Date:** 20020605-20020610
 E.I. Conference No.: 63024
 Nuclear Instruments and Methods in Physics Research, Section A: Accelerators, Spectrometers, Detectors and Associated Equipment (Nucl Instrum Methods Phys Res Sect A) (Netherlands) 2003 502/1 (246-250)
 Publication Date: 20030411
 Publisher: Elsevier
 CODEN: NIMAE   **ISSN:** 0168-9002
 Publisher Item Identifier: S0168900203002821
Item Identifier (DOI): <u>10.1016/S0168-9002(03)00282-1</u>
 Document Type: Conference Paper; Journal   **Record Type:** Abstract
 Treatment: T; (Theoretical)
 Language: English   **Summary Language:** English
 Number of References: 18
 This paper describes the reconfigurable read-out system for the 82944 RICH-1 **channels** of the COMPASS experiment (NA58) at CERN. The system is based on 192 identical large front-end boards (BORA board). BORA was designed for acquiring, digitizing, threshold **subtracting** and **transmitting** event data. The overall operation of the board is controlled and supervised by a DSP tightly interacting with an FPGA that acts as a parallel co-processor. The DSP allows characterizing each analog **channel** by locally **calculating noise** and pedestal. Each BORA communicates with the outside world through two optical fibers and through a **dedicated** DSP network. One optical fiber is used to receive event triggers, and the other one is used to **transmit** event data to subsequent processing stages of the acquisition system. The DSP network allows reconfiguring and reprogramming the DSPs and FPGAs as well as acquiring...
...DOLINA DSP. The read-out system can steadily work up to a trigger rate of 75 kHz with maximum pixel occupancy of 20%, reaching a **transmission** data rate of 5.13 Gbytes/s. (c) 2003 Elsevier Science B.V. All rights reserved.
 Descriptors:

Bidirectional access on HFC CATV networks: Design of a CDMA-based communications system

...coaxial access network. In older upgrades, a PON like architecture was applied in the downstream direction, requiring that special techniques are applied. The CATV upstream **channels** are hampered by ingress **noise** and radiation from short-wave radio, and by non-ideal amplitude and phase characteristics. The most suitable **transmission** technique, as concluded in this thesis is Direct Sequence Code Division Multiple Access (DS-CDMA).

The upstream physical design is based on DS-CDMA, employing preferentially phased Gold codes. Since the system is operating in synchronous mode except during the initialisation procedures, the downstream **channel** has been defined as the timing reference for all upstream **channels**. The **differences** in delay resulting from different physical positions of the **modems** is compensated for by an initialisation procedure.

The Medium Access Control **determines** which **modem** is allowed to use a certain spreading code and time slot. It is therefore important that a **modem** is assigned bandwidth when it is required. A distinction needs to be made between **modems** that actively **transmitting** data, and **modems** that are connected to the network but are not actively sending data. Active **modems** use piggybacking for sending the bandwidth needs to the MAC controller. Idle **modems** use **dedicated** cells instead. Based on these requests, the MAC algorithm **determines** for each **modem** when it is allowed to **transmit**. The **modem determines** for which traffic type the assigned bandwidth is used.

```
Set      Items    Description
S1     2769311   S TRANSCEIVER?? OR TRANSMIT? OR TRANSMISSION?? OR
MODEM??
S2     1928523   S CHANNEL?? OR FREQUENC???
S3       14303   S COMMON(3N)S2
S4         420   S (ESTIMAT??? OR CALCULAT??? OR DETERMIN? OR
APPROXIMAT? OR INTERPOLAT? OR PROBABILITY??? OR STATISTIC??)(3N)S3
S5      947692   S INTERFER? OR CROSS()TALK??? OR NOISE?? OR ALIASING OR
DISTORTION?? OR ARTIFACT??
S6      280650   S (REDUC? OR ATTENUAT??? OR MITIGAT??? OR RID OR
PREVENT??? OR MINIMI??? OR LESSEN? OR DIMINISH??? OR CANCEL? OR
STOP?)(3N)S5
S7          16   S AU=(SUTSKOVER, I? OR SUTSKOVER I? OR BEN()ELI, D? OR
BEN()ELI D?)
S8      422402   S S1 AND (S2 OR S3 OR S4)
S9       66420   S S8 AND (S5 OR S6)
S10        627   S S9 AND DEDICATED
S11         52   S S10 AND (SUBTRACT? OR MINUS OR DIFFERENCE?? OR
PERCENT?)
S12          1   S S11 AND LATTICE
S13         37   S S11 AND IC=H04B?
S14         21   S S13 NOT (S12 OR AD=20031229:20090424/PR)
S15          1   S S14 AND IC=H04K?
S16          7   S S14 AND IC=H04L?
S17          3   S (S14 NOT (S15 OR S16)) AND IC=H04J?
S18          1   S S17 NOT RECEIVER
S19          1   S S7 AND S10
S20          0   S S19 NOT (S12 OR S15 OR S16 OR S18 OR
AD=20031229:20090424/PR)
S21          5   S S7 AND S9
S22          1   S S21 NOT (S12 OR S15 OR S16 OR S18 OR
AD=20031229:20090424/PR)
S23       9558   S (S5 OR S6)(S)(SUBTRACT? OR MINUS OR DIFFERENCE?? OR
PERCENT?)(S)S1
S24          6   S S23 AND S4
S25          5   S S24 NOT (S12 OR S15 OR S16 OR S18 OR S22 OR
AD=20031229:20090424/PR)
S26          4   S S25 AND IC=H04B?
S27          1   S S7 AND S23
S28          0   S S27 NOT (S12 OR S15 OR S16 OR S18 OR S22 OR S26 OR
AD=20031229:20090424/PR)
```

12/3,K/1 (Item 1 from file: 350) Links
   Fulltext available through: Order File History
Derwent WPIX
(c) 2009 Thomson Reuters. All rights reserved.

0006384539 *Drawing available*
WPI Acc no: 1993-184295/199323
XRPX Acc No: N1993-141627
Integrated data processing system with CPU and digital signal processor - integrates functions of CPU and DSP modules as parallel, independently operating functions, tuned for voice applications
Patent Assignee: NAT SEMICONDUCTOR CORP (NASC)
Inventor: AFEK Y; BIRENBAUM A; CARMON I; COHEN R; DORON M; EPSTEIN L; FRAENKEL I; GREENFELD Z; GREISS I; INTRATER A; INTRATER G; KATZRI L; LEVITAN R; OZ O; SANDBANK A; SHIMONY I; TSADIK M; TZADIK Y; VINER O; YOMTOV S

Patent Family (19 patents, 4 countries)

Patent Number	Kind	Date	Application Number	Kind	Date	Update	Type
EP 545581	A2	19930609	EP 1992310568	A	19921119	199323	B
EP 545581	A3	19940209	EP 1992310568	A	19921119	199518	E
US 5487173	A	19960123	US 1991806082	A	19911206	199610	E

...**Original Titles:**Integrated circuit having CPU and DSP for executing vector **lattice** propagation instruction and updating values of vector Z in a single instruction cycle... ...Parallel operating CPU core and DSP module for executing sequence of vector DSP code instructions to generate decoded constellation points in QAM/TCM **modem** application... ...Integrated circuit having CPU core operable for switching between two independent asynchronous clock sources of different **frequencies** while the CPU continues executing instructions. Original Publication Data by AuthorityArgentina**Publication No.** ...**Original Abstracts:**execution by the DSP module and for access by the GP CPU for storage and retrieval of instructions and data. The DSP module includes a **lattice** filter mechanism for executing a single instruction to update propagating values of a vector responsive to the externally provided signal. ... the DSP module is independent of and in parallel with execution of GP instructions by the GP CPU. The system executes a novel QAM\TCM **modem** algorithm... ... The present invention is directed to various **features** of an integrated data processing system that includes a general purpose (GP) CPU core for processing data in accordance with a GP instruction set and... ...**Claims:**being independent of and in parallel with execution of GP instructions by the GP CPU; and wherein the DSP module executes a dual tone multi-**frequency** (DTMF) detection algorithm by executing a single command-list code instruction VCPOLY) that computes ACCEPT **frequency** detectors, REJECT **frequency** detectors and total signal energy; and wherein the GP CPU includes decision logic that identifies a DTMF signal based on the ACCEPT **frequency** detectors, REJECT **frequency** detectors and total signal energy computed by the DSP module.An integrated circuit structure for use in identifying a parallel disconnect signal provided on an analog **transmission** medium, the integrated circuit structure comprising, a central processing unit that executes instructions to perform data processing operations, the data processing operations including a successive approximation analog-to-digital conversion operation to provide a digital output signal based upon an input data signal; a pulse **width** modulation (PWM) element that converts the digital output signal generated by the central processing unit to a square-wave output signal having a duty cycle... ... circuit structure, the external comparator receiving as inputs the output of the external low pass filter and the parallel disconnect signal provided by the analog **transmission** medium and providing said external comparator output a digital signal corresponding to a **difference** between the output of the external low pass filter and the signal provided by the analog **transmission** medium, the input port connected to provide the output of the comparator as the **input** data signal to the central processing unit.... ... command-list code instructions and vector operand data for utilization by the DSP module, the DSP memory element connected to the DSP module by a **dedicated** DSP bus, but not connected to the shared internal bus; and wherein the DSP module includes at least one vector address pointer register that includes an address field that identifies an address of vector operand data that can be retrieved from the DSP memory element by the DSP module **via** the

10

DSP bus for use by the DSP module in executing vector DSP command-list code instructions, an address wrap-around field that facilitates wrap... processing means for processing an externally-provided signal received by the DSP module by executing DSP command-list code instructions, the signal processing means including **lattice** means for executing a first of said command-list code instructions to update propagating values of the vector "Z" responsive to the externally-provided signal... ... said first of said command-list code instructions requires only a single instruction fetch/decode cycle of the DSP module to update the propagating values **of** the vector "Z... ... for preventing the DSP module from executing command-list code instructions which cause access to the shared external memory, whereby the DSP module is temporarily **prevented** from

^15/3,K/1 (Item 1 from file: 350) <u>Links</u>
   Fulltext available through: <u>Order File History</u>
Derwent WPIX

0007353804 *Drawing available*
WPI Acc no: 1995-092610/199513
XRPX Acc No: N1995-073234
Direct sequence code division multiplex access receiver apparatus - uses receiver having data aided multi-user interference canceller with feed forward and feed backward filters and subtracting stage
Patent Assignee: KONINK PHILIPS ELECTRONICS NV (PHIG); PHILIPS ELECTRONICS NV (PHIG); PHILIPS ELECTRONICS UK LTD (PHIG); US PHILIPS CORP (PHIG)
Inventor: EDMONDS J M; MONOGIOUDIS P; MONOGIOUDIS P N

<div align="center">Patent Family (8 patents, 5 countries)</div>

Patent Number	Kind	Date	Application Number	Kind	Date	Update	Type
EP 641102	A2	19950301	EP 1994202349	A	19940818	199513	B
JP 7177124	A	19950714	JP 1994198725	A	19940823	199537	E
EP 641102	A3	19950510	EP 1994202349	A	19940818	199546	E
US 5550810	A	19960827	US 1994295449	A	19940824	199640	E
KR 335711	B	20020904	KR 199421284	A	19940824	200315	E

...**uses receiver having data aided multi-user interference canceller with feed forward and feed backward filters and subtracting stage** ...**Original Titles:**Direct sequence code division multiple access receiver with multiuser **interference canceller** ... ...Recepteur pour acces multiple par multiplexage de code a sequence direct avec annuleur d' **interference** pour utilisation multiples... ...Direct sequence - Code division multiple access receiver with multiuser **interference canceller** ... ...Recepteur pour acces multiple par multiplexage de code a sequence direct avec annuleur d' **interference** pour utilisation multiples **Alerting Abstract** ...The system has a **transmitter** for multiplying a modulating signal with a spreading sequence to form a spread spectrum signal and **transmitting** the signal on a CDMA **channel**. A receiver receives the signals and **cancels** the multiple access **interference**. It uses a feedforward filter, feedback filter and quantiser for producing quantised decisions from information derived from the feedforward filter... ...Circuits make tentative decisions on received information produce an inversion of the equivalent CDMA **channel** in dependence on the cross-correlation values of all users, and adjust the tap weights of the feedforward filter... **Title Terms** .../Index Terms/Additional Words: **INTERFERENCE;** ...
...**SUBTRACT; Class Codes** International Patent Classification IPC Class Level Scope Position Status Version Date ...**H04K-001/02** Main "Version 7" **H04B-0001/707**... **H04B-0001/707**... Original Publication Data by Authority**Argentina****Publication No. Original Abstracts:**A DS-CDMA system comprises at least one **transmitter** and at least **one** receiver operating on a **dedicated** signal **channel** which **is** used **by** other DS-CDMA operators in a non-synchronous way. A receiver for use in such a DS-CDMA system includes a data aided multiuser **interference canceller** (38) comprising **a feedforward** filter (48) connected to a **subtracting** stage (50). A **decision** stage (52) is connected to an output of the **subtracting** stage (50). Decisions **from** the decision stage (52) are stored in a memory which also stores preliminary decisions made on the signal applied to the feedforward filter (48) by a simple receiver (46). These decisions are applied to a feedback filter (58) the output of which is connected to the **subtracting** stage

(50) thereby **removing** the effects of pre-cursive and post-cursive **interference**. The input to, **and** output from,the decision stage 52 are compared and the **difference** is used for **adjusting** the tap weights of the feedforward and feedback filters (48,58). In the case of a single input, single output, the feedforward filter (48) comprises... ... A DS-CDMA system comprises at least one **transmitter** and at least one receiver operating on a **dedicated** signal **channel** which is used by other DS-**CDMA** operators **in** a non-synchronous way. A receiver for use in such a DS-CDMA system includes a data aided multiuser **interference canceller** (38) comprising a feedforward filter (48) connected **to a subtracting** stage (50). A decision stage (52) is connected **to** an output of the **subtracting** stage (50). Decisions from the decision stage (52) **are** stored in a memory which also stores preliminary decisions made on the signal applied to the feedforward filter (48) by a simple receiver (46). These decisions are applied to a feedback filter (58) the output of which is connected to the **subtracting** stage (50) thereby removing the effects of pre-**cursive** and post-cursive **interference**. The input to, and output from, the decision **stage** 52 are compared and the **difference** is used for adjusting the tap weights of **the** feedforward and feedback filters (48,58). In the case of a single input, single output, the feedforward filter (48) comprises a fractionally spaced equalizer which... **Claims:**1. A direct sequence-code division multiple access (DS-CDMA) system comprising a **transmitter** and **a** receiver, the **transmitter** having **means** for multiplying a modulating signal with a spreading sequence in order to form a spread spectrum signal and for **transmitting** the **spread** spectrum signal on a CDMA **channel**, and **the** receiver comprising means for receiving signals on said CDMA **channel**, means **for cancelling** multiple **access interference**, said **means** including feedforward filtering means, feedback filtering means, quantizing means for producing quantized decisions from information derived from the feedforward filtering means, means for making tentative decisions on received information,means for producing an inversion of the equivalent CDMA **channel** in **dependence** on the cross correlation values of all the contemporaneous users and means responsive to the production of the inversion of the equivalent CDMA **channel** for **adjusting** tap weights of at least the feedforward filtering

^16/3,K/1 (Item 1 from file: 350) Links
   Fulltext available through: Order File History
Derwent WPIX

0013479472 *Drawing available*
WPI Acc no: 2003-571428/200354
Related WPI Acc No: 2004-480252
XRPX Acc No: N2003-454320
Signal design to transmit binary information of unequal importance using asymmetric modulation scheme to transmit less important information at lower power level
Patent Assignee: LG ELECTRONICS INC (GLDS)
Inventor: AHN J; AHN J G; AHN J K; KWON H; KWON H C; AN J; GWON H

Patent Family (19 patents, 100 countries)

Patent Number	Kind	Date	Application Number	Kind	Date	Update	Type
EP 1326361	A1	20030709	EP 200228885	A	20021223	200354	B
US 20030131299	A1	20030710	US 2003334782	A	20030102	200355	E
WO 2003058873	A1	20030717	WO 2002KR2402	A	20021220	200357	E

Signal design to transmit binary information of unequal importance using asymmetric modulation scheme to transmit less important information at lower power level Original Titles: Method and device for **transmitting** confirmation signal... ...Signal design to **transmit** binary information of unequal importance... ...Conception de signaux pour **transmission** d'information binaire d'importance inegale... ...APPARATUS FOR **TRANSMITTING** ACKNOWLEDGMENT SIGNAL AND ITS METHOD... ...APPARATUS FOR **TRANSMITTING** ACKNOWLEDGEMENT SIGNAL AND ITS METHOD... ...A response signal **transmission** apparatus and its method... ...Method and apparatus for **transmitting** acknowledgement signals... ...Method and apparatus for **transmitting** acknowledgement signals... ...Method and apparatus for **transmitting** acknowledgement signals... ...METHOD AND APPARATUS FOR **TRANSMITTING** ACKNOWLEDGEMENT SIGNALS... **Alerting Abstract** ...NOVELTY - A response signal from a receiver can be **transmitted** by adjusting the **transmission** power according to the

transmit power obtained when the response signal is ACK or NACK, I.e. of higher or lower importance and the detection threshold of the receiver is... DESCRIPTION - INDEPENDENT CLAIMS are included for a signal **transmission** apparatus, for a method of avoiding errors and for a method of **transmitting** ACK/NACK signals... ...USE - **Transmitting** ACK/NACK signals in mobile communications... ...ADVANTAGE - Increased reliability and power of **transmitted** ACK signals... **Title Terms** .../Index Terms/Additional Words: **TRANSMIT**; **Class Codes** International Patent Classification IPC Class Level Scope Position Status Version ...**Original Abstracts:**wireless communication system by using automatic repeat pray (ARQ) plan, especially claims a response (ACK/NACK) signal power control method for using different powers to **transmit** ACK/NACK signal according to the necessary allowable probability for receiving error of the system. When sending and receiving the ACK/NACK signal in the... ... repeat pray (ARQ) system, because emissive powers of the signal can be differentiated according to each ACK/NACK signal and the ACK/NACK signal is **transmitted** according to the emissive power satisfying the necessary error rate of each signal, it can reduce the necessary power consumption for **transmitting** the NACK signal... ... A method to construct and detect a binary **transmit** signal is disclosed. The method is based on the assumption that certain decision errors are less severe than other decision errors, as e.g. in **transmission** schemes employing ARQ. To this purpose, the important information (e.g. the acknowledgement ACK) is **transmitted** with high power, whereas the less important information (e.g. the non-acknowledgement NACK) is **transmitted** with reduced power. An asymmetric modulation scheme is obtained. The detection threshold to decide at the receiver which of the two signals

16/3,K/2 (Item 2 from file: 350) Links
    Fulltext available through: Order File History
Derwent WPIX

0013330898 *Drawing available*
WPI Acc no: 2003-418296/200339
XRPX Acc No: N2003-333695
Node apparatus in universal mobile telecommunication system, determines down link data channel power level, when modulation technique applied to downlink channel is high order modulation technique
Patent Assignee: SAMSUNG ELECTRONICS CO LTD (SMSU)
Inventor: CHOI S; CHOI S H; LEE H; LEE H U; LEE H W; LEE J; LEE J H; SEO M; SEO M S; LEE C

Patent Family (12 patents, 7 countries)

Patent Number	Kind	Date	Application Number	Kind	Date	Update	Type
US 20030039217	A1	20030227	US 2002222175	A	20020816	200339	B
DE 10239068	A1	20030417	DE 10239068	A	20020826	200339	E
FR 2828968	A1	20030228	FR 200210532	A	20020823	200339	E
GB 2381166	A	20030423	GB 200219508	A	20020822	200339	E
JP 2003134046	A	20030509	JP 2002241134	A	20020821	200339	E

Node apparatus in universal mobile telecommunication system, determines down link data channel power level, when modulation technique applied to downlink channel is high order modulation technique Original Titles: Apparatus and method for **transmitting**/receiving uplink **transmission** power deviation and power level... ...APPARATUS AND METHOD FOR **TRANSMITTING** AND RECEIVING UPLINK **TRANSMISSION** POWER OFFSET AND HIGH-SPEED DOWNLINK SHARED **CHANNEL** POWER LEVEL IN COMMUNICATION SYSTEM EMPLOYING HIGH-SPEED DOWNLINK PACKET ACCESS SYSTEM... ...Apparatus and method for **transmitting**/receiving uplink **transmission** power offset and HS-DSCH power level in a communication system employing HSDPA... ...Apparatus and method for **transmitting**/receiving uplink **transmission** power offset and HS-DSCH power level in a communication system employing HSDPA **Alerting Abstract** ...NOVELTY - The node apparatus has determiner that determines an uplink power offset according to the comparison of different between signal-to-**interference** ratio (SIR) of uplink **dedicated channel** signal and preset target (SIR). Another determiner determines the downlink data **channel** power level, when the modulation technique

applied to the downlink data **channel** is a high order modulation technique. ... uplink power offset and downlink data **channel** power level **transceiver** apparatus; node apparatus controlling method; uplink power offset and downlink power level **transmission**/reception method; uplink **transmission** power controlling method; uplink **transmission** power controlling apparatus; downlink data **channel** power level **transmission** method; downlink data **channel** power level **transmission** apparatus; downlink data **channel** power level **transmission**/reception method; and downlink data **channel** power level **transceiver** apparatus... ... USE - Node apparatus for **transmitting** uplink power offset and downlink data **channel** power level is universal mobile telecommunication system, employing high speed down-link packet access and used in code division multiple access (CDMA) communication system... ... ADVANTAGE - Control **transmission** power of uplink high speed **dedicated** physical control **channel** (HS-DPCCH) in communication system employing high speed downlink packet access (HSDPA... ... DESCRIPTION OF DRAWINGS - The figure shows the **channel** allocation scheme for user equipment (UE) located in a soft handover region in the communication system. Original Publication Data by AuthorityArgentina**Publication No. Original Abstracts:** The invention claims a high-speed packet data communication system, wherein a signal **channel** status determiner measures signal-to-**interference** ratio (SIR) of a first special uplink **channel** signal received from UE, and calculates **difference** between the SIR measured and a pre-set target SIR; a **transmission** power determiner is to compare the **difference** and the pre-set threshold and determine the uplink power deviation of a second special uplink signal **channel** applied to **transmit** control information for the packet data received by UE based on the comparison result; and a **transmitter** sends the determined uplink power deviation to the UE by means of a downlink... ... Ein Paketdatenkommunikationssystem hoher Geschwindigkeit, wobei ein Kanalzustandsbestimmer ein Signal-zu-**Interferenz**-Verhaltnis (SIR) eines Signals eines ersten gewidmeten Aufwartsverbindungskanals misst, welches von einem UE empfangen wird, und eine Differenz zwischen dem gemessenen SIR und einem Ziel... ... A high-speed packet data communication system, wherein a **channel** condition determiner measures a signal-to-**interference** ratio (SIR) of a first uplink **dedicated channel** signal received from a UE, and calculates a **difference** between the measured SIR and a preset target SIR; a **transmission** power determiner compares the **difference** with preset thresholds, and determines an uplink power offset to be applied to a second uplink **dedicated channel transmitting** control information for packet data received at the UE according to a result of the comparison; and a **transmitter transmits** over a downlink the determined uplink power offset to the UE... ... A high-speed packet data communication system, wherein a **channel** condition determiner measures a signal-to-**interference** ratio (SIR) of a first uplink **dedicated channel** signal received from a UE, and calculates a **difference** between the measured SIR and a preset target SIR; a **transmission** power determiner compares the

^16/3,K/3 (Item 3 from file: 350) Links
  Fulltext available through: Order File History
Derwent WPIX

0013070071 *Drawing available*
WPI Acc no: 2003-150250/200315
XRPX Acc No: N2003-118583
Data processing apparatus for radio communication system, filters output of multipliers, before summation and subtraction, to remove noise
Patent Assignee: CURITEL CO (CURI-N); CURITEL COMMUNICATIONS INC (CURI-N); PANTECH & CURITEL CO LTD (PANT-N); SEO B (SEOB-I)
Inventor: SEO B; SEO B H; SUH B H; HUH B

Patent Family (9 patents, 30 countries)

Patent Number	Kind	Date	Application Number	Kind	Date	Update	Type
EP 1265410	A2	20021211	EP 2002254026	A	20020610	200315	B
US 20020186786	A1	20021212	US 2002165709	A	20020607	200315	E
JP 2003018227	A	20030117	JP 2002169135	A	20020610	200317	E
KR 2002093551	A	20021216	KR 200132356	A	20010609	200329	E

Data processing apparatus for radio communication system, filters output of multipliers, before summation and subtraction, to remove noise Alerting Abstract ...NOVELTY - Multipliers (31-33,36,37) multiply long pseudo **noise** (PN) code respectively with in-phase and quadrature pseudo **noises** (Ipn,Qpn), pilot, **dedicated** control, voice and high speed data **transmission channels** (PI,DC,FD,SM). The output of the multipliers are filtered for removing **noise**, after which summation and **subtraction** are performed to produce the final result. ...ADVANTAGE - The data processing speed of the radio **channel** is improved and high quality data is output... ...41,40 Output **channels Title Terms** .../Index Terms/Additional Words: **SUBTRACT**; ... ...**NOISE Class Codes** International Patent Classification IPC Class Level Scope Position Status Version Original Publication Data by Authority**Argentina****Publication No.** ...**Original Abstracts:**processing data using the complex quadrature phase shift keying (CQPSK) is disclosed. The present invention includes plurality of multiplying units for multiplying a long pseudo **noise** (PN) code with an in-phase pseudo **noise** and quadrature pseudo **noise**, and a results of multiplying with a pilot **channel**, a **dedicated** control **channel**, a voice **channel**, a high-speed data **transmission channel**, a result multiplied with **channels** with gain, filtering units for eliminating **noise**, **subtracting** and adding units for calculating final result, and in-phase/quadrature **channel** outputting unit for outputting I-**channel**/Q-channel. The present invention can improve data processing speed of a radio **channel**, increase capacity of data processing in radio communication and also can be applicable to various kinds of radio communication devices transceiving voice, media contents and... ... processing data using the complex quadrature phase shift keying (CQPSK) is disclosed. The present invention includes plurality of multiplying units for multiplying a long pseudo **noise** (PN) code with an in-phase pseudo **noise** and quadrature pseudo **noise**, and a results of multiplying with a pilot **channel**, a **dedicated** control **channel**, a voice **channel**, a high-speed data **transmission channel**, a result multiplied with **channels** with gain, filtering units for eliminating **noise**, **subtracting** and adding units for calculating final result, and in-phase/quadrature **channel** outputting unit for outputting I-**channel/Q-channel**. The present invention can improve data processing speed of a radio **channel**, increase capacity of data processing in radio communication and also can be applicable to various kinds of radio communication devices transceiving voice, media contents and... ... processing data using the complex quadrature phase shift keying (CQPSK) is disclosed. The present invention includes plurality of multiplying units for multiplying a long pseudo **noise** (PN) code with an in-phase pseudo **noise** and quadrature pseudo **noise**, and a results of multiplying with a pilot **channel**, a **dedicated** control **channel**, a voice **channel**, a high-speed data **transmission channel**, a result multiplied with **channels** with gain, filtering units for eliminating **noise**, **subtracting** and adding units for calculating final result, and in-phase/quadrature **channel** outputting unit for outputting I-**channel/Q-channel**. The present invention can improve data processing speed of a radio **channel**, increase capacity of data processing in radio communication and also can be applicable to various kinds of radio communication devices transceiving voice, media contents and... ...**Claims:**processing data in a radio communication system based on a complex quadrature phase shift keying, comprising: a first multiplying means for multiplying a long pseudo **noise** (PN) code and multiplying with an in-phase pseudo **noise** (Ipn) and quadrature pseudo **noise** (Qpn) thereby generating a long in-phase PN code and a long quadrature PN code; a second multiplying means for multiplying the long in-phase pseudo PN code with a pilot **channel** (PI), a **dedicated** control **channel** (DC), a voice **channel** (FD) and a high speed data **transmission channel** (SM); a third multiplying means for multiplying the long quadrature PN code with a pilot **channel** (PI), a **dedicated** control **channel** (DC), a voice **channel** (FD) and a high speed data **transmission channel** (SM); first and second filtering means for filtering the result from the second and the third multiplying means to eliminate a **noise** controlling gains of filtered signals; fourth and fifth multiplying means for multiplying each of filtered signal from the first and second filtering means with a... ... to an eighth gain-controlled signals, wherein the first, the second, the seventh, the eighth gain controlled signals are a gain-controlled in-phase pilot **channel** signal, a gain-controlled in-phase **dedicated** control **channel**, a gain-controlled in-phase voice **channel** and a gain-controlled in-phase high-speed data **transmission channel** signals, and the third, the fourth, the fifth, the sixth gain controlled signals area gain-controlled quadrature pilot **channel** signal, a gain-controlled quadrature **dedicated** control **channel**, a gain-controlled quadrature voice **channel** and a gain-controlled quadrature high-speed data **transmission channel** signals; a **subtracting** means for calculating a first result by adding the first gain-controlled signal and the second gain controlled signal, calculating a second result by adding the third gain-controlled signal and the fourth gain-controlled signal, and calculating a **difference** between the first and the second results; an adding means for calculating a third result by adding the fifth and sixth gain-controlled signals, calculating... ... fourth result by adding the seventh and eighth gain-controlled signals and calculating a sum of the third and the fourth results; an in-

phase **channel** outputting means for outputting the result outputted from the **subtracting** means as an in-phase **channel** (I-**channel**) signal; and a quadrature **channel** outputting means for outputting the result outputted from the adding means as a quadrature **channel** (Q-**channel**) signal... ... processing data in a radio communication system based on a complex quadrature phase shift keying, comprising: a first multiplying means for multiplying a long pseudo **noise** (PN) code and multiplying with an in-phase pseudo **noise** (Ipn) and quadrature pseudo **noise** (opn) thereby generating a long in-phase PN code and a long quadrature PN code; a second multiplying means for multiplying the long in-phase pseudo PN code with a pilot **channel**

16/3,K/4 (Item 4 from file: 350) Links
   Fulltext available through: Order File History
Derwent WPIX
(c) 2009 Thomson Reuters. All rights reserved.

0012908932 *Drawing available*
WPI Acc no: 2002-342422/200238
XRPX Acc No: N2002-269286
Channel estimation method in antenna diversity system, involves determining channel estimate by rotating common pilot channel according to estimated phase difference between common and dedicated pilot channels
Patent Assignee: NOKIA CORP (OYNO); NOKIA MOBILE PHONES LTD (OYNO)
Inventor: AUTIO E; KESKITALO I; KESKITALO L; KINNUNEN P; KOESKITALOU I; OTTIO E; PAJUCOSKY K; PAJUKOSKI K

<div align="center">Patent Family (6 patents, 30 countries)</div>

Patent Number	Kind	Date	Application Number	Kind	Date	Update	Type
EP 1191755	A2	20020327	EP 2001308008	A	20010920	200238	B
BR 200104272	A	20020507	BR 20014272	A	20010926	200238	E
CN 1345136	A	20020417	CN 2001141176	A	20010926	200248	E
JP 2002185376	A	20020628	JP 2001294107	A	20010926	200258	E

Channel estimation method in antenna diversity system, involves determining channel estimate by rotating common pilot channel according to estimated phase difference between common and dedicated pilot channels ...**Original Titles:**Antenna phase estimation algorithm for WCDMA closed loop **transmitter** antenna diversity system ... ...METHOD FOR INFERRING AND DECIDING **CHANNEL** FOR WCDMA CLOSED LOOP **TRANSMITTER** ANTENNA DIVERSITY SYSTEM... ...Antenna phase estimation algorithm for WCDMA closed loop **transmitter** antenna diversity system **Alerting Abstract** ...NOVELTY - The phase **difference** between a **common** pilot **channel** and a **dedicated** pilot **channel** received from an antenna of a diversity system, is computed as a complex coefficient between the **channels**. A **channel** estimate is **determined** by rotating a **common** pilot **channel** according to the **estimated** phase **difference**. USE - For enabling a user equipment (UE) e.g. mobile phone, vehicle telephone to perform **channel** estimation for **channel** received from base station (BS) in antenna diversity system, wideband CDMA telecommunication system, **transmit** antenna diversity system... ...ADVANTAGE - Does not require an estimation of the **noise** variable or the relative powers of the **dedicated** and **common** pilot **channels**. ... ...DESCRIPTION OF DRAWINGS - The figure shows the block diagram of the 3G-WCDMA base station **transmitter** arrangement. **Title Terms** /Index Terms/Additional Words: **CHANNEL**; **Class Codes** International Patent Classification IPC Class Level Scope Position Status Version Date "Version 7" **H04B-0001/707**... ...**H04B-0007/06**... ...**H04B-0007/08**... ...**H04B-0007/26**... ...**H04L-0025/02 H04B-0001/707**... ...**H04B-0007/04**... ...**H04B-0007/08**... ...**H04B-0007/26**... ...**H04L-0025/02** Original Publication Data by AuthorityArgentina**Publication No. Original Abstracts:**This invention teaches a method for use in a wideband CDMA telecommunications system wherein the base station (BS) utilizes **transmit** antenna diversity. The **method** enables the user equipment (UE) to perform a **channel** estimate for **channels received** from two **antennas** of the base station (BS), and includes steps of: (a) computing an estimated phase **difference** between **a** common **pilot channel** and **a dedicated pilot channel** received **from** one **antenna** of the two antennas; and (b) determining the **channel**

estimate **by** rotating **a common** pilot **channel estimate according** to **the estimated** phase **difference,** where the phase **difference** is computed as **a** complex coefficient between the common pilot **channel** and **the dedicated pilot channel.** In **a** second **aspect** this invention teaches a method for use in a **transmit** antenna diversity system **for** enabling the UE to verify an antenna phase shift previously signaled by the UE to the BS. This method includes a first step of: (a... ... This invention teaches a method for use in a wideband CDMA telecommunications system wherein the base station (BS) utilizes **transmit** antenna diversity. The method enables the user equipment (UE) to perform a **channel estimate** for **channels** received from two antennas of the base station (BS), and **includes** steps of: (**a**) computing an estimated phase **difference** between a **common** pilot **channel** and a **dedicated** pilot **channel** received from one **antenna** of the **two** antennas; **and** (b) **determining the channel estimate** by rotating a **common** pilot **channel estimate** according to the estimated phase **difference, where** the phase **difference is** computed **as a** complex coefficient between **the common pilot channel** and the **dedicated** pilot **channel.** In a second aspect this invention **teaches** a **method** for use **in a transmit** antenna diversity system for enabling the UE to verify an antenna phase shift **previously** signaled by the UE to the BS. This method includes a first step of: (a) exploiting prior knowledge of BS rotation angle by considering a... **Claims:**In an antenna diversity system, a method for enabling a user equipment (UE) to perform a **channel** estimate **for a channel** received **from** a base station (BS), comprising steps of:computing an estimated phase **difference** between **a** common **pilot channel** and **a dedicated pilot channel** received **from** one **antenna** of the antenna diversity system; and determining the **channel estimate** by rotating **a common pilot channel estimate** according to **the estimated phase difference,** wherein the phase **difference** is **computed** as a complex **coefficient** between the common pilot **channel** and the **dedicated pilot channel....** ... What is claimed is:1. In an antenna diversity system, a method for enabling a user equipment (UE) to perform a **channel** estimate for a **channel** received from a base station (BS), comprising steps of:computing an **estimated phase difference** between a **common** pilot **channel** and a **dedicated** pilot **channel** received from one antenna of the antenna diversity **system;** and **determining the channel estimate** by rotating a **common pilot channel estimate** according to the estimated phase **difference,** wherein the phase **difference** is computed **as a** complex coefficient between **the common pilot channel** and the **dedicated pilot channel.>**

^^16/3,K/5 (Item 5 from file: 350) <u>Links</u>
   Fulltext available through: <u>Order File History</u>
Derwent WPIX
(c) 2009 Thomson Reuters. All rights reserved.

0010534998 *Drawing available*
WPI Acc no: 2001-137477/200114
XRPX Acc No: N2001-100153
Cross talk interference reducing method for transmission system that uses frequency-translated signals, involves multiplying complex coupling factor with signal on second line
Patent Assignee: TELEFONAKTIEBOLAGET ERICSSON L M (TELF)
Inventor: HJELM M; KARLSSON RUDBERG M; KARLSSON-RUDBERG M; RUDBERG M; RUDBERG M K

Patent Family (11 patents, 90 countries)

Patent Number	Kind	Date	Application Number	Kind	Date	Update	Type
WO 2000059125	A1	20001005	WO 2000SE491	A	20000313	200114	B
AU 200041551	A	20001016	AU 200041551	A	20000313	200114	E
SE 199901141	A	20000930	SE 19991141	A	19990329	200114	E
SE 514948	C2	20010521	SE 19991141	A	19990329	200130	E
EP 1163733	A1	20011219	EP 2000921211	A	20000313	200206	E
			WO 2000SE491	A	20000313		
TW 444445	A	20010701	TW 1999107871	A	19990514	200220	E
KR 2002000553	A	20020105	WO 2000SE491	A	20000313	200244	E
			KR 2001712433	A	20010928		
CN 1353891	A	20020612	CN 2000808256	A	20000313	200262	E
JP 2002540715	W	20021126	JP 2000608515	A	20000313	200307	E

17

Cross talk interference reducing method for transmission system that uses frequency-translated signals, involves multiplying complex coupling factor with signal on second line ...Original Titles:METHOD AND DEVICE FOR **REDUCING** CROSSTALK **INTERFERENCE** ... ...Method and device for **reducing** crosstalk **interference** ... ...METHOD AND DEVICE FOR **REDUCING** CROSSTALK **INTERFERENCE Alerting Abstract** DESCRIPTION - A complex coupling factor for **cross talk interference** is estimated. The estimated factor is multiplied with the signal on the second line to estimate the induced **cross talk interference**, after which the estimated induced **cross talk** is **subtracted** from the signal on the first line. An INDEPENDENT CLAIM is also included for a **transmission** system... ...USE - For **transmission** system that uses **frequency**-translated signals... ...ADVANTAGE - Simplifies and accelerates computation of the estimated **cross talk interference**, thus permitting adaptive **reduction** of **cross talk interference** in real time to accommodate e.g. changing **transmitting** conditions. Allows, at least partly, implementation using **dedicated** hardware for improved speed... ...DESCRIPTION OF DRAWINGS - The figure shows the conceptual diagram of the **cross talk reduction** in a **transmission** line. **Title Terms** .../Index Terms/Additional Words: **INTERFERENCE**; ... ...**TRANSMISSION**; ... ...**FREQUENCY**; **Class Codes** International Patent Classification IPC Class Level Scope Position Status Version Date **H04B-015/00**... ...**H04L-027/26** Main "Version 7" **H04B-0001/10**... ...**H04B-0003/06**... ...**H04B-0003/32**... ...**H04B-0003/46 H04B-0001/10**... ...**H04B-0003/02**... ...**H04B-0003/06**... ...**H04B-0003/46** Original Publication Data by AuthorityArgentina**Publication No. Original Abstracts:**In a **transmission** system which makes **use** of **frequency** translated signals, said **system** having a plurality of lines, a method for reducing crosstalk induced on a signal on a first line of said plurality of lines by a... ... lines, comprising estimating a complex coupling factor for the crosstalk, which when multiplied by the signal on the second line estimates the induced crosstalk, and **subtracting** the estimated induced **crosstalk** from the signal on the first line. The invention comprises an approximation method for multiplying the complex coupling factor by the signal on the second... ... In a **transmission** system which makes use of **frequency** translated signals, **said** system having a plurality of **lines**, a method for reducing crosstalk induced on a signal on a first line of said plurality of lines by a signal on a second line... ... lines, comprising estimating a complex coupling factor for the crosstalk, which when multiplied by the signal on the second line estimates the induced crosstalk; and **subtracting** the estimated induced crosstalk from the signal on **the** first line. The invention comprises an approximation method for multiplying the complex coupling factor by the signal on the second line that operates on the... ... In a **transmission** system which makes use of **frequency** translated signals, said system having a plurality **of** lines, a method for reducing **crosstalk** induced on a signal on a first line of said plurality of lines by a signal on a second line of said plurality of lines, comprising estimating a complex coupling factor for the crosstalk, which when multiplied by the signal on the second line estimates the induced crosstalk, and **subtracting** the estimated induced crosstalk from the signal on the first line. The invention **comprises** an approximation method for multiplying the complex coupling factor by the signal on the second line that operates on the signal on the second line... ... L'invention concerne un systeme de **transmission** utilisant des signaux transposes en **frequence**, ledit systeme possedant plusieurs lignes, et un procede permettant d'attenuer les **perturbations** diaphoniques provoquees sur un signal d'une premiere ligne par un signal d'une seconde ligne. Ce procede consiste a estimer un coefficient de couplage complexe pour les perturbations diaphoniques qui... **Claims:**What is claimed is:1. In a **transmission** system which makes use of **frequency translated** signals, particularly a discrete multi **tone** (DMT) modulated **transmission** system or an OFDM (Orthogonal **Frequency Division** Multiplex) **transmission** system, having a **plurality** of lines **and** in which the modulation may be effected using a fast inverse Fourier transform (IFFT), a method for **reducing** crosstalk **interference** induced on a signal **on** a **first** line of said plurality of lines by a signal on a second line of said plurality of lines, comprising estimating a complex coupling factor for the crosstalk **interference**, which when multiplied by the signal **on** the second line estimates the induced crosstalk **interference**; and **subtracting** the estimated induced crosstalk **interference** from **the** signal on the first **line**; further comprising multiplying the complex coupling factor by the signal on the second line through an approximation method operating on the signal on the second...

16/3,K/6 (Item 6 from file: 350) **Links**
   Fulltext available through: <u>Order File History</u>
Derwent WPIX

0009592072 *Drawing available*
WPI Acc no: 1999-540404/199945
Related WPI Acc No: 1999-035603; 1999-540403; 1999-540408; 1999-540464; 2002-461736; 2003-502784
XRPX Acc No: N1999-400547
Controlling power transmission level with a cellular communications system
Patent Assignee: BENDER P E (BEND-I); PADOVANI R (PADO-I); QUALCOMM INC (QUAL-N)
Inventor: BENDER P E; PADOVANI R

Patent Family (12 patents, 83 countries)

Patent Number	Kind	Date	Application Number	Kind	Date	Update	Type
WO 1999043101	A1	19990826	WO 1999US3683	A	19990219	199945	B
AU 199927760	A	19990906	AU 199927760	A	19990219	200003	E
EP 976206	A1	20000202	EP 1999908295	A	19990219	200011	E

Controlling power transmission level with a cellular communications system Alerting Abstract
...NOVELTY - Base stations (12, 14, 16) **transmit** a pilot **channel** that includes pseudo-random **noise** and information about the power of the **transmitted** signal. The mobile (18) measures the ratio of signal to **noise** on the pilot **channel** and from this makes an estimate of the strength of the received signal. The mobile compares this with the strength of its communications **channel** and **transmits** the ratio of the **difference** between the two back to the central control. ...ADVANTAGE - Does not need a **dedicated** control **channel**. Improved assessment of the quality of reception... **Title Terms** .../Index Terms/Additional Words: **TRANSMISSION**; **Class Codes** International Patent Classification IPC Class Level Scope Position Status Version Date **H04B-007/005**... ...**H04B-007/26** Main "Version 7" **H04B-001/04 H04B-0001/04**... ...**H04B-0007/00**... ...**H04B-0007/005**... ...**H04B-0007/005**... ...**H04B-0007/26**... ...**H04B-0007/26**... ...**H04L-0001/00 H04B-0001/04**... ...**H04B-0007/00**... ...**H04B-0007/005**... ...**H04B-0007/26**... ...**H04L-0001/00** Original Publication Data by AuthorityArgentina**Publication No. Original Abstracts:**A system and method is taught for controlling the power level of **transmissions** within a communication system having a base station, a mobile station, a communication **channel**, and a pilot **channel**. The mobile station determines a signal strength value according to a communication signal received by way of the communication **channel**. A pilot **channel** signal is determined according to a pilot signal **transmitted** by way of the pilot **channel**. The signal to **noise** ratio of the communication signal is determined according to the determined signal strength value and the pilot **channel** signal. The power level of a **transmission** is controlled according to the signal to **noise** ratio. The **noise** level in a communication **channel** within the communication system is estimated. The pilot **channel** signal includes pilot energy and pilot **noise** components.The pilot energy component is removed to provide a remaining pilot signal. Communication system operations are controlled according to the remaining pilot signal. The power levels of **transmissions** are controlled by determining the signal to **noise** ratio of a signal within the communication **channel** and determining a **difference** signal. The **difference** signal is formed by determining the **difference** between determined and desired signal to **noise** ratios. The **difference** signal is **transmitted** between the base station and the mobile station. The pilot **channel** has at least one frame and the power control signal is inserted into the frame. Thus, information representing the strength of the communication signal is **transmitted** to the base by way of the pilot **channel** within the frame.The pilot **channel** can have two information frames for **transmitting** the power control signal a plurality of times... ... A system and method is taught for controlling a power level of **transmissions** in a communication system. A first station of the communication system **transmits** signals on a communication **channel** and a pilot **channel**. A second station of the communication system measures a signal to **noise** ratio of the received signal, determines an expected signal to **noise** ratio of the received signal, determines an indicator in accordance with said measured signal to **noise** ratio and the expected signal to **noise** ratio, and **transmits** the indicator. The indicator is received at the first station the indicator and determines the power level of the next **transmission** according to said received indicator. Additionally, methods and systems for the measurement of the signal to **noise** ratio of the received signal, the determination of the expected signal to **noise** ratio of the received signal, and the determination of the indicator are disclosed... ... A system and method is taught for controlling a power level of **transmissions** in a communication system. A first station of the communication system **transmits** signals on a communication **channel** and a pilot **channel**. A second

station of the communication system measures a signal to **noise** ratio of the received signal, determines an expected signal to **noise** ratio of the received signal, determines an indicator in accordance with said measured signal to **noise** ...

^16/3,K/7 (Item 7 from file: 350) <u>Links</u>
  Fulltext available through: <u>Order File History</u>
Derwent WPIX

0008418509 *Drawing available*
WPI Acc no: 1997-536171/199749
Related WPI Acc No: 1997-536156; 1997-536172; 2002-634586
XRPX Acc No: N1997-446330
RF interference mitigation method for multicarrier modulation - estimating RF interference in accordance with frequency domain model for RF interference and estimated frequency of RF interference and removing estimated RF interference from frequency domain data
Patent Assignee: AMATI COMMUNICATIONS CORP (AMAT-N); AMATI COMMUNICATIONS INC (AMAT-N); BINGHAM J A C (BING-I); TEXAS INSTR INC (TEXI); WIESE B R (WIES-I)
Inventor: BINGHAM J A C; WIESE B R; BINGHAM J

Patent Family (18 patents, 74 countries)

Patent Number	Kind	Date	Application Number	Kind	Date	Update	Type
WO 1997040608	A1	19971030	WO 1997US6384	A	19970417	199749	B
AU 199730547	A	19971112	AU 199730547	A	19970417	199811	E
EP 894390	A1	19990203	EP 1997925397	A	19970417	199910	E
			WO 1997US6384	A	19970417		
CN 1229553	A	19990922	CN 1997195651	A	19970417	200002	E
US 6014412	A	20000111	US 199616251	P	19960419	200010	E

RF interference mitigation method for multicarrier modulation... ...estimating RF interference in accordance with frequency domain model for RF interference and estimated frequency of RF interference and removing estimated RF interference from frequency domain data Original Titles:SCHALTUNG ZUR DIGITALEN HF-**INTERFERENZUNTERDRUCKUNG** ... ...DIGITAL RADIO **FREQUENCY INTERFERENCE CANCELLER** ... ...SUPPRESSEUR D'**INTERFERENCES** SUR DES **TRANSMISSIONS** RF NUMERIQUES... ...SCHALTUNG ZUR DIGITALEN HF-**INTERFERENZUNTERDRUCKUNG** ... ...DIGITAL RADIO **FREQUENCY INTERFERENCE CANCELLER** ... ...SUPPRESSEUR D'**INTERFERENCES** SUR DES **TRANSMISSIONS** RF NUMERIQUES... ...DIGITAL RADIO **FREQUENCY INTERFERENCE CANCELLER** ... ...The relief/moderation of the radio-**frequency interference** in a multicarrier **transmission** system... ...Digital radio **frequency interference canceller** ... ...Digital radio **frequency interference canceller** ... ...Digital radio **frequency interference canceller**. **Mitigating** radio **frequency interference** in multi-carrier **transmission** systems... ...Digital radio **frequency interference canceller**. ... ...Digital radio **frequency interference canceller**. ... ...DIGITAL RADIO **FREQUENCY INTERFERENCE CANCELLER** **Alerting Abstract** ...The method involves obtaining **frequency** domain data which are associated with a **frequency** band. A restricted **frequency** sub-band is identified in the **frequency** band and the **frequency** of the RF **interference** sub-band is estimated in the restricted **frequency** sub-band... ...The RF **interference** is estimated in accordance with a **frequency** domain model for the RF **interference** and the estimated **frequency** of the RF **interference**. The estimated RF **interference** is removed from the **frequency** domain data... ...USE/ADVANTAGE - E.g. for ADSL, VDSL, FTTC. Eliminates or compensates radio **interference** and **reduces** sidelobe **interference**. **Title Terms** .../Index Terms/Additional Words: **INTERFERENCE**; ... ...**FREQUENCY**; **Class Codes** International Patent Classification IPC Class Level Scope Position Status Version Date Original Publication Data by AuthorityArgentina**Publication No. Original Abstracts:**Disclosed are radio **frequency** (RF) **interference cancellation** techniques that effectively estimate RF **interference** to the data signals being received using a **frequency** domain model, and then remove the estimated RF **interference** from the received data signals. Improved techniques for digitally filtering multicarrier modulation samples to **reduce** sidelobe **interference** due to the RF

20

interference are also disclosed... ... The radio **frequency interference** used as the serious|significant disorder|damage|failure for a receiver which can receive a **transmission**-data signal appropriately is removed, or it is compensated.The radio-**frequency** (RF) **interference** to the data signal received is effectively estimated using a **frequency**-domain model,Subsequently, the radio-**frequency** (RF) **interference** denial technique of removing this estimated RF **interference** from a receiving data signal is disclosed.In order to **reduce** the side-lobe **interference** by RF **interference**, the improvement technology which carries out the wave filter of the multi-career|carrier modulation|alteration sample digitally is also disclosed.FIG. 7This invention relates to a radio-**frequency** (RF) **interference** denial (erasure|elimination) device.More Specifically,It is related with RF **interference** denial in a multi-career|carrier **transmission** system... ... Disclosed are radio **frequency** (RF) **interference cancellation** techniques that effectively estimate RF **interference** to the data signals being received using a **frequency** domain model, and then remove the estimated RF **interference** from the received data signals. Improved techniques for digitally filtering multicarrier modulation samples to **reduce** sidelobe **interference** due to the RF **interference** are also disclosed... ... Disclosed are radio **frequency** (RF) **interference cancellation** techniques that effectively estimate RF **interference** to the data signals being received using a **frequency** domain model, and then remove the estimated RF **interference** from the received data signals. Improved techniques for digitally filtering multicarrier modulation samples to **reduce** sidelobe **interference** due to the RF **interference** are also disclosed... ... Disclosed are radio **frequency** (RF) **interference cancellation** techniques that effectively estimate RF **interference** to the data signals being received using a **frequency** domain model, and then remove the estimated RF **interference** from the received data signals. Improved techniques for digitally filtering multicarrier modulation samples to **reduce** sidelobe **interference** due to the RF **interference** are also disclosed... ... Methods and mechanisms for reducing the impact of radio **frequency interference** in multi-carrier data **transmission** systems are disclosed. In one aspect of the invention, dummy tones are used to suppress emissions within restricted **frequency** bands. In another aspect of the invention, signals received on designated quiet tones are detected and used to facilitate **canceling** of RF **interference** on adjacent active tones... ... Disclosed are radio **frequency** (RF) **interference cancellation** techniques that effectively estimate RF **interference** to the data signals being received using a **frequency** domain model, and then remove the estimated RF **interference** from the received data signals. Improved techniques for digitally filtering multicarrier modulation samples to **reduce** sidelobe **interference** due to the RF **interference** are also

18/3,K/1 (Item 1 from file: 350) Links
    Fulltext available through: Order File History
Derwent WPIX

0009639207 *Drawing available*
WPI Acc no: 1999-590935/199950
XRPX Acc No: N1999-435897
Mobile station locating method in communication system
Patent Assignee: MOTOROLA INC (MOTI)
Inventor: GHOSH A; STEWART K A

Patent Family (7 patents, 22 countries)

Patent Number	Kind	Date	Application Number	Kind	Date	Update	Type
WO 1999046880	A1	19990916	WO 1998US24911	A	19981124	199950	B
US 6009091	A	19991228	US 199841898	A	19980313	200007	E
BR 199815691	A	20001205	BR 199815691	A	19981124	200101	E

Alerting Abstract ...NOVELTY - Several base stations are communicated via three types of **frequency** bands which utilize three different spreading codes respectively. The spreading codes (502) define corresponding **channels** utilized for **transmitting** data and control information from mobile station to base stations and **transmitting** information from base station respectively. DESCRIPTION - A mobile station sends communication signal which is received via a **channel** by which location of mobile station based on communication is traced. A time **difference** of arrival (TDOA) or time of arrival (TOA) technique is used

for locating the mobile station. The mobile station broadcasts a probe sequence corresponding via a **Dedicated** Physical Location **Channel** (DPLCH) (501). An INDEPENDENT CLAIM is also included for an apparatus for locating mobile station within a communication system... ...ADVANTAGE - A high signal to **noise** ratio at a distant base station without an undesirable mobile station **transmit** power envelope variation is obtained by utilizing spreading codes with orthogonal channelization codes and mobile station having **Dedicated** Physical Located **Channel**. ... ...DESCRIPTION OF DRAWINGS - The figure shows the block diagram of mobile station spreading technique for wide band CDMA system incorporating a location sub-**channel**. ... ...501 **Dedicated** Physical Location **Channel Class Codes** International Patent Classification IPC Class Level Scope Position Status Version Date **H04B-007/26** Main **H04B-0007/26**... ...**H04J-0011/00**... ...**H04J-0013/00 H04B-0007/26**... ...**H04J-0011/00**... ...**H04J-0013/00** Original Publication Data by AuthorityArgentina**Publication No. Original Abstracts:**A **Dedicated** Physical Location **Channel (DPLCH)** is utilized **by** a mobile station (913) to support subscriber location functions. The DPLCH is spread by an Orthogonal Variable Spreading Factor (OVSF) code CL (502) of length 256 which is distinct from those OVSF codes assigned to other **channels** utilized by the mobile station (913). **When** a power-up function (PUF) is received by the mobile station (913), the DPLCH sub-**channel** amplitude is then modified relative to **the** other **channels** being utilized by the mobile station (**913**) using gain module GL (503) prior to combination (504) with the other **channels**. A **Dedicated** Physical Location **Channel** (DPLCH) is utilized by a mobile station (913) to support subscriber **location** functions. The **DPLCH** is spread by an Orthogonal Variable Spreading Factor (OVSF) code CL (502) of length 256 which is distinct from those OVSF codes assigned to other **channels** utilized by the mobile station (913). When a power-up function (PUF) is received **by** the mobile station (913), the DPLCH sub-**channel** amplitude is then modified relative to the other **channels** being utilized by the mobile **station** (913) using gain module GL (503) prior to **combination** (504) with the other **channels**. A **Dedicated** Physical Location **Channel** (DPLCH) is utilized by a mobile station (913) to support subscriber location functions. The DPLCH is **spread** by an **Orthogonal** Variable Spreading Factor (OVSF) code CL (502) of length 256 which is distinct from those OVSF codes assigned to other **channels** utilized by the mobile station (913). When a power-up function (PUF) is received by the mobile station (913), the DPLCH sub-**channel** amplitude is then modified relative to the other **channels** being utilized by the mobile station (913) using gain module GL (503) prior **to** combination (504) with the other **channels**. Selon...**Claims:**method for mobile station location within a communication system, the method comprising the steps of:communicating with a plurality of base stations via a first **frequency** band using a **first** spreading code, the first spreading code defining a first **channel** utilized for **transmitting data** from the **mobile** station to the plurality of base stations;communicating with the plurality of base stations via the first **frequency** band using a second spreading **code**, the second spreading code defining a second **channel** utilized for **transmitting** control information **from** the mobile **station** to the plurality of base stations; andcommunicating with the plurality of base stations via the first **frequency** band using a third spreading code, the **third** spreading code defining a third **channel** utilized for **transmitting** information to the plurality **of** base stations **that** is utilized for mobile station location within the communication system.

^22/3,K/1 (Item 1 from file: 350) Links
    Fulltext available through: Order File History
Derwent WPIX
(c) 2009 Thomson Reuters. All rights reserved.

0014031629 *Drawing available*
WPI Acc no: 2004-213583/200420
XRPX Acc No: N2004-169225
Communication system has lattice interfered channel that has underlying channel with at least one lattice vector on input or output side, and through which mapped input data are sent at rate of not more than 0.7 bit per dimension
Patent Assignee: DSPC TECHNOLOGIES LTD (DSPC-N); INTEL CORP (ITLC)
Inventor: BEN-ELI D; SHANY Y; **SUTSKOVER I**

Patent Family (2 patents, 1 countries)

Patent Number	Kind	Date	Application Number	Kind	Date	Update	Type

| US 20040030979 | A1 | 20040212 | US 2002214630 | A | 20020807 | 200420 | B |
| US 7036071 | B2 | 20060425 | US 2002214630 | A | 20020807 | 200628 | E |

Communication system has lattice interfered channel that has underlying channel with at least one lattice vector on input or output side, and through which mapped input data are sent at rate of not more than... Original Titles:Practical coding and metric calculation for the lattice **interfered channel** ... ...Practical coding and metric calculation for the lattice **interfered channel** ...Inventor: **SUTSKOVER I Alerting Abstract** ...NOVELTY - An encoder-modulator maps the input data to a signal constellation having signal points in predetermined dimensions. A lattice **interfered channel** (100) has an underlying **channel** (102) with an addition of at least one lattice vector (104,106) at the input or output side. The mapped input data are sent through the lattice **interfered channel** at a rate of not more than 0.7 bit per dimension. ... a **transmitter;**a data **transmission method** in communication system;a **signal** processing method in communication system;a receiver; anda communication device... ... ADVANTAGE - Ensures effective **transmission** of predetermined data from a **transmitter** to a receiver through effective use and **implementation** of lattice **interfered channel.**DESCRIPTION OF DRAWINGS - The figure shows the block diagram illustrating lattice **interfered channel.**100Lattice **interfered channel**102Underlying **channel**Title Terms** .../Index Terms/Additional Words: **INTERFERENCE; CHANNEL; Class Codes** Original Publication Data by AuthorityArgentina**Publication No.** ...Inventor name & address:**Sutskover, Ilan... ...Sutskover, Ilan Original Abstracts:**A communication system includes a lattice **interfered channel** to **transmit data from** a **transmitter** to a receiver. **In** one embodiment, an encoding-modulation scheme having a rich signal constellation is used to encode data at a total rate of 0.7 bit/dimension or less before **transmission** into the lattice **interfered channel**. In another **embodiment, decoding** metric approximation techniques are used to process signals received from the lattice **interfered channel**. In still **another embodiment**, multilevel code (MLC) decoding is used to jointly decode an error correction code component and a lattice/MLC component of a received signal. The error... ... A communication system includes a lattice **interfered channel** to **transmit** data from a **transmitter** to **a receiver. In one** embodiment, an encoding-**modulation** scheme having a rich signal constellation is used to encode data at a total rate of 0.7 bit/dimension or less before **transmission** into the lattice **interfered channel**. In another embodiment, **decoding** metric approximation techniques **are used** to process signals received from the lattice **interfered channel**. In still another embodiment, multilevel code (MLC) **decoding is** used to jointly decode an error correction code component and a lattice/MLC component of a received signal. The error correction code component may then... ...**Claims:**system comprising:an encoder-modulator to map input data into a signal constellation having more than 2k signal points in k dimensions; anda lattice **interfered channel** having an underlying **channel** together with at least one of the following: addition of **at least** one lattice vector **at** an input of the underlying **channel** and addition of at least one lattice vector at an output of the underlying **channel;wherein** said mapped input data is **transmitted** through said lattice **interfered channel** at a rate **of** no greater than 0.7 bits/dimension.... ... What is claimed is:13. A method for use in processing a received signal in a communication system having a lattice **interfered channel**, said lattice **interfered channel** having an associated lattice Lambda, comprising: identifying a point in the lattice Lambda that is closest to a received vector;obtaining a difference **between the** identified point **and the** received vector; andapproximating a bit likelihood measure using the difference between the identified point and the received vector, wherein approximating includes calculating a sum of probabilities associated with a subset of lattice points within lattice Lambda,wherein prior to **transmission**, input data is mapped into a signal constellation having more than 2k signal points in k dimensions for **transmission** through the lattice **interfered channel** at a rate of no greater than 0.7 bits/dimension

26/3,K/1 (Item 1 from file: 350) Links
    Fulltext available through: Order File History
Derwent WPIX
(c) 2009 Thomson Reuters. All rights reserved.

0014302999 *Drawing available*
WPI Acc no: 2004-490032/200447
XRPX Acc No: N2004-386543

Transmission power control method for communication system e.g. CDMA, involves setting power of downlink channel for mobile station based on reception quality information when time difference is equal or less than preset threshold

Patent Assignee: NTT DOCOMO INC (NITE); NTT IDO TSUSHINMO KK (NITE)

Inventor: ISHII M; ISHII M I P D N D I; NAKAMURA T; NAKAMURA T I P D N D I; SATO T; SATO T I P D N D I; ISHII Y; SATOO T

Patent Family (10 patents, 34 countries)

Patent Number	Kind	Date	Application Number	Kind	Date	Update	Type
EP 1432142	A2	20040623	EP 200329064	A	20031217	200447	B
JP 2004201095	A	20040715	JP 2002368341	A	20021219	200447	E
US 20040132475	A1	20040708	US 2003737860	A	20031218	200447	E
CN 1510847	A	20040707	CN 200310121866	A	20031219	200467	E
EP 1432142	B1	20050810	EP 200329064	A	20031217	200554	E

Alerting Abstract ...that the transmission power is adapted for positional relationships among mobile stations and a radio state of each mobile station, hence prevents unnecessary power consumption, **reduces interference** to other mobile stations, and increase a downlink capacity... **Class Codes** International Patent Classification IPC Class Level Scope Position Status Version Date **H04B-007/005** Main **H04B-0001/00**... ...**H04B-0001/69**... ...**H04B-0007/005**... ...**H04B-0007/005**... ...**H04B-0007/26**... ...**H04B-0007/26 H04B-0001/00**... ...**H04B-0001/69**... ...**H04B-0007/005**... ...**H04B-0007/005**... ...**H04B-0007/005**... ...**H04B-0007/26**... ...**H04B-0007/26** Original Publication Data by AuthorityArgentina**Publication No. Original Abstracts:**The object of the present invention to provide a **transmission** power control method which controls a **transmission** power of a downlink common channel so that the **transmission** power is adapted to a radio state of each mobile station, and thereby makes it possible to prevent unnecessary power consumption, reduce interference to other mobile stations, and increase a downlink capacity. The **transmission** power control method includes (A) acquiring reception quality information of a downlink for a mobile station (S103), (B) measuring a time **difference** (S104) between when an uplink signal is received from the mobile station and when a downlink signal to be **transmitted** to the mobile station occurs, (C) comparing the measured time **difference** with a predetermined threshold (S105), and (D) setting a **transmission** power (S106) of a downlink common channel for mobile stations in accordance with the reception quality information, when the time **difference** is equal to or less than the predetermined threshold... ... The object of the present invention to provide a **transmission** power control method which controls a **transmission** power of a downlink common channel so that the **transmission** power is adapted to a radio state of each mobile station, and thereby makes it possible to prevent unnecessary power consumption, reduce interference to other mobile stations, and increase a downlink capacity. The **transmission** power control method includes (A) acquiring reception quality information of a downlink for a mobile station, (B) measuring a time **difference** between when an uplink signal is received from the mobile station and when a downlink signal to be **transmitted** to the mobile station occurs, (C) comparing the measured time **difference** with a predetermined threshold, and (D) setting a **transmission** power of a downlink common channel for mobile stations in accordance with the reception quality information, when the time **difference** is equal to or less than the predetermined threshold... ... The object of the present invention to provide a **transmission** power control method which controls a **transmission** power of a downlink common channel so that the **transmission** power is adapted to a radio state of each mobile station, and thereby makes it possible to prevent unnecessary power consumption, reduce interference to other mobile stations, and increase a downlink capacity. The **transmission** power control method includes (A) acquiring reception quality information of a downlink for a mobile station, (B) measuring a time **difference** between when an uplink signal is received from the mobile station and when a downlink signal to be **transmitted** to the mobile station occurs, (C) comparing the measured time **difference** with a predetermined threshold, and (D) setting a **transmission** power of a downlink common channel for mobile stations in accordance with the reception quality information, when the time **difference** is equal to or less than the predetermined threshold. ...**Claims:**power of a **common channel** is **calculated** based on the receiving quality of the said down-link,The transmission...

26/3,K/2 (Item 2 from file: 350) <u>Links</u>
    Fulltext available through: <u>Order File History</u>
Derwent WPIX
(c) 2009 Thomson Reuters. All rights reserved.

0014040456 *Drawing available*
WPI Acc no: 2004-222635/200421
Device for controlling high speed shared control channel transport power in time division duplexing code division multiple access communication system by using high speed downlink packet access system and method therefor
Patent Assignee: SAMSUNG ELECTRONICS CO LTD (SMSU)
Inventor: HWANG S O; KIM J G; KIM Y B; LEE J S; LI X Q; ZHANG S W; HWANG S; KIM J; KIM Y; LEE J; LI X; ZHANG S

Patent Family (2 patents, 1 countries)

Patent Number	Kind	Date	Application Number	Kind	Date	Update	Type
KR 2003088607	A	20031120	KR 200226278	A	20020513	200421	B

Class Codes International Patent Classification IPC Class Level Scope Position Status Version Date
H04B-0007/26... ...H04B-0007/26 H04B-0007/26... ...H04B-0007/26 Original Publication Data by
Authority Argentina **Publication No. Claims:**[CLAIM 1] The **transmitting** power control method of the method for the time division duplexing WCDMA system using the high-speed forwarding packet connection method **transmitting** the measurement report and controlling the TX power of the common control channel comprising the primary channel signal, from the base station and the process it receives the common control channel signal; it produces the path loss which is **difference** between the received power of the primary channel signal and the process, of measuring the **interference** power of the common control channel signal and received power and **interference** power to the measurement report; and of **transmitting** the measurement report through the second channel... ...CLAIM 6] The **transmitting** power control method including the TX power of the process, of receiving the measurement report and primary channel and the process of controlling the TX power of the common control channel with the target signal to **interference** ratio of the common control channel and path loss of the method for controlling the TX power of the common control channel in the time division duplexing WCDMA system using the high-speed forwarding packet connection method comprising the path loss which is **difference** between the **interference** power of the received power of the primary channel and the common control channel from the user terminal... ...CLAIM 7] The **transmitting** power control method of claim 6, wherein the process of controlling the TX power of the common control channel adds the target signal to **interference** ratio of the common control channel after **subtracting** the path loss in the TX power of the primary channel... ...CLAIM 10] The **transmitting** power control method of claim 9, wherein the process of controlling the TX power of the common control channel adds the target signal to **interference** ratio of the common control channel after **subtracting** the signal-to-**interference** ratio in the TX power of the **common** control **channel** and it **determines**. [

^26/3,K/3 (Item 3 from file: 350) <u>Links</u>
    Fulltext available through: <u>Order File History</u>
Derwent WPIX
(c) 2009 Thomson Reuters. All rights reserved.

0012808717 *Drawing available*
WPI Acc no: 2002-665793/200271
XRPX Acc No: N2002-526755
Downlink power control method in radio access network, involves regulating transmit power level on common transport channel, based on received signal strength information and signal-to-interference information
Patent Assignee: TELEFONAKTIEBOLAGET ERICSSON L M (TELF)
Inventor: LIESHOUT G V; PERSSON M; RUNE G; VAN LIESHOUT G

Patent Family (4 patents, 98 countries)

Patent Number	Kind	Date	Application Number	Kind	Date	Update	Type
US 20020094833	A1	20020718	US 2001260891	P	20010112	200271	B
			US 2001989105	A	20011121		
WO 2002056498	A2	20020718	WO 2002SE49	A	20020111	200271	E
AU 2002219755	A1	20020724	AU 2002219755	A	20020111	200427	E
AU 2002219755	A8	20050915	AU 2002219755	A	20020111	200569	E

Class Codes International Patent Classification IPC Class Level Scope Position Status Version Date **H04B-007/00... ...H04B-007/005** Main **H04B-0007/005... H04B-0007/005...** Original Publication Data by AuthorityArgentina**Publication No. Original Abstracts:**A radio network control node that determines the **transmit** power of a **common** or shared downlink transport channel regulates that power based on one or more factors. The downlink **transmit** power regulation makes **common** downlink transport channel **transmissions** more efficient and **effective** in terms of delivering services to users, maximizing capacity, and reducing unnecessary interference. Examples of one or more factors that may be considered in regulating the **transmit** power on a **common** transport channel include (but are not limited to) include one or more measurements made by the user equipment of received downlink **transmissions** such as received **signal** strength, signal-to-**interference** ratio, error rates **like** bit error rate and block error, etc. Other potential factors could include current conditions in the cell such as traffic volume and **percentage** of maximum base **station transmit** power currently being **used**. The service(s) requested for each common transport channel user may also be taken into account. The controlling radio network node for the user connection uses one or more of these factors to adapt the downlink **transmit** power of the **common** transport channel. That power level adaptation may occur directly or indirectly via another radio network controller or base station node. The **transmit** power on the **common** transport channel may be regulated in general, per user connection, block-by-block, etc... ... A radio network control node that determines the **transmit** power of a common or shared **downlink** transport **channel** regulates that power **based** on one or more factors. The downlink **transmit** power regulation makes common downlink transport channel **transmissions more** efficient and effective and effective in terms **of** delivering services to users, maximizing capacity, and reducing unnecessary interference. Examples of one or more factors that may be considered in regulating the **transmit** power on a common transport channel include (but **are** not limited do) include one or more measurements made by the user equipment of received downlink **transmissions** such as received signal strength, signal-to-**interference ratio**, error rates bit error rate and block **error**, etc. Other potential factors could include current conditions in the cell such as traffic volume and **percentage** of maximum base station **transmit** power currently being **used**. The service(s) requested **for** each common transport channel user may also be taken into account. The controlling radio network node for the user connection uses one or more of these factors to adapt the downlink **transmit** power of the common transport channel. That power **level** adaptation may occur directly or indirectly via another radio network controller or base station node. The **transmit** power on the common transport channel may be **regulated** in general, per user connection, block-by-block, etc... ...**Claims:**radio network node coupled to a base station transmitting information over a radio interface on a common transport channel shared by plural mobile stations, a **method** comprising:**determining** one or more conditions relating to a transmit power level for transmitting information over the radio interface to a mobile station using the common transport channel, and regulating the transmit power level on the **common** transport **channel** based on the **determined** one or more conditions.

26/3,K/4 (Item 4 from file: 350) Links
   Fulltext available through: Order File History
Derwent WPIX

0012413202 *Drawing available*
WPI Acc no: 2002-357557/200239
Synchronous demodulation apparatus and method in cdma communication system
Patent Assignee: SAMSUNG ELECTRONICS CO LTD (SMSU)
Inventor: HUH S H; HWANG S G

Patent Family (2 patents, 1 countries)

Patent Number	Kind	Date	Application Number	Kind	Date	Update	Type
KR 2001066407	A	20010711	KR 199968122	A	19991231	200239	B

Alerting Abstract DESCRIPTION - A synchronous demodulation apparatus contains a PCCPCH(Primary **Common** Control Physical **CHannel**) code **estimator**(202), a pilot symbol extractor(212), a channel estimator(222), and a normalizer(226). The PCCPCH code estimator(202) executes a despreading operation after acquiring the code synchronization of the signal **transmitted** through a PCCPCH. The pilot symbol extractor(212) extracts a pilot symbol, located at the last of a slot for synchronous demodulation, from the signal despreaded by the PCCPCH code estimator(202). The channel estimator(222) estimates a channel from the extracted PCCPCH pilot symbol to compensate phase and amplitude **distortions** due to fading and Doppler. The normalizer(226) normalizes the channel value estimated by the channel estimator(222) in consideration of the power **difference** between the PCCPCH and a DPCH(Dedicated Physical CHannel). **Class Codes** International Patent Classification IPC Class Level Scope Position Status Version Date **H04B-0001/69... ...H04B-0001/69 H04B-0001/69... ...H04B-0001/69**

[File 9] **Business & Industry(R)** Jul/1994-2009/Apr 22

[File 15] **ABI/Inform(R)** 1971-2009/Apr 24

[File 16] **Gale Group PROMT(R)** 1990-2009/Apr 02
File 16: UD/banner does not reflect last processed date

[File 20] **Dialog Global Reporter** 1997-2009/Apr 23

[File 47] **Gale Group Magazine DB(TM)** 1959-2009/Apr 14

[File 75] **TGG Management Contents(R)** 86-2009/Mar W3

[File 80] **TGG Aerospace/Def.Mkts(R)** 1982-2009/Apr 01

[File 88] **Gale Group Business A.R.T.S.** 1976-2009/Apr 23

[File 112] **UBM Industry News** 1998-2004/Jan 27
File 112: This file is closed. For more recent UBM/CMP records, please search DIALOG Newsroom files.

[File 148] **Gale Group Trade & Industry DB** 1976-2009/Apr 10
File 148: The CURRENT feature is not working in File 148. See HELP NEWS148.

[File 160] **Gale Group PROMT(R)** 1972-1989

[File 264] **DIALOG Defense Newsletters** 1989-2009/Apr 23

[File 369] **New Scientist** 1994-2009/Apr W2

[File 370] **Science** 1996-1999/Jul W3
File 370: This file is closed (no updates). Use File 47 for more current information.

[File 484] **Periodical Abs Plustext** 1986-2009/Apr W3
File 484: Despite the gap in UDs all content is present.

[File 570] **Gale Group MARS(R)** 1984-2009/Apr 02

[File 620] **EIU:Viewswire** 2009/Apr 22

[File 621] **Gale Group New Prod.Annou.(R)** 1985-2009/Mar 20

[File 623] **Business Week** 1985-2009/Apr 24

[File 624] **McGraw-Hill Publications** 1985-2009/Apr 24

[File 634] **San Jose Mercury** Jun 1985-2009/Apr 22

[File 635] **Business Dateline(R)** 1985-2009/Apr 23

[File 636] **Gale Group Newsletter DB(TM)** 1987-2009/Apr 03

[File 647] **UBM Computer Fulltext** 1988-2009/Feb W3

[File 696] **DIALOG Telecom. Newsletters** 1995-2009/Apr 23

[File 674] **Computer News Fulltext** 1989-2006/Sep W1
File 674: File 674 is closed (no longer updates).

[File 810] **Business Wire** 1986-1999/Feb 28

[File 813] **PR Newswire** 1987-1999/Apr 30

[File 587] **Jane`s Defense&Aerospace** 2009/Mar W4

```
Set      Items     Description
S1     4337861     S TRANSCEIVER?? OR TRANSMIT? OR TRANSMISSION?? OR MODEM??
S2     6456269     S CHANNEL?? OR FREQUENC???
S3       14222     S COMMON(3N)S2
S4         151     S (ESTIMAT??? OR CALCULAT??? OR DETERMIN? OR APPROXIMAT? OR
INTERPOLAT? OR PROBABILITY??? OR STATISTIC??)(3N)S3
S5     2274028     S INTERFER? OR CROSS()TALK??? OR NOISE?? OR ALIASING OR
DISTORTION?? OR ARTIFACT??
S6      215132     S (REDUC? OR ATTENUAT??? OR MITIGAT??? OR RID OR PREVENT???
OR MINIMI??? OR LESSEN? OR DIMINISH??? OR CANCEL? OR STOP?)(3N)S5
S7           5     S AU=(SUTSKOVER, I? OR SUTSKOVER I? OR BEN()ELI, D? OR
BEN()ELI D?)
S8        5044     S (S5 OR S6)(S)(SUBTRACT? OR MINUS OR DIFFERENCE?? OR
PERCENT?)(S)S1
S9           0     S S8(S)S4
S10         21     S S8(S)S3
S11         15     RD  (unique items)
S12          3     S S11 NOT PY>2003
S13          2     S S12 NOT BISTATIC
S14          0     S S7 AND S8
```

13/3,K/1 (Item 1 from file: 88) Links
Gale Group Business A.R.T.S.

Author Abstract: High-frequency single-sideband (HF-SSB) radio communication suffers from highly variable propagation conditions and high levels of **interference noise**. One **common distortion** is **frequency** shifting of the received signal due to **differences** in carrier frequencies at **transmitter** and receiver, or to Doppler shifts due to the **transmission** path. This paper presents a novel and efficient technique to compensate for this frequency offset using only the received speech signal to determine and correct...

Text:

13/3,K/2 (Item 1 from file: 587) <u>Links</u>
Jane`s Defense&Aerospace
10892604   **Word Count:** 5572
Radio tomorrow

INTERNATIONAL DEFENSE REVIEW (IDR)   MARCH 01, 2001 v. 034 no. 003
Section Heading: FEATURE
By: Rupert Pengelley

...may be in sight. Taken to its logical conclusion, the
advent of "software defined" radio (SDR) technology could well lead
to the replacement of tactical **transceivers** by what might more
appropriately be described as general-purpose RF (radio frequency)
devices.

Certainly future tactical voice and data radios are unlikely to look...

...1980s to the next
generation of multiband, multimode SDRs. Those cited by the US Army
include the increased speed and power of embedded processors,
enabling **modem** functions to be performed by digital signal
processors; improved analog-to-digital converters, with higher
conversion rates and increased dynamic operating ranges; and the
development...intelligence (C{4}I) capabilities to the warfighters.
This family will cover an operating spectrum from 2-2,000MHz
initially, and will be capable of **transmitting** voice, video, and
data... JTRS is not a one-size-fits-all system. Rather, it is a
family of radios that are interoperable, affordable and...

...I radio is intended to exploit a
CSMA-based wideband waveform being developed by BAE in association
with BBN to provide the TOC-to-TOC **transmission** capability for those
brigade combat teams belonging to the Army's second digitized
division (1 CAV) and the third of the US Army's new...

...five channels in its ground application, six for
aviation, two for dismounted applications, and one for handheld
applications.) Consideration is being given to using a **common** three-
channel stackable radio for both ground and aviation applications,

offering enhanced economy of scale and redundancy. The Block II
draft RFP was expected before the end...120km point-to-
point range) using a vertical-incidence SINCGARS-type whip antenna.
(Though it could not receive such signals, the IWS could generate
skywave **transmissions** for sending messages to base stations over
even longer ranges, according to ITT.)

To maintain such links "anywhere, anytime", the SUO SAS
communication network is...

...provided by embedding serial probes
in the bit patterns. These retune digitally matched filters in the
receiver faster than the channel decorrelation time, overcoming
multipath **interference** from buildings and obstacles. The software
tunable digital synthesizer automatically changes frequency (up to
500/sec) throughout the full frequency range, using direct sequence
spread spectrum rather than frequency hopping. The coding rate, data
rate, power and frequency may be changed on every packet
transmission.

Some partisan engineers are inclined to dismiss JTRS as "a future-
looking product whose time has passed." Even so, SUO SAS itself is
billed as...was already a feature of several
modern tactical radio systems and that SDRs, like their
predecessors, embody a receiver (or two) as well as a **transmitter.**
The thought therefore arises that this receive capacity could
usefully be exploited for signal intelligence (SIGINT) as well as
for communication. Pursuing this line of...

...to the services at the start of FY03. Both
teams are working on subsystem risk reduction, including co-channel
and co-site mitigation. A key **difference** between ACN and standard
rebroadcast systems is that waveform translation takes place, the
signal being demodulated and remodulated in another waveform (and on
another frequency...

...Aerospace concerning vitreous antennas. These
allow apertures to be stacked like pancakes on substrates, the
material between them being electrically transparent to the other
layers/**transmitters,** and giving coverage from UHF through S-band.
MEMs are used to reconfigure the array electrically for the
appropriate frequency, their cantilevered electrostatic design
approach...any type of communications, be it
satellite, hand-held, or wideband. It will have a communications
network routing architecture that will be independent of the
transmission media, and will be fully adaptive in terms of quality
of service versus network conditions and traffic demands.

MOSAIC is described by David Keetley, director...

...are two requirements: what type
of service are you asking for, and what speed of service and time of
delivery or precedence – as, say, the **difference** between fire orders
or conferencing."

US006865232B1

(54) **MULTI-CARRIER TRANSMISSION SYSTEMS**

(75) Inventors: **Mikael Isaksson**, Lulea (SE); **Magnus Johansson**, Lulea (SE); **Harry Tonvall**, Lulea (SE); **Lennart Olsson**, Lulea (SE); **Tomas Stefansson**, Lulea (SE); **Hans Ohman**, Lulea (SE); **Gunnar Bahlenberg**, Lulea (SE); **Anders Isaksson**, Lulea (SE); **Goran Okvist**, Lulea (SE); **Lis-Marie Ljunggren**, Lulea (SE); **Tomas Nordstrom**, Lulea (SE); **Lars-Ake Isaksson**, Lulea (SE); **Daniel Bengtsson**, Lulea (SE); **Siwert Hakansson**, Lulea (SE); **Ye Wen**, Lulea (SE)

(73) Assignee: **STMicroelectronics N.V.**, Amsterdam (NL)

(*) Notice: Subject to any disclaimer, the term of this patent is extended or adjusted under 35 U.S.C. 154(b) by 0 days.

(56) **References Cited**

U.S. PATENT DOCUMENTS

5,400,322 A	*	3/1995	Hunt et al.	370/468
5,479,447 A	*	12/1995	Chow et al.	375/260
5,652,772 A		7/1997	Isaksson et al.	
5,867,528 A	*	2/1999	Verbueken	375/222
6,064,692 A	*	5/2000	Chow	375/219
6,072,779 A	*	6/2000	Tzannes et al.	370/252
6,370,156 B2	*	4/2002	Spruyt et al.	370/480

* cited by examiner

Primary Examiner—Betsy L. Deppe
(74) *Attorney, Agent, or Firm*—Lisa K. Jorgenson; Allen, Dyer, Doppelt, Milbrath & Gilchrist, P.A.

(57) **ABSTRACT**

A multi-carrier transmission system has a plurality of transceivers, each having a receiver and a transmitter. Data is transmitted between the transceivers by modulating the data onto a multiplicity of carrier waves in the form of multi-bit symbols, wherein each carrier wave constitutes a channel, and wherein the number of bits per symbol (the bit loading), varies between channels and, within a channel, with time, so that each channel has associated therewith a bit loading parameter. In operation, the multi-carrier system is adapted to synchronously update, at the transceivers, the bit loading parameters associated with each channel by transmission of data over a control channel, in that the control channel is established, at system start-up, on a predetermined one of the multiplicity of carrier waves whose identity is known to the transceivers, and in that the control channel is, after start-up, changed from the predetermined channel to a further channel, selected by the first transceiver on the basis of channel characteristics.

28 Claims, 19 Drawing Sheets
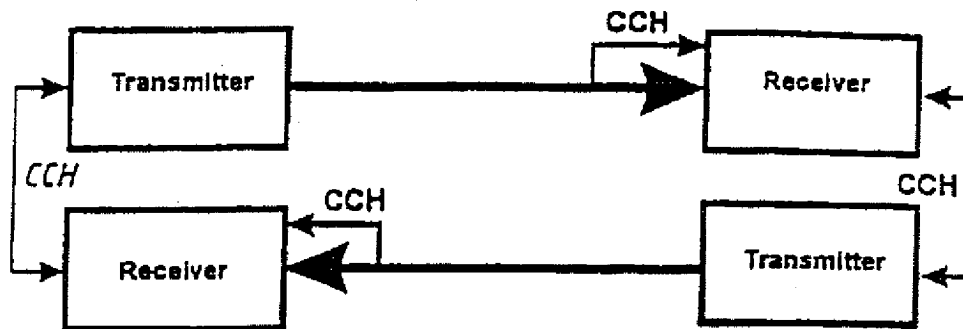
(19) **United States**

(12) **Patent Application Publication** (10) Pub. No.: US 2002/0126768 A1
ISAKSSON et al. (43) Pub. Date: Sep. 12, 2002

(54) **CONTROL CHANNELS FOR TELECOMMUNICATIONS TRANSMISSION SYSTEMS**

(76) Inventors: MIKAEL ISAKSSON, LULEA (SE); MAGNUS JOHANSSON, LULEA (SE); HARRY TONVALL, LULEA (SE); LENNART OLSSON, LULEA (SE); TOMAS STEFANSSON, LULEA (SE); HANS OHMAN, LULEA (SE); GUNNAR BAHLENBERG, LULEA (SE); ANDERS ISAKSSON, LULEA (SE); GORAN OKVIST, LULEA (SE); LIS-MARIE LJUNGGREN, LULEA (SE); TOMAS NORDSTROM, LULEA (SE); LARS-AKE ISAKSSON, LULEA (SE); DANIEL BENGTSSON, LULEA (SE); SIWERT HAKANSSON, LULEA (SE); YE WEN, LULEA (SE)

Correspondence Address:
CHRISTOPHER F. REGAN
ALLEN, DWYER, DOPPELT, MILBRATH & GILCHRIST, PA
P.O. BOX 3791
ORLANDO, FL 32802-2330 (US)

(*) Notice: This is a publication of a continued prosecution application (CPA) filed under 37 CFR 1.53(d).

(21) Appl. No.: 09/147,745

(22) PCT Filed: Sep. 1, 1997

(86) PCT No.: PCT/SE97/01458

(30) Foreign Application Priority Data

Sep. 2, 1996 (SE) 9603195-0

Publication Classification

(51) Int. Cl.^{7} H04L 5/14
(52) U.S. Cl. 375/298

(57) **ABSTRACT**

In certain types ol transmission system using nQ,₁M it may be desirable to use a control applications in multicarrier snrstems with variable bitloading it is particularly desirible that the control channel data be separable from user data when the value of n. i.e the bitloading. or constellation identifier are unknown. Binary data is transmitted using nQAM modulation. The binary data comprises both user data and cointro,l clata. This means that a control channel is superimposed on a user data channel within the same nQAM constellation. Separation of said control data is lacilitated by arranging control data points to have either unique phase, or unique amplitude, values. These unique values are not employed for user data points.

Digital receiver unit

Analog front-end

Digital transmitter unit
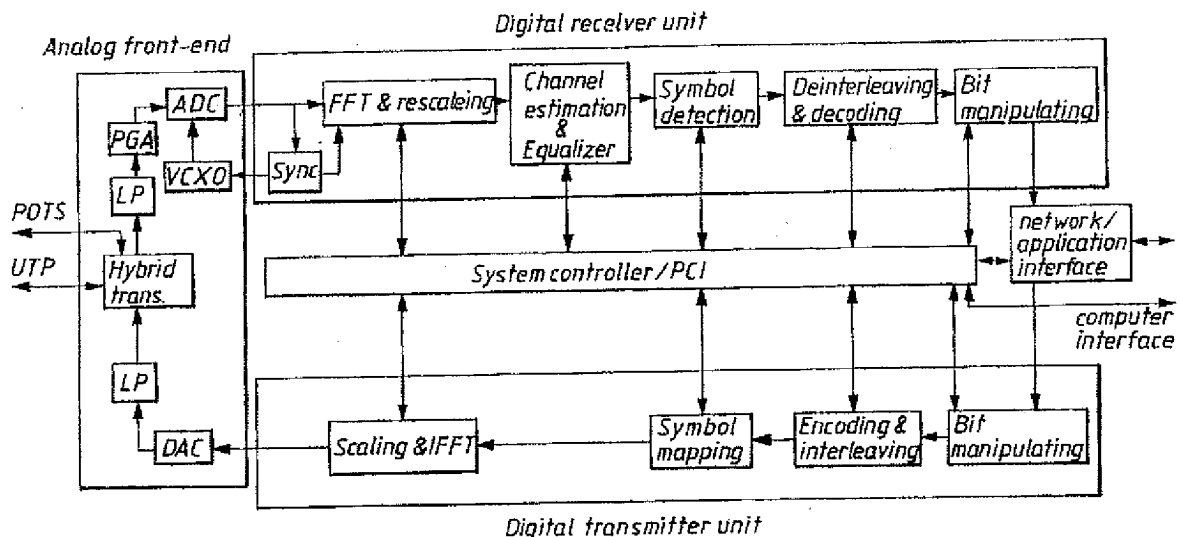
See → [0199], [0299]

(12) **United States Patent**   (10) **Patent No.:**   **US 6,538,986 B2**

Isaksson et al.   (45) **Date of Patent:**   **Mar. 25, 2003**

(54) **DATA TRANSMISSION SYSTEM AND METHOD USING NQAM CONSTELLATION WITH A CONTROL CHANNEL SUPERIMPOSED ON A USER DATA CHANNEL**

(75) Inventors: **Mikael Isaksson**, Lulea (SE); **Magnus Johansson**, Lulea (SE); **Harry Tonvall**, Lulea (SE); **Lennart Olsson**, Lulea (SE); **Tomas Stefansson**, Lulea (SE); **Hans Ohman**, Lulea (SE); **Gunnar Bahlenberg**, Lulea (SE); **Anders Isaksson**, Lulea (SE); **Goran Okvist**, Lulea (SE); **Lis-Marie Ljunggren**, Lulea (SE); **Tomas Nordstrom**, Lulea (SE); **Lars-Ake Isaksson**, Lulea (SE); **Daniel Bengtsson**, Lulea (SE); **Siwert Hakansson**, Lulea (SE); **Ye Wen**, Lulea (SE)

(73) Assignee: **STMicroelectronics N.V.**, Amsterdam (NL)

(*) Notice: Subject to any disclaimer, the term of this patent is extended or adjusted under 35 U.S.C. 154(b) by 0 days.

(21) Appl. No.: **09/147,745**

(22) PCT Filed: **Sep. 1, 1997**

(86) PCT No.: **PCT/SE97/01458**

§ 371 (c)(1),
(2), (4) Date: **Jun. 1, 1999**

(87) PCT Pub. No.: **WO98/10553**

PCT Pub. Date: **Mar. 12, 1998**

(65) **Prior Publication Data**

US 2002/0126768 A1 Sep. 12, 2002

(30) **Foreign Application Priority Data**

Sep. 2, 1996 (SE) 9603195

(51) Int. Cl.[7] H04J 11/00; H04J 3/12; H04L 23/02; H04L 5/12

(52) U.S. Cl. 370/207; 375/261; 370/527

(58) Field of Search 370/204, 206, 370/207, 208, 464, 465, 203, 498, 522, 527; 375/259, 261, 262, 295, 298, 260

(56) **References Cited**

U.S. PATENT DOCUMENTS

4,627,077 A	*	12/1986	Armstrong	....	375/261
5,022,053 A	*	6/1991	Chung et al.	....	375/265
5,105,443 A	*	4/1992	Betts et al.	....	375/265

(List continued on next page.)

FOREIGN PATENT DOCUMENTS

DE   44 35 833   5/1995

Primary Examiner—Kwang Bin Yao
Assistant Examiner—Kevin C. Harper
(74) *Attorney, Agent, or Firm*—Allen, Dyer, Doppelt, Milbrath & Gilchrist, P.A.; Lisa K. Jorgenson

(57) **ABSTRACT**

A transmission system using nQAM. A control channel is superimposed on a nQAM data channel. It is desirable to separate control channel data from user data without using a higher level protocol layer. In multi-carrier systems with variable bit-loading it is particularly desirable that the control channel data be separable from user data when the value of n, that is the bit-loading, or constellation identifier are unknown. Binary data is transmitted using nQAM modulation. The binary data includes both user data and control data. This means that a control channel is superimposed on a user data channel within the same nQAM constellation. Separation of the control data is facilitated by arranging control data points to have either a unique phase or unique amplitude values. These unique values are not employed for user data points.

15 Claims, 14 Drawing Sheets
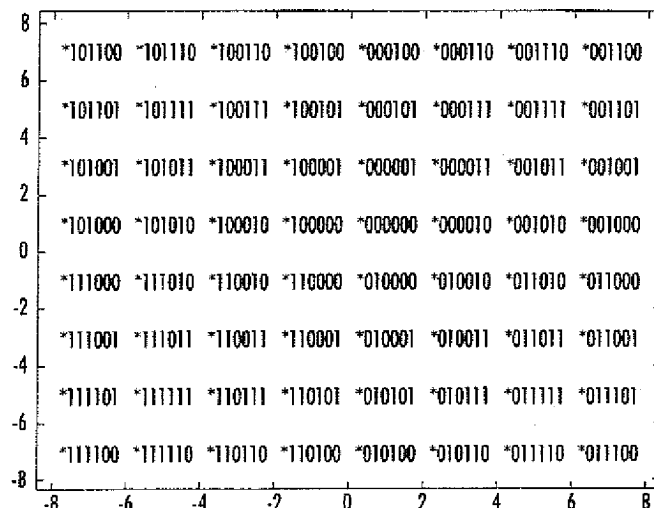
Advanced Signal Processing Algorithms for 3rd Generation Wireless Mobile Systems

THÈSE NUMÉRO 2550 (2002)

PRÉSENTÉE AU DÉPARTEMENT DE SYSTÈMES DE COMMUNICATIONS

ÉCOLE POLYTECHNIQUE FÉDÉRALE DE LAUSANNE

POUR L'OBTENTION DU GRADE DE DOCTEUR ÈS SCIENCES

PAR

Alessandro Nordio

Ingénieur en Télécommunications,
Politecnico di Torino, Italie

Composition du Jury:

Prof. Bixio Rimoldi, président du Jury
Prof. Giuseppe Caire, directeur de thèse
Prof. Sergio Benedetto, corapporteur
Prof. Pierre Comon, corapporteur
Prof. Raymond Knopp, corapporteur
Prof. Ruediger Urbanke, corapporteur

Lausanne, EPFL
March, 2002

Acknowledgments

First of all, I would like to thank my advisor, Prof. Giuseppe Caire for the support and the advices he gave me during my Ph.D.

I'm also grateful to the members of my defense committee, Prof. Sergio Benedetto, Prof. Pierre Comon, Prof. Raymond Knopp, Prof. Bixio Rimoldi, and Prof. Ruediger Urbanke for their contributions with valuable remarks to the improvement of the thesis.

Prof. Piere Humblet and Prof. Raymond Knopp have my gratitude for their precious suggestions and constructive discussions.

A big thanks goes to Giuseppe Montalbano, for his contributions, help and constant encouragement during these years.

Thanks for the friendship to my officemates and the people I met at Eurecom Institute: Max, Daniela, Chris, Houda, Alain, Dominique, Jussi, Cristina(Chiquita), Masato, Albert(Tio), Marco, Aawatif and many others.

A special thanks goes to my *colocatrice*, Daniela, for the friendship and help she gave me.

I would like also to thank my family, and in particular Cristina for their every day support and encouragement.

March 2002

Advanced Signal Processing Algorithms for 3rd Generation Wireless Mobile Systems

Alessandro Nordio

Sintesi

Motivata dall'interesse mondiale per i sistemi cellulari di terza generazione, questa tesi affronta il problema di migliorare l'affidabilità del livello fisico dei ricevitori di terza generazione che utilizzano la tecnica W-CDMA, proponendo algoritmi semplici e a bassa complessità adatti ad essere implementati su sistemi esistenti. Il lavoro è stato sviluppato nell'ambito di una collaborazione tra Eurécom e EPFL il cui obiettivo è quello di realizzare una piattaforma *Software Radio* capace di convalidare algoritmi avanzati per il trattamento del segnale. La ricerca si focalizza su molti aspetti del livello fisico, tra cui sincronizzazione, *multi-user detection*, e il progetto di algoritmi per l'interfaccia tra il livello fisico e l'hardware.

Per quanto riguarda la sincronizzatione consideriamo l'acquisizione iniziale della temporizzazione per i sistemi DS-CDMA, considerando canali affetti da fading e multipath. Nel nostro modello la Stazione Base diffonde un segnale di sincronizzazione composto da un gruppo di chip modulati, ripetuti periodicamente e separati da lunghi intervalli di tempo. Dopo opportune ipotesi semplificative deriviamo lo stimatore a massima verosimiglianza della temporizzazione risolvendo un problema di massimizzazione vincolata. Il nostro stimatore a massima verosimiglianza ha una complessità proporzionale al numero di campioni di segnale trattati. Per mezzo di simulazioni le prestazioni dello stimatore a massima verosimiglianza vengono poi confrontate con quelle fornite da altri stimatori di temporizzazione proposti in letteratura. Lo stimatore proposto fornisce buone prestazioni indipendentemente dal tipo di canale considerato. In più è poco sensibile alle variazioni dello spettro Doppler del canale e fornisce buone prestazioni sia in condizioni di fading veloce che di fading lento.

In modo da aumentare la capacità del sistema, proponiamo successivamente un semplice ricevitore iterativo multiutente a cancellazione parallela di interferenza con equalizzazione retroazionata per sistemi CDMA. Nel nostro ricevitore, una stima del segnale interferente (interferenza da accesso multiplo e interferenxa inter simbolica) è ottenuto pesando le decisioni hard prodotte da decodificatori di Viterbi.

La stima dell'interferenza è poi sottratta dal segnale ricevuto in modo da migliorare la decodifica nell'iterazione successiva. Utilizzando un'analisi asintotica delle prestazioni per sistemi CDMA con spreading casuale, ottimizziamo i pesi della retroazione ad ogni iterazione. Poi consideriamo due effetti (tra loro correlati) che limitano le prestazioni del ricevitore: la polarizzazione dell'interferenza residua e l'effetto *ping-pong*. Mostriamo che l'algoritmo proposto può essere migliorato compensando la polarizzazione nel calcolo dei pesi della retroazione e proponiamo una modifica dell'algoritmo base in modo da evitare effetti *ping-pong*. Tale modifica permette inoltre di ottenere una più alta capacità del sistema e una più veloce convergenza alle prestazioni del singolo utente. L'algoritmo proposto è stato convalidato, tramite simulazioni, in un ambiente compatibile con le specifiche UMTS-TDD, includendo canali selettivi in frequenza, fading, utenti asincroni e controllo di potenza. Per tali applicazioni i decodificatori SISO (implementati ad esempio con l'algoritmo BCJR) non

sono dunque necessari per ottenere efficienze spettrali elevate, e, nella maggior parte dei casi, semplici decodificatori di Viterbi sono sufficienti.

In questa tesi presentiamo poi algoritmi a bassa complesssità per l'interfaccia tra il livello fisico e l'hardware adatti ad essere implementati su terminali *Software Radio*. Gli algoritmi proposti rendono la frequenza di campionamento indipendente dalla frequenza di simbolo e utilizzano la tecnica del campionamento a frequenza intermedia per la conversione analogico-digitale e digitale-analogico. Come applicazione particolare valutiamo l'effetto della distorsione introdotta da tali algoritmi sulla stima di canale, in un ambiente UMTS-TDD.

Descriviamo infine l'architettura della piattaforma *Software Radio* sviluppata ad Eurécom e capace di fornire comunicazioni in tempo reale. La piattaforma è attualmente utilizzata per l'implementazione di protocolli e algortimi di trattamento del segnale di terza generazione come UMTS e CDMA2000. Viene fornita una descrizione dell'hardware con esempi di implementazione software sia su DSP ad alte prestazioni che su microprocessori standard.

Advanced Signal Processing Algorithms for 3rd Generation Wireless Mobile Systems

Alessandro Nordio

Abstract

Motivated by the worldwide activity around third generation mobile communication systems, this thesis addresses the problem of improving the physical layer reliability of W-CDMA third generation transceivers by designing simple and low complexity algorithms suited to be implemented on a real system. The work was developed in a framework of a joint project between Eurécom and EPFL whose objective is to design a real-time Software Defined Radio platform able to validate advanced signal processing algorithms.

The research focuses on several aspects of the physical layer such as synchronization, multi-user detection, and design of the front-end signal processing.

About the synchronization we consider initial timing acquisition in DS-CDMA when propagation is affected by multipath and fading and where the Base Station broadcasts a synchronization pilot signal in the form of bursts of modulated chips transmitted periodically and separated by long silent intervals. Subject to certain simplifying assumptions we derive the Maximum Likelihood (ML) estimator by solving a constrained maximization problem. Our ML timing estimator has constant complexity per observation sample. The relation to other estimation methods is addressed, and performance comparisons are provided by simulation. The proposed estimator yields good performance independently of the multipath-intensity profile of the channel, provided that the delay spread is not larger than a given maximum spread. Moreover, our estimator is fairly robust to the mismatch in the fading Doppler spectrum and provides good performance for both fast and slow fading.

In order to increase the system capacity we propose a low complexity multiuser joint Parallel Interference Cancellation decoder and Turbo Decision Feedback Equalizer for CDMA. In our scheme, an estimate of the interference signal (both MAI and ISI) is formed by weighting the hard decisions produced by conventional (i.e., hard-output) Viterbi decoders. The estimated interference is subtracted from the received signal in order to improve decoding in the next iteration. By using asymptotic performance analysis of random-spreading CDMA, we optimize the feedback weights at each iteration. Then, we consider two (mutually related) performance limitation factors: the bias of residual interference and the *ping-pong* effect. We show that the performance of the proposed algorithm can be improved by compensating for the bias in the weight calculation, and we propose a modification of the basic PIC algorithm, which prevents the ping-pong effect and allows higher channel load and/or faster convergence to the single-user performance. The proposed algorithm is validated through computer simulation in an environment fully compliant with the specifications of the time-division duplex mode of 3rd generation systems, contemplating a combination of TDMA and CDMA and including frequency-selective fading channels, user asynchronism, and power control. For such application, Soft-Input Soft-Output decoders (e.g.implemented by the forward-backward BCJR algorithm) are not needed to attain very high spectral efficiency, and simple conventional Viterbi decoding suffices for most practical settings.

Moreover we present low-complexity algorithms for transmitter and receiver front-end suited to the implementation of Software Defined radio terminals. The proposed algorithms make the processing sampling frequency independent of the symbol rate of the digitally modulated signal and use the "IF-sampling" technique for D/A and A/D conversion. As a case-study, we consider a training-based joint multiuser channel estimation and we show that our front-end algorithms work nicely when coupled with an efficient FFT-based joint channel estimator.

Eventually we describe a software radio architecture developed for providing real-time wide-band radio communication capabilities in a form attractive for advanced 3G system research. It is currently being used to implement signaling methods and protocol similar, but not limited to, evolving 3G radio standards (e.g. UMTS, CDMA2000). An overview of the hardware system is provided along with example software implementation on both high performance DSP systems and conventional microprocessors.

Contents

List of Figures

List of Tables

Acronyms

3GPP	3rd Generation Partnership Project
A/D	Analog to Digital
BER	Bit Error Rate
BPSK	Binary Phase Shift Keying
BS	Base Station
CDF	Cumulative Density Function
CDMA	Code Division Multiple Access
CPU	Central Processing Unit
DAQ	Data Acquisition Card
DFE	Decision Feedback Equalization or Decision Feedback Equalizer
DFT	Discrete time Fourier Transform
DS-CDMA	Direct Sequence - CDMA
DSP	Digital Signal Processor or Digital Signal Processing
D/A	Digital to Analog
EPFL	École Politechnique Fédérale de Lausanne
ETSI	European Telecommunications Standards Institute
FDD	Frequency Division Duplex
FIR	Finite Impulse Response
FFT	Fast Fourier Transform
FPGA	Field Programmable Gate Array
GPRS	General Packet Radio Service
GSM	Global System for Mobile communications
IC	Interference Canceler
IDFT	Inverse Discrete Fourier Transform
IF	Intermediate Frequency
i.i.d.	Independent and identically distributed
ISI	Inter Symbol Interference
JML	Joint Maximum Likelihood
KKT	Karush-Kuhn-Tucker
LO	Local Oscillator
LS	Least Squares
LVDS	Low-Voltage Differential Signaling
MAI	Multiple Access Interference
MF	Matched Filter or Matched Filtering
MIP	Multipath Intensity Profile

ML	Maximum Likelihood
MMX	Multi-Media eXtension
MT	Mobile Terminal
MUD	Multi User Detection
PC	Personal Computer
PCI	Peripheral Component Interconnect
PIC	Parallel Interference Cancellation
PN	Pseudo Noise
QPSK	Quaternary Phase Shift Keying
RF	Radio Frequency
RHS	Right Hand Side
RMSE	Root Mean Square Error
SDR	Software Defined Radio
SIC	Serial Interference Cancellation
SIMD	Single Instruction Multiple Data
SINR	Signal to Interference plus Noise Ratio
SISO	Soft Input Soft Output
TDD	Time Division Duplex
UMTS	Universal Mobile Telecommunication System
UTRA	UMTS Terrestrial Radio Access
VHDL	Very High Speed Integrated Circuit Hardware Description Language
WAP	Wireless Application Protocol
W-CDMA	Wideband Code Division Multiple Access
w.r.t	with respect to
WSS-US	Wide Sense Stationary Uncorrelated Scattering

List of Symbols

a	Constant scalar
$\mathbf{a}$	Constant vector
$\mathbf{A}$	Constant matrix
a	Variable scalar
$\boldsymbol{a}$	Variable vector
$\boldsymbol{A}$	Variable matrix
$a(t)$	Continuous-time function of the variable t
$a[n]$	n^{th} element of the vector $\boldsymbol{a}$
$A(f)$	Discrete Fourier transform of the vector $\boldsymbol{a}$
$\delta(t)$	Dirac delta in the variable t
$\delta_{i,j}$	Kronecker delta
$\delta[n]$	Discrete time delta
e	Neper constant
$\mathbf{I}$	Identity matrix
$\mathbf{I}_N$	$N \times N$ Identity matrix
j	Imaginary unit
$(\cdot)^*$	Complex conjugate operator
$(\cdot)^{\text{T}}$	Transpose operator
$(\cdot)^{\text{H}}$	Hermitian operator
$\star$	Convolution operator
$\mathrm{E}[\cdot]$	Expectation operator
$1\{\cdot\}$	Indicator function
$\otimes$	Kronecker product
$[x]_+$	Positive part of x
$\mathcal{N}(m, v)$	Gaussian distribution with mean m and variance v
$\mathcal{N}_{\mathbb{C}}(m, v)$	Gaussian complex distribution with mean m and variance v
$\mathcal{A} \setminus \mathcal{B}$	Complement of the set $\mathcal{B}$ with respect to the set $\mathcal{A}$

Chapter 1

Introduction

1.1 Historical perspective

The first revolution in mobile telephony can be identified with the migration from analog systems (so called first generation (1G), such as TACS and AMPS [1]) to digital systems (second generation (2G), such as GSM, IS54, IS95 [1]). The existing second generation (2G) digital mobile standards offer bit rates up to 10 kbit/s and have experienced phenomenal growth since their launch. Now they are rapidly evolving towards the so called 2.5G systems including, for example, the GPRS (General Packed Radio Service) which offers air-interface transfer rates up to 115 kbit/s. GPRS is a standard oriented to packed data communications developed by the European Telecommunications Standards Institute (ETSI) and represents an essential step towards third generation (3G) systems such as the Universal Mobile Telecommunication System (UMTS) currently under development and soon available on the market. UMTS will provide both traditional telecommunication services and new Internet-based services over the same network with higher bit rates (from 384 kbit/s up to 2 Mbit/s) and will use radio frequencies around 2 GHz. Two main modes are currently considered for the UMTS standard: Time Division Duplex (TDD) and Frequency Division Duplex (FDD). The FDD mode is intended for applications in public macro and micro cell environments with wide area coverage and typical data transfer rates of up to 384 kbit/s. The TDD mode provides advantages for micro and pico cells and is especially suitable for environments with high traffic density (e.g. business areas, city centers, airports) and indoor coverage where large data rates are required.

 In order to provide this high performance, 3G systems need an improved physical layer. A huge amount of work has already been dedicated to the design of third generation transceivers, including for example the RAKE receiver, Multi-User Detec-

tion (MUD), multiple antennas, joint adaptive spatio-temporal signal processing and modern coding techniques such as "Turbo Codes" at both transmitter and receiver. Nevertheless, most algorithms are limited to a theoretical stage (a-part from few cases such as the RAKE receiver and Turbo Codes) and their practical feasibility remains a major issue.

At present, most algorithms are tested only through computer simulation which often introduces a certain simplifications to model a real system. On the other hand, studies done by the main telecommunications companies about the feasibility and on software implementation of these solutions are not disclosed to the open literature.

In this context in 1999 the Eurécom Institute and EPFL (École Politechnique Fédérale de Lausanne) started a joint project whose objective is to study and implement a real-time Software Defined Radio (SDR) platform able to provide measurements in real transmission conditions and aiming at validating advanced mobile communication algorithms.

Motivated by this project, the work presented in this thesis focuses on the analysis and design of a Wideband Code Division Multiple Access (W-CDMA) SDR platform, an architecture characterized by relatively few integrated circuits or hardware components except for some high performance Digital Signal Processors (DSPs). The platform has been initially targeted for the UMTS-TDD standard although other standards could be implemented. In other words, the UMTD-TDD standard has been considered as a reference for the research developed in these years for the platform project. The aim was to improve the solutions proposed by the norm with more efficient and reliable algorithms, which concern many aspects of the transceiver physical layer signal processing chain. In particular, the work of this thesis focuses on the following aspects:

- Design of the transceiver front-end signal processing;

- Synchronization;

- Multi-user detection;

Some considerations that motivated the work on these items are shortly discussed in the rest of this chapter.

1.2   Front-end signal processing and the Software Radio concept

In the future the proliferation of wireless mobile communications systems will require radio terminals to be able to reconfigure themselves to handle several different standards. These terminals represent a really attractive solution to provide universal connectivity to the users and must be designed by using Software Defined Radio techniques. The basic idea of SDR is that some parameters characteristic of the transmission system are chosen and programmed in software instead of using analog or digital dedicated hardware. Software mainly means generality, flexibility, and robustness, properties that nowadays have extreme relevance in the mobile communication context. SDR is a very broad term involving several levels in the protocol stack (e.g., see

[2], [3], [4] and references therein). At the physical layer, SDR requires signal processing algorithms suited to implementation on a programmable CPU. The goal is to move the software toward the antenna, performing operations like *channel selection* [5, 6], *up- and down-conversion* [7], synchronization and detection in the all-digital domain, by using high performance Digital Signal Processors (DSPs).

In a modern transceiver, for example, the digital baseband signal produced by the transmitter is sent to the A/D converter, up-converted to Radio Frequency (RF) and then sent to the antenna. At the receiver side the RF signal incoming from the antenna is downconverted to baseband and sampled before being processed. The *up* and *down-conversion* operations are performed in hardware, passing through an Intermediate Frequency (IF) usually ranging from tens to hundreds of MHz. The base-band signal processing, instead, is constrained to certain parameters (signal bandwidth, chip or symbol rate) imposed by the implemented standard. In order to meet these constraints the hardware is created "ad hoc", with the disadvantage of not being able to support other standards characterized, by different parameters.

The advantage of Software Radio instead, is that some parameters characteristic of the transmission system, such as the IF, the modulation scheme, the IF to baseband conversion, the baseband processing and other features are chosen and programmed in software. This solution enables the same hardware architecture to support many standards providing a software interface between the baseband processing and the hardware constraints. In practice, since the Intermediate Frequency is a parameter dependent on the analog modulation devices, in a SDR transceiver the software governing the system is supposed to process the transmitter baseband signal in order to match it to the IF. This processing mainly consists in applying re-sampling techniques at both transmitter and receiver ends. In general, resamplers should be designed in order to allow resampling by non rational factors.

In fact, a part of the work presented in this thesis concerns the design of such re-sampling techniques. Many front-end algorithms are proposed and compared, with particular attention to the computational complexity. For the transmitter side we discuss an efficient generation of an IF analog signal from the baseband digital signal, while, at the receiver side, we propose efficients methods to generate a digital baseband signal from the IF analog signal.

The proposed resampling techniques for the front-end signal processing, however, have an impact on the performance of the physical layer signal processing functions as for example channel estimation and data detection. This impact mainly consists of a degradation of the receiver performance in terms, for example, of Signal to Interference plus Noise Ratio (SINR) and Bit Error Rate (BER). For this reason the proposed techniques have been chosen and validated in a realistic UMTS-TDD system by finding a trade-off between degradation and computational cost.

1.3 Synchronization

Signal processing requires, in general, perfect synchronization between the transmitter and the receiver clocks. The synchronization is acquired when the receiver is switched on and then tracked while transmitting and receiving data. In UMTS-TDD, in order to facilitate the acquisition of the synchronization, a particular downlink signal is

broadcasted by the Base Station (BS). In order to assure reliable communications, the synchronism must be reliably and rapidly acquired. A good synchronization algorithm has a dramatic impact on the synchronization time, especially when the radio channel introduces severe degradations to the signal. Classical systems use simple algorithms although, in general, when the channel is affected by multipath and fading they show quite poor performance.

In this thesis we present a Maximum Likelihood (ML) approach to the synchronization problem when the BS signal is corrupted by the presence of a multipath fading channel. The derived ML detector provides reliable timing estimations and, at the same time, it jointly estimates the channel Multipath Intensity Profile (MIP). This approach leads to an algorithm providing better performance compared to classical synchronization systems.

1.4   Multi user detection

In a typical CDMA system several users access simultaneously the same radio channel. This situation is common in a CDMA systems like the UMTS-TDD where the received signal can contain the superposition of several user signals. In such systems the Multiple Access Interference (MAI), caused by the users accessing the radio channel at the same time depends on the correlation between their spreading sequences. The solution provided by the UMTS-TDD norm consist of assigning orthogonal sequences to the users in order to nullify the MAI and by simple matched filtering the received signal using filters matched to the spreading sequences of each user. This idea, however, finds its limitations in a non perfect synchronization between users which destroys the orthogonality of the sequences. In any case, even with good synchronization and tracking algorithms, asynchronism between users is introduced by the propagation delays and orthogonality is destroyed by the fading multipath channels. In order to reduce the MAI effect, Multi User Detection [8] techniques seem very promising, providing outstanding performance, superior to the conventional Single User Detectors and allowing very high channel loads. Multi User Detection, traditionally regarded as an ensemble of techniques to detect uncoded data in a multiple access waveform channel, are the subject of intensive studies in the recent years (see for example [8] and references therein). The proposed solutions, however, often require computational complexities not affordable by the available technology so that their implementation in the communications systems under development is still not considered, at least in the first system release. On the other hand, Information Theory shows that much larger channel loads can be achieved provided that a *non-linear* multiuser joint detector and decoder is employed [9, 10]. This may range from the impractically complex optimal joint decoder to practically appealing successive interference cancellation approaches (stripping) [11, 12] where decoded and re-encoded users are subtracted from the received signal.

In this thesis, with the aim of providing simple and practical solutions for the implementation on the SDR platform, a Chapter is dedicated to the development of a low-complexity Iterative Parallel Interference Cancellation Multiuser Detection algorithm, that, at the same time, performs joint channel decoding and Decision Feedback Equalization. This algorithm can be easily implemented and used for real time appli-

cations with the available technology.

1.5 Thesis outline and contributions

The thesis is organized as follows: Chapter 2 gives an overview on the UMTS-TDD standard main features introducing the general system model of the transmitter and the receiver along with part of the notation used through this work.

Chapter 3 presents the derivation of the Joint ML timing estimator for the UMTS-TDD mode in the presence of multipath fading channels. Comparisons with the performance of other timing estimators are provided. The results shown in this Chapter have been published in the following papers:

- G. Caire, P. A. Humblet, G. Montalbano, and A. Nordio,"Slot-timing maximum likelihood estimation with bursty pilot signals for DS-CDMA in multipath fading channels," Proc. IEEE Globecom 2000, S. Francisco, CA, November 2000.

- G. Caire, P. A. Humblet, G. Montalbano, and A. Nordio,"Initial synchronization in DS-CDMA via bursty pilot signals," to appear on IEEE Trans. on Communications, 2002

Chapter 4 develops a simple and high performance multi user detector with joint decoding and decision feedback equalization. Related publications are

- A. Nordio, G. Caire, and M.Hernandez, "Design and Performance of a Low-Complexity Iterative Multiuser Joint Decoder Based on Viterbi Decoding and Parallel Interference Cancellation," Proceedings of ICC 2002, NewYork, May 2002.

- A. Nordio, G. Caire, and M.Hernandez, "Low-Complexity Turbo Equalization and Multiuser Decoding for TDMA-CDMA" submitted to IEEE Transactions on Wireless Communications, February 2002.

Chapter 5 addresses some low complexity algorithms for a SDR transceiver front-end. Results, show that the proposed techniques represents a valid solutions for implementation. The work presented in this Chapter has been partially published in

- G. Caire, P. A. Humblet, G. Montalbano, and A. Nordio,"Transmission and reception front-end architectures for software radio," Proc. ECWT 2000, Paris, France, September 2000.

The architecture of the W-CDMA SDR platform developed at Eurécom Institute is presented in Chapter 6. A description of the hardware set-up and of the employed signal processing algorithms is also given. Parts of this Chapter are contained in the following publications

- C. Bonnet, G. Caire, A. Enout, P. A. Humblet, G. Montalbano, A. Nordio, and D. Nussbaum,"A software radio platform for new generation of wireless communication systems," Proc. 12th Tyrrhenian Intern. Workshop on Digital Comm.: Software radio technologies and services, Porto Ferraio, Italy, September 2000.

- C. Bonnet, G. Caire, A. Enout, P. A. Humblet, G. Montalbano, A. Nordio, and D. Nussbaum,"A software radio testbed for UMTS TDD systems," Proc. of IST Mobile Communications Summit 2000, October 2000.

- C. Bonnet, G. Caire, A. Enout, P. A. Humblet, G. Montalbano, A. Nordio, and D. Nussbaum,"Open Software Radio Platform for New Generations of Mobile Systems," Proc. of 3rd European DSP Education and Research Conf., Paris, France, September 2000.

- C. Bonnet, G. Caire, A. Enout, P. A. Humblet, G. Montalbano, A. Nordio, D. Nussbaum, T.Höhne, R. Knopp, B. Rimoldi, "An open software-radio architecture supporting advanced 3G+ systems," Annales des télécommunications, tome 56, n.5-6, Paris, France, Mai-Juin 2001.

Finally in Chapter 7 the general conclusions of this thesis are pointed out.

Chapter 2

A system model based on the

UMTS-TDD physical layer

The Universal Mobile Communications System [13] consists of a set of standards and new technologies conceived a few years ago and it is still under development. The aim of this standard is to provide to the users high-quality wireless multimedia broad-band communications, by extending todays mobile technologies (like GSM, WAP, GPRS [1]). This choice was motivated by the increasing need of multimedia appli-cations usually requiring high data rates such as pictures, graphics, video communi-cations, video on demand, mobile Internet access and other wide-band information as well as voice and data.

The development of UMTS has the support of many major telecommunications operators and manufacturers worldwide. Several organizations take care of the UMTS standardization as, for example, the 3rd Generation Partnership Project (3GPP) which is a collaboration agreement that brings together a number of telecommunications stan-dards bodies like the European Telecommunications Standards Institute. One of the 3GPP scopes is to produce globally applicable technical specifications and technical reports for 3rd generation mobile systems, including a new radio interface known as UTRA (UMTS Terrestrial Radio Access) based on the W-CDMA technology. Two main modes are considered for the UTRA: the Frequency Division Duplex [14] mode and the Time Division Duplex [15] mode. Although the UMTS standard considers for these modes several levels of the protocol stack, the research developed in this thesis only focuses on the UMTS-TDD physical layer, considering, in particular, the standard proposed by 3GPP.

A short overview of the UMTS-TDD physical layer is presented in the following. Later, inspired by its main characteristics, we describe the transmitter and receiver
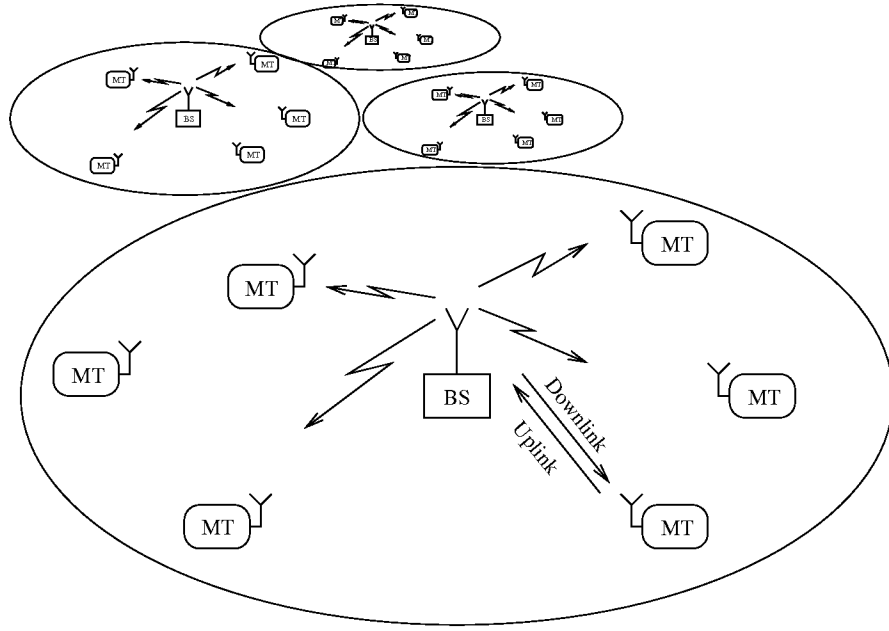
Figure 2.1: General structure of a cellular wireless system

models used in this thesis. The interested reader can find more details on the UMTS-TDD 3GPP standard in [13].

2.1   Overview on the UMTS-TDD physical layer

2.1.1   The multiple access strategy

UMTS is a cellular system schematically represented in Figure 2.1. In the Figure, a cell is the region where a Mobile Terminal (MT) can access the network through a certain Base Station. Usually communications between MTs and BS are bi-directional. In the literature the words *uplink* and *downlink* [1] refer to the communication links going from the MTs to the BS and from the BS to the MTs respectively.

The BSs, however, are more complicate than the MTs because they organize the flows of information transmitted and received by the MTs according to rules, scheduling, and algorithms defined in the supported protocols. Communication protocols that drive these systems are organized in layers and, in particular, the *physical layer* or layer 1 generates the radio signals to be transmitted and applies suitable signal processing algorithms to the received signals in order to assure reliable communications. Like for other digital systems, the UMTS baseband processing is performed in the all digital domain while the analog devices only take care of up- and down-conversion operations, acting from baseband or an Intermediate Frequency to the Radio Frequency. The UMTS-TDD layer 1 acts from the bit level to the Digital to Analog (D/A) or Analog to Digital (A/D) converters. It includes signal processing algorithms as synchronization, channel estimation, data detection, channel encoding and decoding, modulation, demodulation, and it implements the multiple access technique used to regulate
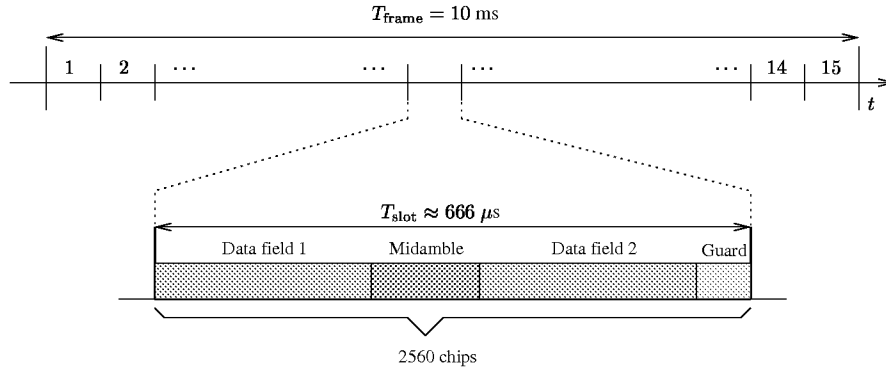
Figure 2.2: The UMTS-TDD slot structure

the access of the transceivers to the radio resources.

The UMTS 3GPP standard proposes different multiple access techniques for the FDD and TDD modes. The standard for TDD physical layer [13] recommends a combination of Time Division Multiple Access (TDMA) and Direct Sequence Code Division Multiple Access (DS-CDMA) techniques [1].

On the TDMA side, time is organized as a concatenation of frames lasting $T_{\text{frame}} = 10$ ms where each frame is divided in 15 *slots* of length $T_{\text{slot}} \approx 666 \,\mu\text{s}$. The MTs and the BS are allowed to transmit only in certain slots of the frame, called uplink and downlink slots respectively. These are dynamically assigned according to certain requirements as for example the uplink and downlink data rates, quality of service, and cell-load.

The slot allocation strategy includes the possibility for more than one MT to transmit at the same time and in the same slot, causing Multiple Access Interference (MAI) between MT signals at the BS receiver. By using CDMA techniques, interfering signals are separated by means of spreading sequences.

2.1.2 Spreading and scrambling

In the UMTS-TDD mode, a spreading sequence is a vector of chips belonging to the QPSK [1] constellation. The spreading sequence length, L, is also called *spreading factor*. In the standard, the chip time, T_c, is defined such that $T_{\text{slot}} = 2560\,T_c$, that is, 2560 chips take place in a slot, yielding a chip-rate $R_c = 1/T_c = 3.84$ Mchips/s. A simplified slot structure is depicted in Figure 2.2. Spread data and control information occupy only two parts of the slot, in the Figure labeled "Data Field 1" and "Data Field 2", respectively. The field "Midamble" is used for channel estimation purposes and the guard time "Guard" is a silent interval separating the slots.

The standard employs Walsh-Hadamard [16] spreading sequences with spreading factors of powers of two and in the range $1 \leq L \leq 16$. Moreover the system can assign to the users different spreading factors in order to provide different data rates. The Walsh-Hadamard spreading sequences of length $L = 2^l$, for a positive integer l, are the rows of the $L \times L$ Walsh-Hadamard matrix $\mathbf{H}_L$ generated by the following

recursive procedure:

$$\mathbf{H}_{2L} = \begin{bmatrix} \mathbf{H}_L & \mathbf{H}_L \\ \mathbf{H}_L & -\mathbf{H}_L \end{bmatrix} \tag{2.1}$$

with initial condition

$$\mathbf{H}_1 = 1. \tag{2.2}$$

The cross-correlation matrix of the Walsh-Hadamard sequences is proportional to the identity matrix,

$$\mathbf{R_{H_L}} = \mathbf{H}_L^{\mathrm{T}} \mathbf{H}_L = L\mathbf{I}_L. \tag{2.3}$$

Since the MAI is proportional to the correlation between spreading sequences, the advantage of using Walsh-Hadamard sequences is to nullify the MAI at the receiver. We have to point out that this consideration is valid only in the case of perfectly synchronous users. When users are asynchronous and their relative offsets contain a fraction of T_c, (2.3) no longer holds. Moreover, since there are only L orthogonal sequences of length L, this choice provides a maximum load of 1 user per chip. In a general case, if the multiple access interference is not negligible as for example when using non-orthogonal spreading sequences or with Walsh-Hadamard sequences and asynchronous users, the MAI can be reduced by employing Multi User Detection (MUD) techniques [8] for the moment still not considered by the norm. This issue is broadly discussed in Chapter 4.

The MAI, however, is not the only source of interference at the receiver. In fact a complete model should take into account also the cell-to-cell interference (i.e. the interference caused by transceivers of an adjacent cell). In particular in the UMTS-TDD mode, MTs of adjacent cells, can be assigned to the same spreading sequences, causing cell-to-cell interference between data signals. In order to reduce this effect cells are characterized by *scrambling sequences* that multiply the transmitted chips. The scrambling sequences are initially known by the BS and then acquired by the MTs during the synchronization process.

2.1.3   Synchronization

The frame and slot timings depend on the BS clock which is used as time reference by the MTs. This means that every MT has to acquire the BS time reference before starting communication in the cell. This process of timing acquisition is called *synchronization*.

In the UMTS-TDD mode synchronization is performed in two steps, called primary and secondary synchronization respectively. These are facilitated by the BS which broadcasts to the MTs some synchronization signals located in a known position of the frame. For the primary synchronization the BS broadcasts in a downlink slot a burst made of 256 modulated chips,

$$\boldsymbol{s}_{\mathrm{ps}} = \Big[s_{\mathrm{ps}}[0], \dots, s_{\mathrm{ps}}[255] \Big]$$

separated by long silent intervals and repeated indefinitely at a known rate. The primary synchronization sequence, $\boldsymbol{s}_{\mathrm{ps}}$, is common to all the cells and is known by the MTs. When a MT is switched on, it first detects the presence and the timing of the primary synchronization.
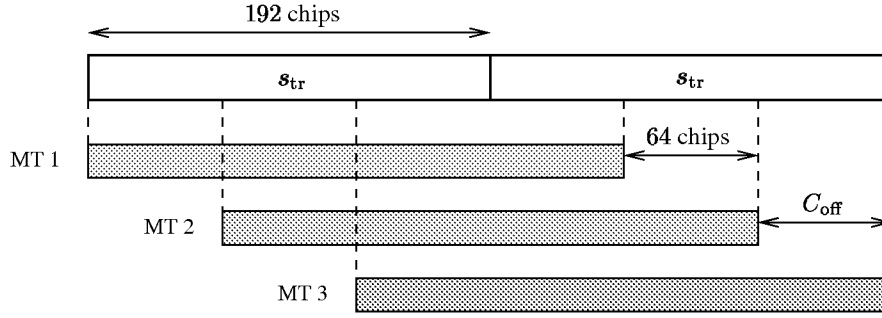
Figure 2.3: Generation of training sequences for the UMTS-TDD "Midamble type 2"

The detection of the frame timing is facilitated by the structure of the primary synchronization sequence, designed in order to have a very peaky aperiodic autocorrelation function. Moreover the sequence s_{ps} is a hierarchical sequence made of two base sequences of length 16 chips, s_{ps_1} and s_{ps_2}. The primary synchronization sequence is then given by

$$s_{\mathrm{ps}} = s_{\mathrm{ps}_1} \otimes s_{\mathrm{ps}_2} \tag{2.4}$$

where ($\otimes$ denotes Kronecker product [17]) and where

$$s_{\mathrm{ps}_1} = [-1,-1,-1,-1,-1,-1,+1,+1,-1,+1,-1,+1,-1,+1,+1,-1]$$
$$s_{\mathrm{ps}_2} = [-1,-1,-1,+1,+1,-1,+1,+1,-1,-1,-1,+1,-1,+1,-1,-1]$$

This feature in the design of the sequence is useful to reduce the complexity of the synchronization algorithm as shown in Chapter 6.

When the frame time reference of at least one BS is successfully acquired, the MT searches for some secondary synchronization signal broadcasted by the BS and carrying additional information that characterizes the BS (e.g. the slot timing and the scrambling sequence index). Once all these parameters have been identified, the MT can set up a connection with the BS. For more information on the UMTS-TDD synchronization procedures refer to [14, 15].

2.1.4   Midamble and channel estimation

In wireless communication the transmitted signals are degraded by the radio channel that must be correctly estimated at the receiver in order to improve the reliability of the communications. In the literature a huge amount of work has been published on channel estimation, and many techniques have been proposed.

The UMTS-TDD standard defines a training sequence based channel estimation, where a sequence of known modulated chips is sent by the transmitter in the field "Midamble" of the slot (see Figure 2.2). In a given slot the training sequence chips are built from a common periodic base sequence,

$$s_{\mathrm{t}} = \left[s_{\mathrm{t}}[0], s_{\mathrm{t}}[1], \ldots, s_{\mathrm{t}}[P_{\mathrm{tr}}] - 1] \right]^{\mathrm{T}}$$

of period P_{tr} by adding a cyclic extension of length C_{ext}, providing a total midamble length of $P_{\mathrm{tr}} + C_{\mathrm{ext}}$ chips. In an uplink slot, for example, the MTs allowed to transmit

Table 2.1: UMTS-TDD midamble parameters

	P_{tr}	C_{ext}	C_{off}	U
Midamble 1	456	56	57	8
Midamble 2	192	64	64	3

build their training sequences using a cyclic shift of s_t by an integer multiple of C_{off} as shown in Figure 2.3. This technique that allows a joint estimation of all the channels is described in [18], [19], and with some modifications in [20], and references therein. Usually P_{tr} is an integer multiple of C_{off} such that the ratio $P_{tr}/C_{off} = U$ indicates the maximum number of channels that the system can jointly estimate; C_{off} also represents the maximum length of the channel impulse response that can be estimated.

The TDD standard defines two midambles of sizes 512 and 256 chips which parameters are summarized in the Table 2.1 and allowing the joint channel estimation of $U = 8$ and $U = 3$ users respectively. An example of midamble generation is given in Figure 2.3. More details on the channel estimation signal processing for the UMTS-TDD mode are given in Chapter 6.

2.1.5   Pulse shaping filter

The last item discussed in this short overview of the UMTS-TDD physical layer is the transmission filter which shapes the spectrum of the transmitted signal by providing a finite output bandwidth. The UMTS standard proposes, as pulse-shaping filter the root-raised cosine waveform $\psi(t)$ whose spectrum is given by

$$
\Psi(f) = \begin{cases} \sqrt{T_c} & |f| \leq \dfrac{1 - r_{off}}{2T_c} \\[2ex] \sqrt{\dfrac{T_c}{2}\left[1 - \sin\left(\dfrac{\pi T_c}{r_{off}}\left(|f| - \dfrac{1}{2T_c}\right)\right)\right]} & \dfrac{1 - r_{off}}{2T_c} \leq |f| \leq \dfrac{1 + r_{off}}{2T_c} \\[2ex] 0 & |f| \geq \dfrac{1 + r_{off}}{2T_c} \end{cases} \tag{2.5}
$$

and where

$$
\Psi(f) = \int_{-\infty}^{\infty} \psi(t) e^{-j2\pi ft} \, dt
$$

In the standard, the roll-off factor is set to $r_{off} = 0.22$ so that the total bandwidth of the UMTS signal is given by

$$
W_\psi = \frac{1}{T_c}(1 + r_{off})
$$

Since the chip-rate is $R_c = 3.84$ Mchips/s this corresponds to the bandwidth $W_\psi = 4.68$ MHz.

2.2   General system model

Driven by the main characteristics of the UMTS-TDD 3GPP system described in the previous Sections we introduce in the following the block diagram of a TDMA-CDMA transceiver on which the work presented in this thesis is based. Along with the description we introduce part of the notation used in the following Chapters. Because of the generality of this architecture the UMTS-TDD physical layer can be seen as a particular case and will be used through this thesis as a reference for comparisons.

2.2.1   Transmitter

In Figure 2.4 the block diagram of a TDMA-CDMA transmitter for both MT and BS is depicted. Information bits, denoted in the following by the vector b, and provided by the upper layers of the protocol stack, are channel-encoded, interleaved, modulated, and spread. The channel encoder labeled "ENC" in the Figure can be any code with coding-rate R. Blocks of encoded bits are interleaved with the interleaver Π and then modulated using a modulation alphabet $\mathcal{A}$ (BPSK or QPSK [16]). Symbols, denoted by the vector

$$a = \left[a[0], a[1], \dots \right]$$

have energy

$$\mathcal{E} = \left(\log_2 |\mathcal{A}| \right) R E_b$$

where $|\mathcal{A}|$ is the cardinality of the modulation alphabet $\mathcal{A}$ and where E_b is the energy associated to each information bit. In this system we consider complex spreading sequences with spreading factor L, given by the complex column vectors

$$s_u = \left[s_u[0], s_u[1], \dots, s_u[L-1] \right]^{\mathrm{T}}$$

where u is the sequence index and where the elements $s_u[l]$ belong to the QPSK constellation.

When the BS communicates at the same time with U MTs its output signal is the sum of U contributions, each one characterized by different symbols and spreading sequences as shown in Figure 2.4(b).

In both cases, after spreading, complex chips are sent to the block labeled "Digital and Analog front-end" that provides a RF signal to send to the antenna. For most systems in this block the D/A converter, which separates the digital signal processing from the analog devices is located. The position of the D/A converter inside the "Digital and Analog front-end" block depends on the platform. An in-depth discussion of the baseband to RF signal processing for the transmitter is given in Chapter 5.

In the theoretical studies presented in Chapters 3 and 4, for the sake of simplicity, we only consider the baseband processing, i.e. the "Digital and Analog front-end" block in Figure 2.4 is neglected. In this case, assuming an analog pulse-shaping filter $\psi(t)$, the baseband signal sent to the antenna is given by

$$x(t) = \sqrt{\mathcal{E}} \sum_k a[k] \sum_{l=0}^{L-1} s[l] \psi(t - lT_c - kT) \qquad (2.6)$$

(a) MT transmitter
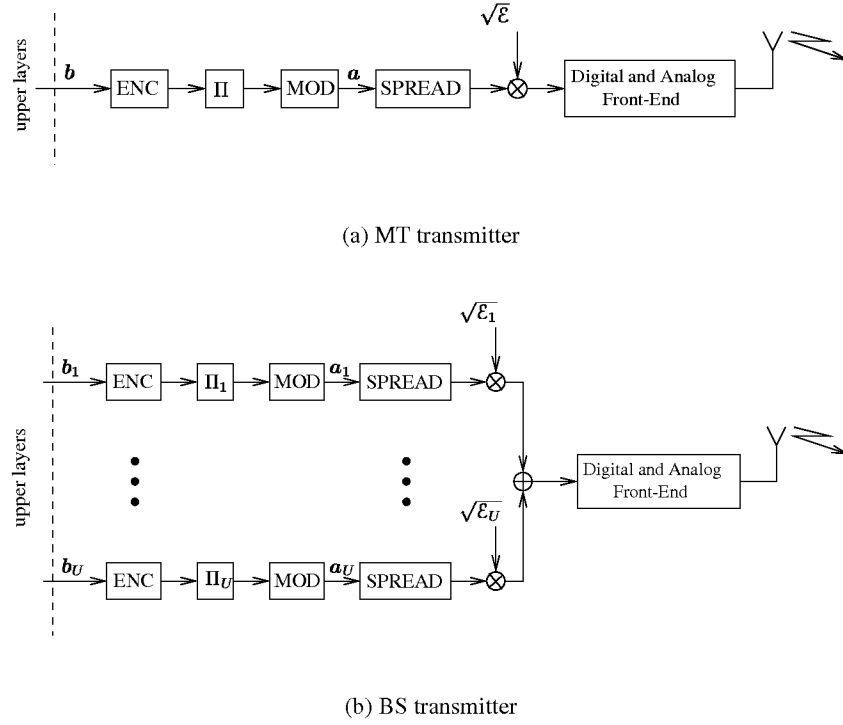
(b) BS transmitter

Figure 2.4: General scheme of the BS and MT transmitters

for a MT transmitter and by

$$x(t) = \sum_{u=1}^{U} \sqrt{\mathcal{E}_u} \sum_k a_u[k] \sum_{l=0}^{L-1} s_u[l]\psi(t - lT_c - kT) \tag{2.7}$$

for the BS transmitter. The symbol period is denoted by $T_s = LT_c$.

Although this system model has been focused on data transmission (which may involve coding and spreading) it can also represent the transmission chain for synchronization and training sequence signals. In fact, these can be seen as special cases where synchronization sequence chips and the training sequence chips are considered as source symbols while channel encoding, interleaving, and spreading blocks do not perform any operation.

2.2.2   Channel

The transmitted signal is corrupted by the radio channel which is characterized by the environment where radio signals propagate. The propagation conditions are in general assumed time-varying owing to the movement of the MT with respect to the BS although other effects can be involved (objects moving, changes of the weather, etc). Complete channel models, taking into account all these effects, are usually very complicated and when applied in the study of advanced signal processing techniques often lead to non-tractable solutions. A commonly used and simple channel model often used in the literature, is the Wide-Sense Stationary Uncorrelated Scattering model
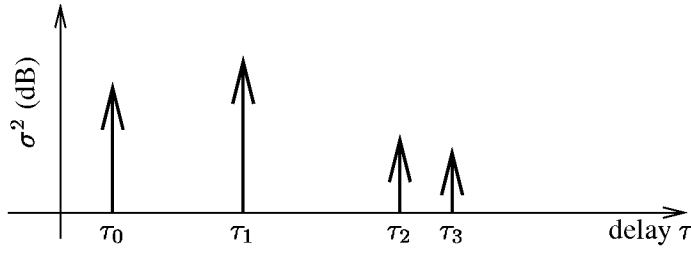
Figure 2.5: Representation of a channel MIP

(WSS-US [16]) with Rayleigh fading and multipath impulse response, represented by

$$h(t,\tau) = \sum_{p=0}^{P-1} c_p(t)\delta(\tau - \tau_p) \tag{2.8}$$

where the time-varying complex channel impulse response $h(t,\tau)$ is a function of the time t and of the delay τ. In this model the echoes of the RF signal reflected by the scatterers are grouped into P independent subsets, called paths, characterized by the delays τ_p and a set of time-varying mutually independent complex path gains $c_p(t)$ modeled as random processes with distribution $\mathcal{N}_{\mathbb{C}}(0,\sigma_p^2)$. Usually these channels are defined by a Multipath Intensity Profile (MIP) [1], given by the delays vector

$$\boldsymbol{\tau} = [\tau_0,\tau_1,\ldots,\tau_{P-1}] \tag{2.9}$$

and by the relative path powers vector

$$\boldsymbol{\sigma}^2 = [\sigma_0^2,\sigma_1^2,\ldots,\sigma_{P-1}^2] \tag{2.10}$$

An example of MIP is given in Figure 2.5. The MIP of certain propagation conditions have been standardized [21] with the purpose of giving a common reference for testing signal processing algorithms.

The solutions proposed in this work have been tested using some of the standard channels as well as with other MIP created "ad hoc" in order to show particular behaviors of the algorithms.

2.2.3 Receiver

The considerations done for the transmitter front-end hold for the receiver whose general structure is depicted in Figure 2.6. An in-depth discussion on the RF to base-band signal processing represented in the Figure by the block "Analog and Digital Front End" is given in Chapter 5.

For the rest of the thesis, for simplicity, we assume baseband transmission. We will denote by $y(t)$ the continuous time baseband received signal and by the vector

$$\boldsymbol{y} = \Big[y[0],y[1],\ldots\Big]^{\mathrm{T}}$$

its discrete-time version, sampled at rate $R_s = N_c/T_c$ where N_c is a suitable integer that satisfies the Nyquist criterion.
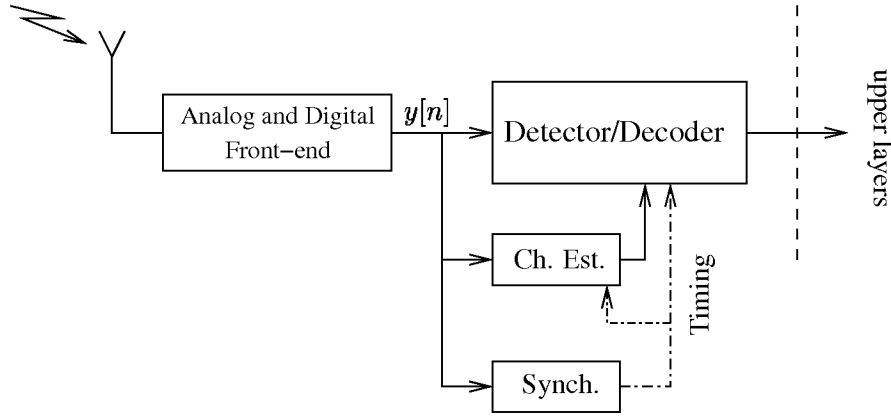
Figure 2.6: Scheme of a TDMA-CDMA receiver

In the uplink case where U MTs are transmitting at the same time the baseband signal at the BS receiver is given by

$$y(t) = \sum_{u=1}^{U} \int_{-\infty}^{\infty} h_u(t, t - \tau) x_u(\tau) \, d\tau + \nu(t) \qquad (2.11)$$

where

- $\nu(t)$ is the noise contribution, a complex Gaussian random process with zero mean and power spectral density I_0 that takes into account the thermal noise and cell-to-cell interference (assumed Gaussian)

- $x_u(\tau)$ is the continuous-time complex baseband signal produced by the transmitter of the uth MT given by (5.1)

- $h_u(t, \tau)$ is the channel connecting the uth MT to the BS

In a downlink slot instead the only channel involved is the one that links the BS antenna to the MT receiver, so that the received signal is

$$y(t) = \sum_{u=1}^{U} \int_{-\infty}^{\infty} h(t, t - \tau) x_u(\tau) \, d\tau + \nu(t) \qquad (2.12)$$

Since we restrict this system model to a single cell, considering a single BS, the cell-to-cell interference is assumed to be part of the total noise variance.

The synchronization block, present only in the MT, estimates the timing of the BS signal and provides a time reference to the receiver. The synchronization process is active when the MT is switched on or when, for some reason, the MT looses the synchronization and must re-acquire the timing. Using the slot timing informations the channel estimation block identifies the midamble into the slot, processes the training sequence signal, and provides channel estimates to the detector/decoder. The derivation of an efficient signal processing technique providing the channel estimates is given in Section 5.5.

Eventually, the detector/decoder processes the signal contained in the slot data fields, estimates the information bits, and sends it to the upper layers. It performs operations like matched filtering, despreading, demodulation, deinterleaving and decoding.

In this system model we do not specify the structure of the detector/decoder, leaving it enough general to include the Single User Detector receiver proposed by the UMTS-TDD norm as well as the Multi User Detection and decoding techniques developed in Chapter 4.

Chapter 3

Maximum likelihood burst timing acquisition

We consider the initial timing acquisition in DS-CDMA when propagation is affected by multipath and fading and where the base-station broadcasts a synchronization pilot signal in the form of bursts of modulated chips transmitted periodically and separated by long silent intervals. Subject to certain simplifying assumptions we derive the maximum likelihood (ML) estimator by solving a constrained maximization problem. Our ML timing estimator has constant complexity per observation sample. The relation to other estimation methods is addressed, and performance comparisons are provided by simulations. The proposed estimator yields good performance independently of the multipath-intensity profile of the channel, provided that the delay spread is not larger than a given maximum spread. Moreover, our estimator is fairly robust against the mismatch in the fading Doppler spectrum and provides good performance for both fast and slow fading.

3.1 Introduction and motivation

In a wireless mobile system synchronization represents a major issue. As introduced in Section 2.1.3 a MT before starting communication with the BS must acquire its timing. When data transmission occurs with a slot structure, as for the UMTS-TDD mode, the basic time reference is the slot and frame timing. In third generation wireless communication systems [22] timing acquisition is facilitated by a pilot signal transmitted by the BS. In the UMTS standard this signal is called *primary synchronization signal*. In both FDD and TDD [14, 15] modes, the primary synchronization signal (already

19

described in Section 2.1.3) is bursty, i.e., it is non-zero only for a small fraction of time compared with the slot duration. The first task of the MT when it is switched on consists of detecting the presence and the timing of the primary synchronization signal. Motivated by this scheme, we consider the general problem of initial slot timing acquisition in a DS-CDMA system with a bursty pilot signal in the presence of an unknown multipath fading channel.

In [23] a maximum likelihood (ML) timing estimator is derived by assuming that the channel MIP is known at the receiver, and in [24, 25] the ML criterion is applied by modeling the channel as deterministic unknown and constant with time. Unfortunately the multipath intensity profile is not known *before* initial acquisition and, since the initial synchronization phase may last several slots, the algorithms based on the constant channel assumption might perform poorly in the presence of time-varying fading.

In this Chapter, we obtain a low-complexity slot timing estimator requiring a minimum amount of prior knowledge and yielding good performance on a wide range of channel MIPs and fading Doppler bandwidths. Since both the channel MIP and the noise plus interference power spectral density are not known at the receiver, we formulate a joint ML problem where all these parameters have to be estimated. We derive the ML estimator by solving a constrained maximization problem via the Karush-Kuhn-Tucker (KKT) conditions [26]. In order to obtain a tractable solution we make several simplifying assumptions. When these are not satisfied, our estimator is not exactly ML and may suffer from mismatch. The proposed estimator is compared with the simple estimator for flat fading [16], with the too optimistic estimator of [23], and with the estimator of [24] for two typical channel MIPs under both the assumption of slow fading (constant channel) and fast fading. Computer simulations show that the proposed joint ML estimator exhibits good performance in all these conditions and it is fairly robust to mismatch of the assumed fading statistics.

3.2   Signal model

The continuous-time complex baseband received signal is given by

$$y(t) = \zeta(t, \theta) + \nu(t) \tag{3.1}$$

where $\nu(t)$ represents noise plus interference, modeled as a zero-mean complex circularly symmetric Gaussian process with power spectral density I_0, and $\zeta(t, \theta)$ is the received synchronization signal component, given by

$$\zeta(t, \theta) = \sum_{m=0}^{M-1} \int h(t, t - \tau) x(\tau - \theta - mT) \, d\tau \tag{3.2}$$

where θ is the slot timing, $x(t)$ is the bursty pilot waveform of duration T_{ps}, $T \gg T_{\mathrm{ps}}$ is the period of repetition of $x(t)$, $h(t, \tau)$ is the time-varying multipath channel impulse response and M is the number of transmitted pilot bursts. Because of the slot periodicity, θ must be estimated modulo T. The channel is assumed to follow the WSS-US [16] model with Rayleigh fading and multipath impulse response given by (2.8) where the channel MIP is defined by the delays vector $\boldsymbol{\tau} = [\tau_0, \ldots, \tau_{P-1}]$
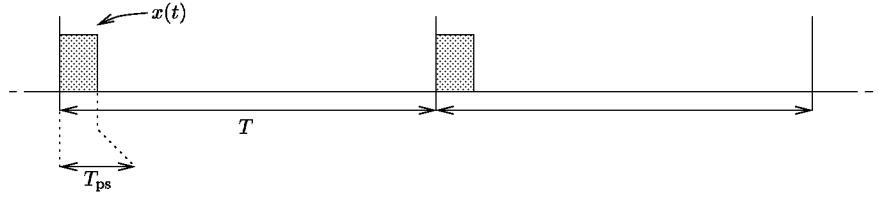
Figure 3.1: Bursty synchronization signal at the transmitter

and by the path variances $\boldsymbol{\sigma} = [\sigma_0^2, \ldots, \sigma_{P-1}^2]$. Since T_{ps} is much shorter than T, we assume that the channel coherence time T_{coh} [16] satisfies $T_{\mathrm{ps}} < T_{\mathrm{coh}} \leq T$. This implies that the channel is almost constant during each mth burst, but changes independently from burst to burst. Since T_{ps} is very short [1] this condition is referred to as *fast fading*, and holds approximately for $\frac{1}{T} \leq B_d < \frac{1}{T_{\mathrm{ps}}}$, where B_d is the fading Doppler bandwidth. Moreover, we assume that the delays τ_p are constant over the whole observation window of duration MT. In practical systems [19] the period T ranges from one slot period to one frame period and the multipath delays vary at a much lower rate than the slot rate. Thus this assumption is satisfied. Subject to the above assumptions, $\zeta(t, \theta)$ in (3.2) can be rewritten as

$$\zeta(t, \theta) = \sum_{m=0}^{M-1} \sum_{p=0}^{P-1} c_{mp} x(t - \theta - \tau_p - mT) \tag{3.3}$$

where c_{mp} are complex zero-mean circularly-symmetric Gaussian mutually uncorrelated random variables such that $\mathrm{E}\left[c_{mp} c_{nq}^*\right] = \sigma_p^2 \delta_{m,n} \delta_{p,q}$.

The pilot waveform is given by

$$x(t) = \sum_{n=0}^{N-1} s_n \psi(t - nT_c) \tag{3.4}$$

where T_c is the chip duration, s_n is a sequence of N chips known at the receiver and $\psi(t)$ is the chip-shaping pulse band-limited to $[-W_\psi/2, W_\psi/2]$ with $\frac{1}{T_c} \leq W_\psi \leq \frac{2}{T_c}$. In a digital receiver implementation the signal is low-pass filtered and sampled at a convenient rate $W > W_\psi$. Hence, baseband processing is performed in discrete time. We assume $W = N_c/T_c$, where $N_c > 1$ is the number of samples per chip. Let $Q = WT$ denote the number of samples per pilot repetition period, and define the discrete-time observed signal as

$$\boldsymbol{y} = \left[y[0], \ldots, y[MQ - 1]\right]^{\mathrm{T}}$$

After a straightforward derivation, it is possible to write $\boldsymbol{y}$ in the compact form

$$\boldsymbol{y} = \boldsymbol{Sc} + \boldsymbol{\nu} \tag{3.5}$$

---

[1] In the UMTS standard proposal [14, 15] the pilot waveform consists of a sequence of 256 chips convolved with a root-raised cosine chip-shaping pulse. Thus with good approximation we may say that $T_{\mathrm{ps}} \approx 270$ chip periods, whereas T can range from one slot (2560 chips) to one frame period (15 slots).
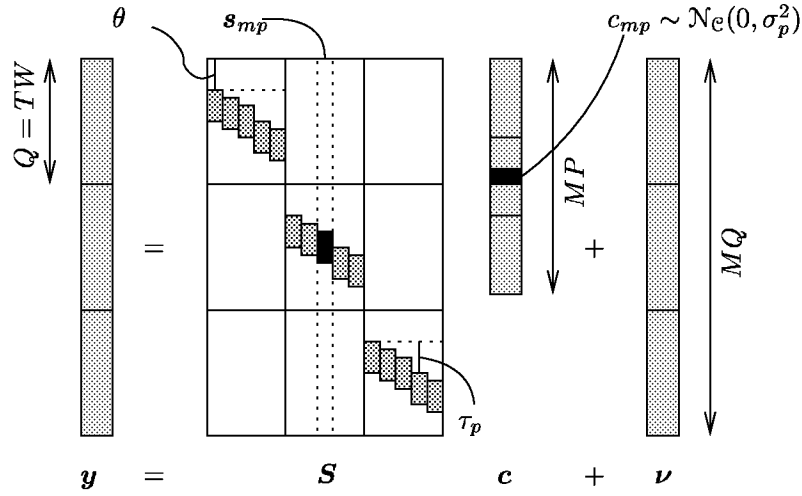
Figure 3.2: Model of the bursty synchronization signal

where $\boldsymbol{\nu} \triangleq \left[\nu[0],\ \ldots,\ \nu[MQ-1]\right]^{\mathrm{T}}$ is the vector of interference plus noise samples, $\boldsymbol{c} \triangleq \left[\boldsymbol{c}_0^{\mathrm{T}}, \ldots, \boldsymbol{c}_{M-1}^{\mathrm{T}}\right]^{\mathrm{T}}$, with $\boldsymbol{c}_m \triangleq \left[c_{m0}, \ldots, c_{m(P-1)}\right]^{\mathrm{T}}$, contains all MP channel path coefficients over the M periods, and where $\boldsymbol{S}$ is the $MQ \times MP$ matrix whose $(mP+p)^{\mathrm{th}}$ column, for $m = 0, \ldots, M-1$ and $p = 0, \ldots, P-1$, is given by

$$\boldsymbol{s}_{mp} \triangleq \Big[\underbrace{0, \ldots, 0}_{mQ}, s_p[0], \ldots, s_p[Q-1],\ \underbrace{0, \ldots, 0}_{(M-m-1)Q}\ \Big]^{\mathrm{T}} \tag{3.6}$$

where

$$s_p[i] = \frac{1}{\sqrt{W}} \sum_{n=0}^{N-1} s_n \psi(i/W - \theta - \tau_p - nT_c) \tag{3.7}$$

Notice that the dependence of $\boldsymbol{y}$ on θ is *hidden* in the matrix $\boldsymbol{S}$ as shown in Figure 3.2. Since the columns of $\boldsymbol{S}$ are obtained by translating the same waveform, they have all the same square magnitude, equal to the energy $\mathcal{E}$ of the pilot waveform. Then, without loss of generality we can include the term $\mathcal{E}$ into the path variances σ_p^2, and consider $|\boldsymbol{s}_{mp}|^2 = 1$ for all m, p and delay θ. Under our assumptions, $\boldsymbol{y}$ is a zero-mean complex circularly-symmetric Gaussian random vector with covariance matrix

$$\boldsymbol{R}_y = \boldsymbol{S}\boldsymbol{\Lambda}\boldsymbol{S}^{\mathrm{H}} + I_0\mathbf{I}_{MQ} \tag{3.8}$$

where the superscript $(\cdot)^{\mathrm{H}}$ denotes the Hermitian transpose, $\mathbf{I}_m$ indicates the $m \times m$ identity matrix and where $\boldsymbol{\Lambda}$ is the covariance matrix of $\boldsymbol{c}$, given by $\boldsymbol{\Lambda} = \mathbf{I}_M \otimes \boldsymbol{\Lambda}_c$ with $\boldsymbol{\Lambda}_c = \mathrm{diag}(\sigma_0^2, \ldots, \sigma_{P-1}^2)$.

3.3 Maximum likelihood problem formulation

The log-likelihood function for the parameters vector $\boldsymbol{\theta} = (\theta, \tau, \sigma, I_0)$ is immediately obtained as [27]

$$\mathcal{L}(\boldsymbol{y}|\boldsymbol{\theta}) = -\log\det(\boldsymbol{R}_y) - \boldsymbol{y}^{\mathrm{H}}\boldsymbol{R}_y^{-1}\boldsymbol{y} \tag{3.9}$$

Notice that the number of channel paths P is also unknown and it is implicitly contained in the parameters $\boldsymbol{\tau}$ and $\boldsymbol{\sigma}$. By applying the matrix inversion lemma [17] to (3.8) we get

$$\boldsymbol{R}_y^{-1} = \frac{1}{I_0}\mathbf{I}_{MQ} - \frac{1}{I_0^2}\boldsymbol{S}\boldsymbol{\Lambda}^{\frac{1}{2}}\left(\mathbf{I}_{MP} + \frac{1}{I_0}\boldsymbol{\Lambda}^{\frac{1}{2}}\boldsymbol{S}^{\mathrm{H}}\boldsymbol{S}\boldsymbol{\Lambda}^{\frac{1}{2}}\right)^{-1}\boldsymbol{\Lambda}^{\frac{1}{2}}\boldsymbol{S}^{\mathrm{H}} \qquad (3.10)$$

Now, we make the key assumption that the columns of $\boldsymbol{S}$ are mutually orthogonal. In particular, this is approximately verified if the delays τ_p are sufficiently spaced apart (more than T_c) and if the sequence of chips s_n has a very peaky aperiodic autocorrelation function. In practice, the pilot sequence s_n is quite long ($N = 256$ in UMTS [19]) and paths spaced by less than one chip interval are substantially treated as a single path (they are not *resolvable* [16]). Thus, our assumption is not very restrictive. If $\boldsymbol{S}$ has orthonormal columns, (3.10) reduces to

$$\boldsymbol{R}_y^{-1} = \frac{1}{I_0}\left(\mathbf{I}_{MQ} - \boldsymbol{S}\boldsymbol{\Sigma}\boldsymbol{S}^{\mathrm{H}}\right) \qquad (3.11)$$

where

$$\boldsymbol{\Sigma} = \mathbf{I}_M \otimes \mathrm{diag}\left(\frac{\xi_0}{1+\xi_0},\ldots,\frac{\xi_{P-1}}{1+\xi_{P-1}}\right)$$

, and where we define the path average signal-to-noise ratio (SNR) $\xi_p = \sigma_p^2/I_0$, for $p = 0,\ldots,P-1$. Subject to the same assumption, the determinant of $\boldsymbol{R}_y$ is readily obtained as

$$\det(\boldsymbol{R}_y) = \left[\prod_{p=0}^{P-1}(1+\xi_p)\right]^M I_0^{MQ} \qquad (3.12)$$

By using (3.11) and (3.12) in (3.9) and by defining the total received signal energy $E_y = |\boldsymbol{y}|^2$ and the vector of path average SNRs $\boldsymbol{\xi} = (\xi_0,\ldots,\xi_{P-1})$, we obtain the log-likelihood function in the form

$$\mathcal{L}(\boldsymbol{y}|\boldsymbol{\theta}) = \frac{1}{I_0}\left[\sum_{p=0}^{P-1}\frac{\xi_p}{1+\xi_p}X(\theta+\tau_p) - E_y\right] - MQ\log I_0 - M\sum_{p=0}^{P-1}\log(1+\xi_p), \qquad (3.13)$$

where we define

$$X(\theta+\tau_p) \overset{\triangle}{=} \sum_{m=0}^{M-1}\left|\boldsymbol{s}_{mp}^{\mathrm{H}}\boldsymbol{y}\right|^2 \qquad (3.14)$$

The term $X(\theta+\tau_p)$ is obtained by summing for $m = 0,\ldots,M-1$ the squared magnitude of the output of a discrete time filter with impulse response matched to the delayed pilot waveform $x(t - \theta - mT - \tau_p)$. Then, this is the output of a sort of *square-law diversity combiner* [16] collecting the signal energy over all the M pilot repetition periods, for a given guess of the timing θ and multipath component with delay τ_p. We shall refer to these terms as the *received path energies* at delay $\theta + \tau_p$. From the implementation point of view, $X(\theta + \tau_p)$ for all $p = 0,\ldots,P-1$ can be calculated by sampling at delays $\theta + \tau_p$ the output of the *same* filter matched to $x(t)$.

3.4   Approximated ML estimation

In order to find the ML estimate of θ, we should jointly estimate also the other unknown parameters $\boldsymbol{\tau}, \boldsymbol{\xi}$ and I_0. For simplicity of exposition, we first assume that the delays $\boldsymbol{\tau}$ are known. Then, for any given value of θ we want to maximize the log-likelihood function with respect to $\boldsymbol{\xi}$ and I_0, i.e., we want to solve the constrained maximization problem

$$\begin{cases} \text{maximize} & \mathcal{L}(\boldsymbol{y}|\theta, \boldsymbol{\xi}, \boldsymbol{\tau}, I_0) \\ \text{subject to} & \boldsymbol{\xi} \geq \mathbf{0}, \quad I_0 \geq 0 \end{cases} \tag{3.15}$$

This can be solved by using the KKT method [26]. In this section we let $X_p \triangleq X(\theta + \tau_p)$ for the sake of notation simplicity.

We have the following:

Proposition 1.   The solution of the maximization problem (3.15) is given by

$$\xi_p = \left[\frac{1}{\beta} X_p - 1\right]_+, \quad I_0 = \frac{\beta}{M}, \quad \beta = \frac{E_y - \sum_{p \in \mathcal{D}} X_p}{Q - D} \tag{3.16}$$

where $[\cdot]_+$ denotes positive part, and where we define the set of indexes $\mathcal{D} = \{p \in [0, P-1] : X_p > \beta\}$, of cardinality $|\mathcal{D}| = D$. Moreover, this solution exists and is unique for any set of received signal energies $\{X_p : p = 0, \ldots, P-1\}$, for all $Q > P$ and $M \geq 1$ and for all E_y such that $\sum_{p=0}^{P-1} X_p < E_y < \frac{Q}{P} \sum_{p=0}^{P-1} X_p$.

Proof. See Appendix 3.A.1.

Solution (3.16) has the following intuitive interpretation: β acts as an adaptive threshold level. If $X_p > \beta$ then $\theta + \tau_p$ is a good candidate for being a true channel path.

Let π be the permutation of P indexes sorting the X_p's in non-decreasing order, i.e., such that

$$X_{\pi(0)} \geq X_{\pi(1)} \geq \cdots \geq X_{\pi(P-1)}$$

Then, by substituting the solution of Proposition 1 into (3.13) we obtain the maximized log-likelihood function in the form

$$\overline{\mathcal{L}}(\boldsymbol{y}|\theta, \boldsymbol{\tau}) \triangleq \max_{\boldsymbol{\xi}, I_0} \mathcal{L}(\boldsymbol{y}|\boldsymbol{\theta}) = -(Q - D) \log \frac{E_y - \sum_{p=0}^{D-1} X_{\pi(p)}}{Q - D} - \log \prod_{p=0}^{D-1} X_{\pi(p)} \tag{3.17}$$

The exact ML joint estimator of $\boldsymbol{\theta}$ is obtained by further maximizing $\overline{\mathcal{L}}(\boldsymbol{y}|\theta, \boldsymbol{\tau})$ with respect to all possible $\boldsymbol{\tau}$ and θ. While maximization with respect to θ involves searching in a one-dimensional real space, with complexity $\mathcal{O}(Q)$, the maximization with respect to $\boldsymbol{\tau}$ requires a search over P-dimensional real spaces for all $P = 1, 2, \ldots$, which is highly impractical.

In order to circumvent this hurdle, we restrict the search over a set of tentative delay vectors $\boldsymbol{\tau}$ selected according to some criteria. At the same time, the set of tentative $\boldsymbol{\tau}$ should enforce the condition that the delays are separated by more than T_c, which guarantees that the columns of $\boldsymbol{S}$ are approximately orthonormal. The selection of the tentative $\boldsymbol{\tau}$ is based on the following proposition and heuristic considerations.

Proposition 2. For a given fixed θ, let $\{\tau_p : p = 0, 1, \ldots\}$ be a sequence of delays such that the sequence of corresponding received energies $\{X_p : p = 0, 1, \ldots\}$ is non-increasing. Then, the sequence of log-likelihood functions $\{\overline{\mathcal{L}}(y|\theta, \tau_0, \ldots, \tau_p) : p = 0, 1, \ldots\}$ is non-decreasing. Moreover, if for some $D \geq 1$ the condition

$$X_D \leq \beta_D \overset{\triangle}{=} \frac{E_y - \sum_{i=0}^{D-1} X_i}{Q - D} \tag{3.18}$$

holds, then

$$\max_{p \geq 0} \overline{\mathcal{L}}(y|\theta, \tau_0, \ldots, \tau_p) = \overline{\mathcal{L}}(y|\theta, \tau_0, \ldots, \tau_{D-1})$$

Proof. See Appendix 3.A.2.

From Proposition 2 it follows that we can construct a set of "nested" tentative delay vectors of dimension $P = 1, 2, \ldots$ in sequence, by appending more and more delays corresponding to decreasing received energies. The maximum of the log-likelihood function over the (infinite) delay vector sequence is found when, for some (finite) integer D the condition (3.18) holds. Furthermore, we observe that:

1. The log-likelihood function increases with the received energy sum

$$A = \sum_{p=0}^{D-1} X_{\pi(p)}$$

   and decreases with the product

$$B = \prod_{p=0}^{D-1} X_{\pi(p)}$$

   For a given value of A, $\overline{\mathcal{L}}(y|\theta, \tau)$ is maximized by a "peaky" distribution of the path energies X_p's. In fact, the product B is maximum for the uniform distribution $X_{\pi(0)} = \cdots = X_{\pi(D-1)} = A/D$ while it is small if the received energies are spread, i.e., if $X_{\pi(0)} \gg X_{\pi(1)} \gg \cdots \gg X_{\pi(D-1)}$ (notice that $X_{\pi(D-1)} > \beta > 0$, so B cannot be zero).

2. In practice, systems are designed to handle multipath channels up to a given maximum delay spread T_d (see e.g. [19]) (defined here as $T_d \overset{\triangle}{=} \max_p \tau_p - \min_p \tau_p$ [16]). Then, for a given θ, the channel paths are expected to be contained in a time window $[\theta, \theta + T_d]$, where T_d is known *a priori*.

Driven by the above two considerations, a meaningful choice of the sequence of delays $\{\tau_p : p = 0, 1, \ldots\}$ is to choose for each p the delay $\tau_p \in [0, T_d]$ for which X_p is maximum and τ_p has not appeared before in the sequence. Moreover, since the paths should be separated by at least one chip interval, we place around each chosen τ_p a *forbidden region* of size $2T_c$. The newly selected delays should not belong to the forbidden regions of already selected delays. The resulting approximated ML algorithm is given as follows.
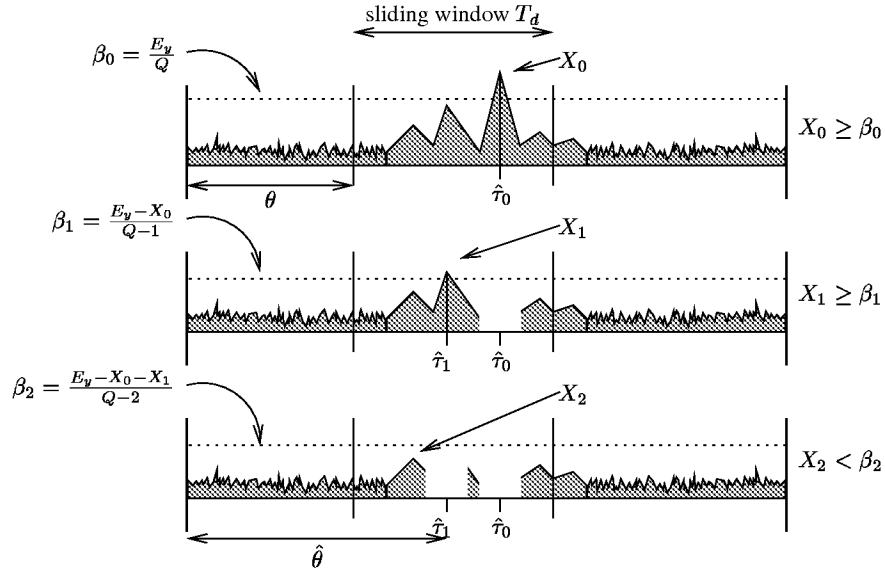
Figure 3.3: An example of the Joint Maximum Likelihood algorithm behaviour

Initial timing estimation.   For all $\theta \in [0, T]$ we compute the value $\widehat{\mathcal{L}}(\boldsymbol{y}|\theta)$ given by the recursion: initialize $p = 0$, $\beta_0 = E_y/Q$, and the search interval $\mathcal{S}_0 = [0, T_d]$, then

1. Select $\tau_p = \arg \max_{\tau \in \mathcal{S}_p} X(\theta + \tau)$, and let $X_p = X(\theta + \tau_p)$.

2. If $X_p > \beta_p$, let $\beta_{p+1} = \frac{E_y - \sum_{i=0}^{p} X_i}{Q - p - 1}$, let $\mathcal{S}_{p+1} = \mathcal{S}_p \setminus [\tau_p - T_c, \tau_p + T_c]$,[2] then increment p by 1 and go to step 1.

3. If $X_p \le \beta_p$ or if $\mathcal{S}_{p+1}$ is empty, compute

$$\widehat{\mathcal{L}}(\boldsymbol{y}|\theta) = -(Q - p) \log \beta_p - \log \prod_{i=0}^{p-1} X_i$$

and exit the recursion.

Finally, the estimated slot timing is given by $\widehat{\theta} = \theta_m + \widehat{\tau}_0$, where

$$\theta_m = \arg \max_{\theta \in [0,T]} \widehat{\mathcal{L}}(\boldsymbol{y}|\theta) \tag{3.19}$$

and where $\widehat{\tau}_0$ is the estimated delay of the first path (also provided by the above algorithm) corresponding to θ_m.

As far as implementation is concerned, some considerations are in order.

- Up to now, we considered the parameter θ as continuous. However, in a digital implementation, the search for the maximum of $\widehat{\mathcal{L}}(\boldsymbol{y}|\theta)$ is done on a discrete set of values. The most computationally demanding operation is the computation of the matched filter output $z_{mp}(\theta) = \boldsymbol{s}_{mp}^{\mathrm{H}} \boldsymbol{y}$ involved in the calculation of $X(\theta +$

---

[2]The notation $\mathcal{A} \setminus \mathcal{B}$ denotes the complement of the set $\mathcal{B}$ with respect to the set $\mathcal{A}$.

τ_p) (see (3.14)). In most practical applications it is sufficient to acquire the slot timing with an error of less than one chip. Therefore, a very fine discretization of θ is not needed. In our numerical examples, we discretize θ with step $1/W$, so that we need just a matched filter operating at the signal sampling rate W, whose output is given by

$$z[i] = \sum_j y[j]x((j+i)/W)^*$$

The receiver accumulates the squared matched filter outputs in a vector buffer $\boldsymbol{v}_b = \left[v_b[0], \ldots, v_b[Q-1]\right]$ such that

$$v_b[i] = \sum_{m=0}^{M-1} |z[mQ+i]|^2$$

The search of the delays and the search for the maximum in (3.19) is performed over the discrete values $\{t_k = k/W : k = 0, \ldots, Q-1\}$ by processing the data buffer $\boldsymbol{v}_b$. Assuming θ uniformly distributed, the minimum possible Mean Square Error resulting from discretization is given by the variance of a uniformly distributed random variable over $\left[-\frac{1}{2W}, +\frac{1}{2W}\right]$, i.e., by $\frac{1}{12W^2}$. This is referred to as "discretization error" in Section 3.5.

- We have implicitly assumed that the pilot bursts fall approximately in the middle of the observation intervals $[mT, (m+1)T]$. However, the initial timing reference of the MT is arbitrary, and the pilot bursts may fall across the boundaries of the observation intervals. Since the slot timing is defined modulo T, in order to solve this problem it is sufficient to apply the estimation algorithm by treating the data buffer $\boldsymbol{v}_b$ as a *circular buffer*.

- The complexity of the proposed algorithm is linear in the observation size QM, as opposed to other timing algorithms based on Least-Squares (LS) [24] or subspace decomposition, which require matrix-vector multiplication or matrix eigen-analysis (see e.g. [28] and references therein).

- As byproducts of initial timing estimation, the proposed method also provides estimates for the interference plus noise power spectral density I_0, for the path SNRs ξ_p, for the path delays τ_p and for the number of paths P. These can be used to speed-up some terminal setup procedures [15, 14]. For example, the delays corresponding to the largest path SNRs can be used to initialize the fine delay search of a rake receiver, and the knowledge of I_0 can be exploited to initialize the power control loop.

3.5 Results

We compare the performance of our estimator, hereafter denoted by joint ML (JML), with the following estimators:
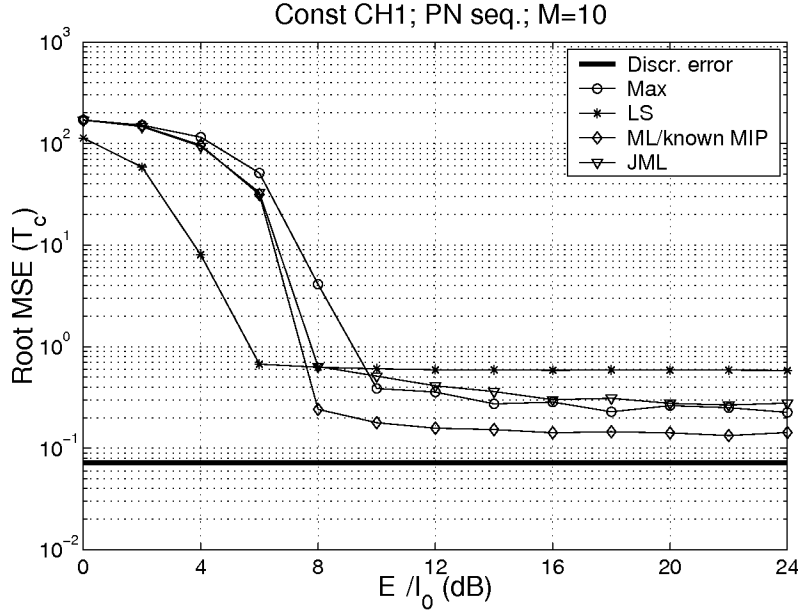
Figure 3.4: RMSE with constant CH1 vs. $\mathcal{E}/I_0$ for $M = 10$ accumulated bursts

- The least computationally intensive estimator that selects as estimated delay the position of the maximum element in the buffer v_b, in the sequel denoted as the "MAX" estimator.

- The approximated least-squares estimator (denoted by "LS") which is an approximation of the exact LS estimator that coincides with the ML estimator subject to the assumption of constant channel. In fact, when the channel is constant during the observation interval the ML slot timing estimator is given by [24, 25]

$$\hat{\theta} = \arg \max_{\theta} \bar{y}^H \bar{S} (\bar{S}^H \bar{S})^{-1} \bar{S}^H \bar{y} \qquad (3.20)$$

where $\bar{y} = \frac{1}{M} \sum_{m=1}^{M} y_m$, $y_m = \left[y[(m-1)Q], \ldots, y[mQ-1] \right]^T$, and where $\bar{S}$ is the $Q \times L$ convolution matrix whose l^{th} column is given by

$$\bar{s}_l = \left[s_l[0], \ldots, s_l[Q-1] \right]^T$$

where

$$s_l[i] = \frac{1}{\sqrt{W}} \sum_{n=0}^{N-1} s_n \psi((i-l-1)/W - nT_c - \theta)$$

and L is the channel delay spread expressed in sample periods. From the implementation point of view the algorithm corresponds to filtering the received signal $\bar{y}$ with a filter matched to the pilot waveform, windowing the filtered signal by the $L \times L$ matrix $(\bar{S}^H \bar{S})^{-1}$, taking the magnitude square of the output signal and finding the maximum. Even though the matrix $(\bar{S}^H \bar{S})^{-1}$ can be precomputed this approach is extremely computational intensive since it requires
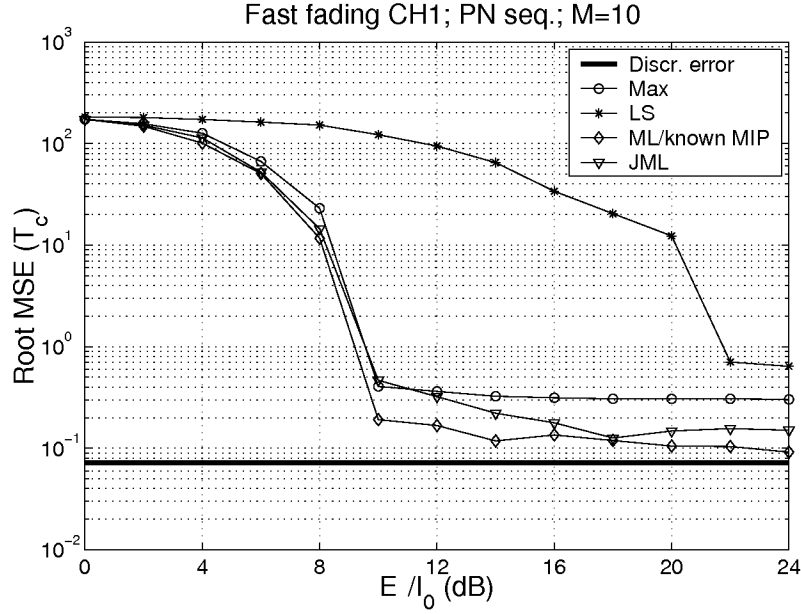
Figure 3.5: RMSE with fast fading CH1 vs. $\mathcal{E}/I_0$ for $M = 10$ accumulated bursts

the computation of L scalar products per output sample (i.e. for each possible θ). Therefore we consider the more practical approximated LS estimator based on the assumption $\bar{S}^{\mathrm{H}}\bar{S} \approx \mathbf{I}$, also proposed in [24].

- The ML estimator with perfect knowledge of both the channel MIP and the interference power spectral density I_0 (denoted by "ML/known MIP") proposed in [23]. Since all the parameters but θ are known the log-likelihood function (3.13) for this estimator reduces to

$$\mathcal{L}(\boldsymbol{y}|\theta) = \sum_{p=0}^{P-1} \frac{\xi_p}{1+\xi_p} X(\theta + \tau_p) \tag{3.21}$$

As performance measure we use the root-mean square error (RMSE) of the estimated slot timing normalized with respect to the chip interval (i.e., it is expressed in fraction of T_c) and the cumulative density function (CDF) $F_e(E)$ of the sum of the energies of the paths falling in the estimated window $W_e = \left[\hat{\theta}, \hat{\theta} + T_d\right]$, normalized with respect to the total channel energy. The CDF gives the probability that the fraction of the total channel energy "captured" inside W_e is below a given level E. Since in general the performance of the subsequent synchronization phase, involving BS identification, frame synchronization etc., depends on the fraction of captured channel energy (no matter which algorithm is used), the CDF is able to characterize the performance of the whole synchronization procedure, independently of the particular algorithm employed in the second phase.

In our examples the chip-shaping pulse is root-raised cosine with roll-off factor $\alpha = 0.22$. As pilot sequence, we used a PN sequence of length $N = 255$ and the UMTS primary synchronization sequence of length $N = 256$ defined in [13]. The
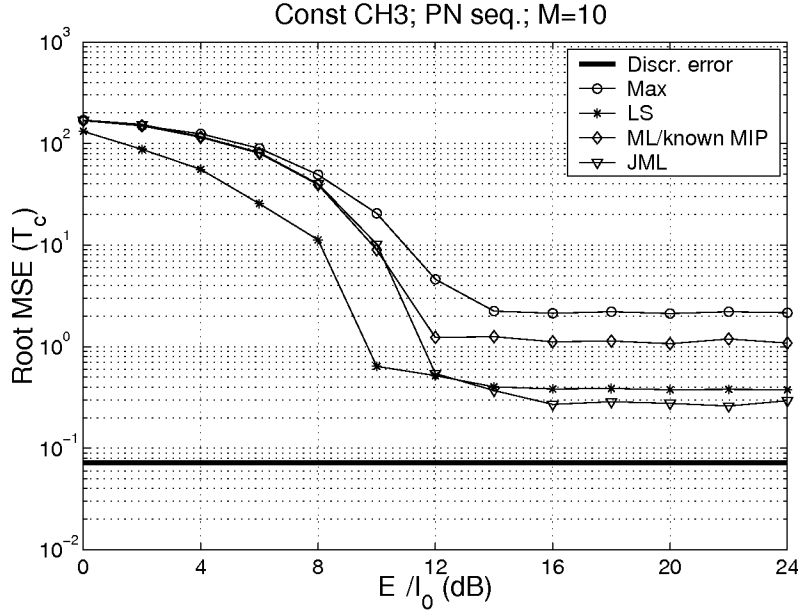
Figure 3.6: RMSE with constant CH3 vs. $\mathcal{E}/I_0$ for $M = 10$ accumulated bursts

receiver sampling rate is $W = 4/T_c$ and both the pilot repetition interval and the slot duration are equal to $T = 625\,T_c$, corresponding to $Q = 2500$ samples (in reality Q may be much larger but we were limited by the simulation time). In our simulations we considered four typical channel MIPs described in table 3.1 and denoted by CH1, CH2, CH3, and CH4. CH1 is specified as a standard channel test in [21] and it has been chosen because it satisfies our working assumptions. CH3 was created "ad hoc" in order to test the algorithm on a channel which does not satisfy our assumptions. In fact CH3 has non-separable paths. Eventually, CH2 and CH4 were created "ad hoc" in order to put in evidence the energy-capture performance and to test the *outlier error* performance of the estimator, i.e., the capability of locating θ within a window.

Figures 3.4–3.7 show the timing RMSE versus the pilot energy to interference plus noise ratio $\mathcal{E}/I_0$ for channel MIPs CH1 and CH3 under both constant and fast fading conditions. We refer to fast fading conditions when the channel coherence time is much smaller than the period of repetition of the pilot (but still larger than the pilot duration). Notice that the "JML" and the "ML/known MIP" estimators are mismatched for constant channel, while the "LS" estimator is mismatched for fast fading. The number of accumulated bursts is fixed to $M = 10$.

The "LS" estimator performs very poorly in the presence of fast fading because is mismatched (see figures 3.5 and 3.7). Indeed in the presence of fast Rayleigh fading, as in our scenario, the amplitude of the averaged received signal $\bar{\boldsymbol{y}} = \frac{1}{M} \sum_m \boldsymbol{y}_m$ decreases as the number of accumulated bursts M increases. On the contrary the "JML" estimator shows good performance also in the presence of a constant channel despite it is mismatched in this case. Moreover it always performs closely to the "ML/known MIP" estimator.
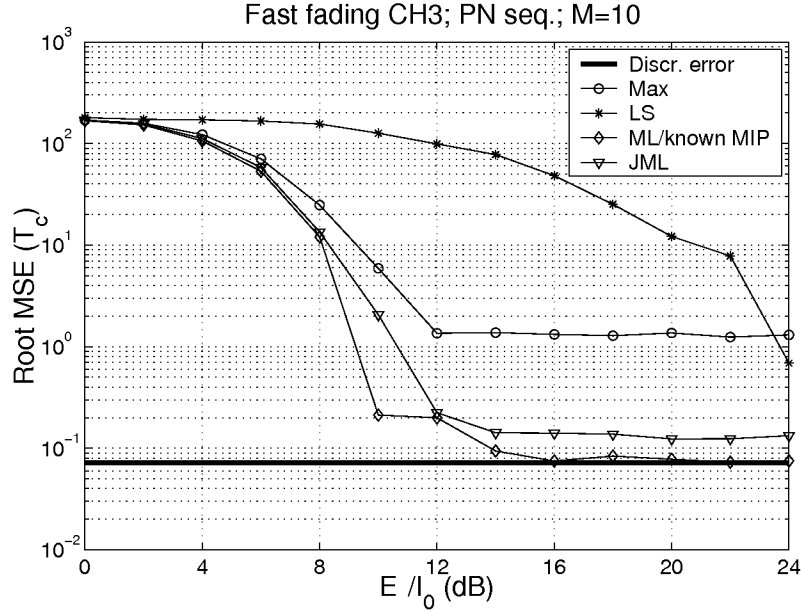
Figure 3.7: RMSE with fast fading CH3 vs. $\mathcal{E}/I_0$ for $M = 10$ accumulated bursts

Extensive simulations show that increasing M reduces the $\mathcal{E}/I_0$ needed to achieve a given RMSE, without affecting the relative behaviors of the estimators.

Figures 3.8–3.11 show the CDF $F_e(E)$ of the fraction of channel energy captured in the window W_e for channels CH2 and CH4. In these figures the CDF of the "MAX" estimator shows abrupt transitions each corresponding to the loss of the channel energy associated with a path. For instance, in the case of channel MIP CH2, the transition occurs at $E = -3\,\mathrm{dB}$ that corresponds to the loss of half the channel energy. This effect is due to a false lock of the "MAX" estimator on the the second path of the channel.

In the presence of fast fading the "JML" estimator generally outperforms all other estimators but the "ML/known MIP" that is based on non-realistic assumptions. With slow fading our estimator performs better than the "MAX" and the "LS" estimators for high $\mathcal{E}/I_0$ (i.e. greater than 10 dB when $M = 10$ as evidenced by figures 3.4 and 3.6) even though it is mismatched.

Finally figures 3.12 and 3.13 compare the performance of the "JML" estimator in terms of RMSE versus $\mathcal{E}/I_0$ for fast fading channel CH1 and CH3 when using the UMTS and the PN sequence, for $M = 10$ accumulations. Performance are worse with the UMTS sequence due to its worse acyclic autocorrelation properties.

3.6   Conclusions

Motivated by the initial BS acquisition procedure of UMTS, we considered the problem of slot timing estimation based on bursty pilot signals. Subject to some simplifying working assumptions, we derived a low-complexity algorithm based on joint ML estimation of the slot timing, of the multipath intensity profile and of the interference
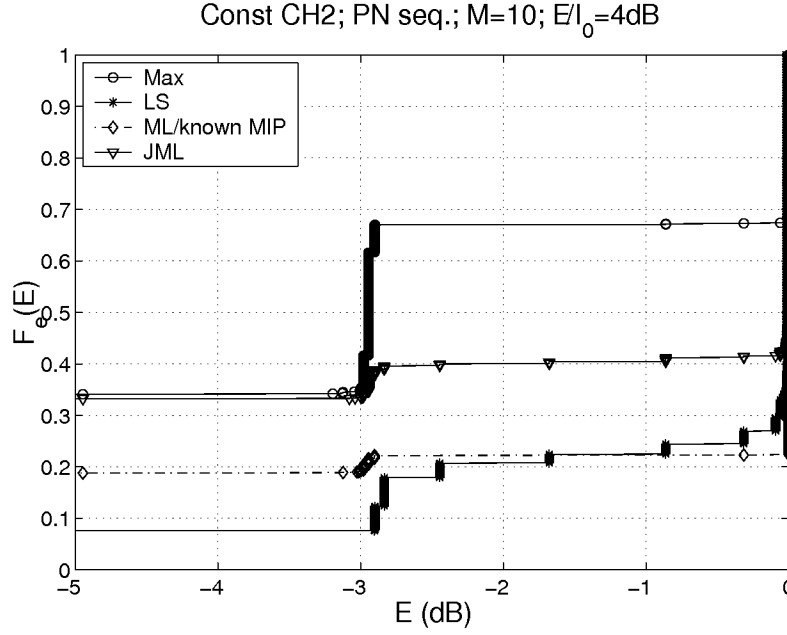
Const CH2; PN seq.; M=10; E/I$_0$=4dB

Figure 3.8: CDF with constant CH2 for $\mathcal{E}/I_0 = 4\,$dB and $M = 10$ accumulated bursts

plus noise power spectral density and we solved the likelihood function maximization problem by using the KKT conditions. Comparisons with other algorithms such as the simple peak detection, the ideal algorithm that exploits perfect knowledge of the channel multipath intensity profile and an approximated least-squares are provided. The proposed algorithm shows good performance in all the considered conditions, especially for very sparse channels and under fast fading conditions. Moreover it shows significant robustness to mismatch namely to the presence of constant channels and non-ideal acyclic autocorrelation properties of the pilot sequence.

3.A   Appendix

3.A.1   Proof of Proposition 1

We restate the maximization problem (3.15) more in general as follows. For arbitrary P, let $\{X_p : p = 0, \ldots, P-1\}$ be a non-increasing non-negative sequence, let $Q > P$ and $M > 1$ be arbitrary integers and let $\sum_{p=0}^{P-1} X_p < E_y < \frac{Q}{P} \sum_{p=0}^{P-1} X_p$. We want to maximize the function

$$f(\boldsymbol{\xi}, I_0) = \frac{1}{I_0} \left[\sum_{p=0}^{P-1} \frac{\xi_p}{1+\xi_p} X_p - E_y \right] - MQ \log I_0 - M \log \prod_{p=0}^{P-1} X_p$$

subject to $\boldsymbol{\xi} \geq \mathbf{0}$ and $I_0 \geq 0$.

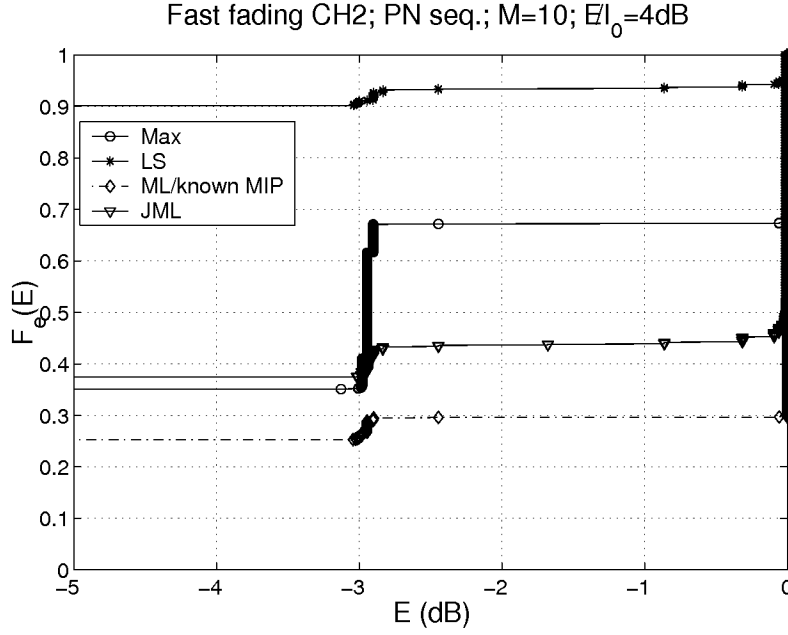The KKT necessary conditions for a (local) maximum point of the objective func-

Fast fading CH2; PN seq.; M=10; E/I$_0$=4dB

Figure 3.9: CDF with fast fading CH2 for $\mathcal{E}/I_0 = 4\,\mathrm{dB}$ and $M = 10$ accumulated bursts

tion in the constraint set yield the system of inequalities

$$\frac{\partial}{\partial \xi_i} f(\boldsymbol{\xi}, I_0) \leq 0, \qquad \text{for} \quad i = 0, \ldots, P - 1$$
$$\frac{\partial}{\partial I_0} f(\boldsymbol{\xi}, I_0) \leq 0 \tag{3.22}$$

where strict equality must hold if $\xi_i > 0$ or $I_0 > 0$.

By solving the inequality for ξ_i we obtain $\xi_i \geq X_i/(MI_0) - 1$. Since the RHS of the inequality for ξ_i is negative if $\xi_i = 0$ and $X_i/(MI_0) < 1$, we conclude that the solution is given by

$$\xi_i = \left[\frac{X_i}{\beta} - 1 \right]_+ \tag{3.23}$$

where we let $\beta = MI_0$. By substituting this into the inequality for I_0, we obtain

$$\beta = \frac{E_y - \sum_{p=0}^{D-1} X_p}{Q - D} \tag{3.24}$$

where $D \leq P$ is the minimum integer for which $X_D < \beta$. Notice that since $E_y > \sum_{p=0}^{P-1} X_p$, then $\beta > 0$ thus $I_0 > 0$ and (3.23), (3.24) satisfy the KKT necessary conditions.

Next, we prove that this solution exists and is unique. Finally, we prove that this is actually the *global* maximizer for our problem.

Existence. For $d = 1, \ldots, P$, let

$$\beta_d = \frac{E_y - \sum_{p=0}^{d-1} X_p}{Q - d} \tag{3.25}$$

and define the set $\mathcal{D}_d = \{X_p : X_p > \beta_d\}$. The solution (3.23), (3.24) exists if the equation $|\mathcal{D}_d| = d$ has a solution for some $D \in \{1, \ldots, P\}$.

By definition of β_d, we have that $X_0 > \beta_1$. If for $1 \leq p \leq P - 1$ the condition $X_p > \beta_p$ is never verified, then the solution is obviously $D = 1$. Otherwise, there must exist some $1 \leq p \leq P - 1$ such that $X_p > \beta_p$. Let d be the maximum of such indexes. We can write

$$
\begin{aligned}
X_d &> \beta_d \\
&= \frac{E_y - \sum_{p=0}^{d-1} X_p}{Q - d} \\
&= \frac{Q - d - 1}{Q - d - 1}\left(\frac{E_y - \sum_{p=0}^{d-1} X_p}{Q - d} + \frac{X_d}{Q - d} - \frac{X_d}{Q - d}\right) \\
&= \frac{Q - d - 1}{Q - d}\beta_{d+1} + \frac{X_d}{Q - d}
\end{aligned}
\tag{3.26}
$$

which implies $X_d > \beta_{d+1}$. Since by construction $d = \max\{p : X_p > \beta_p\}$, then $X_{d+1} \leq \beta_{d+1}$, which implies that $D = d + 1$ is a solution.

Uniqueness. Suppose that there exist $1 \leq D < D' \leq P$ such that $|\mathcal{D}_D| = D$ and $|\mathcal{D}_{D'}| = D'$, i.e.,

$$
\begin{cases}
X_p > \beta_D & \text{for } 0 \leq p \leq D - 1 \\
X_p \leq \beta_D & \text{for } D \leq p \leq P - 1
\end{cases}
\tag{3.27}
$$

and

$$
\begin{cases}
X_p > \beta_{D'} & \text{for } 0 \leq i \leq D' - 1 \\
X_p \leq \beta_{D'} & \text{for } D' \leq i \leq P - 1
\end{cases}
\tag{3.28}
$$

By following the same steps of (3.26) we can show that

$$
\beta_d > X_d \Rightarrow \beta_{d+1} > X_d
\tag{3.29}
$$

Then, starting from (3.27) we can write the chain of inequalities $\beta_D \geq X_D \Rightarrow \beta_{D+1} \geq X_D \geq X_{D+1} \Rightarrow \beta_{D+2} \geq X_{D+1} \geq X_{D+2} \Rightarrow \cdots \Rightarrow \beta_{D'} \geq X_{D'-1}$, which contradicts (3.28).

We conclude that the solution must be unique.

Global maximum. The function $f(\boldsymbol{\xi}, I_0)$ is not concave in $\mathbb{R}_+^{P+1}$. However, it is continuous on the (convex) constraint $\mathbb{R}_+^{P+1}$ and $f(\boldsymbol{\xi}, I_0) \to -\infty$ if any of its variables grows without bound. By continuity, the global maximum of $f(\boldsymbol{\xi}, I_0)$ is finite and the maximizer must have all finite components, therefore it must satisfy the necessary KKT conditions. Since the solution (3.23), (3.24) exists and is unique, it must be the global maximizer.

3.A.2   Proof of Proposition 2

Let $\{X_p : p = 0, 1, \ldots\}$ denote a sequence of non-increasing path energies. If for some D the condition (3.18) holds, then $\beta_D \geq X_p$ for all $p \geq D$ and, by Proposition 1, the function $\mathcal{L}(\boldsymbol{y}|\theta, \xi_0, \ldots, \xi_p, \tau_0, \ldots, \tau_p, I_0)$ for all $p \geq D$ is maximized with respect to the ξ_i's and I_0 by letting $\beta = \beta_D = (E_y - \sum_{i=0}^{D-1} X_i)/(Q - D)$, $I_0 = \beta/M$ and $\xi_i = [X_i/\beta - 1]_+$. Since β_D is determined only by the X_i's for $i = 0, \ldots, D-1$, by adding
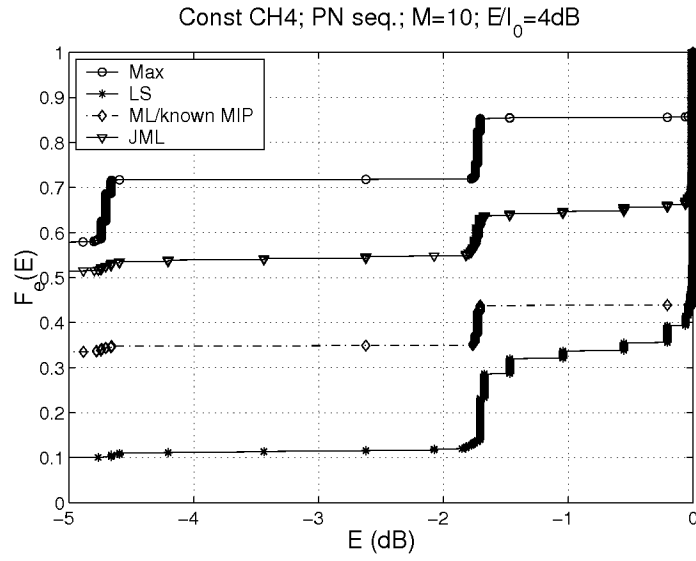
Figure 3.10: CDF with constant CH4 for $\mathcal{E}/I_0 = 4\,\text{dB}$ and $M = 10$ accumulated bursts
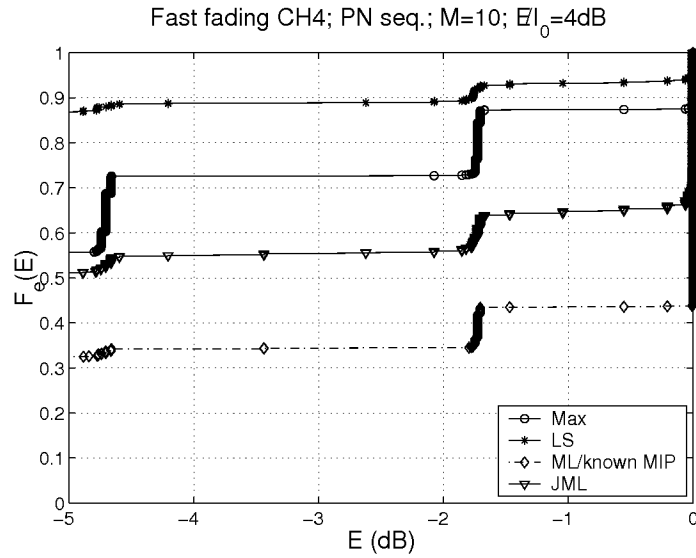

Figure 3.11: CDF with fast fading CH4 for $\mathcal{E}/I_0 = 4\,\text{dB}$ and $M = 10$ accumulated bursts
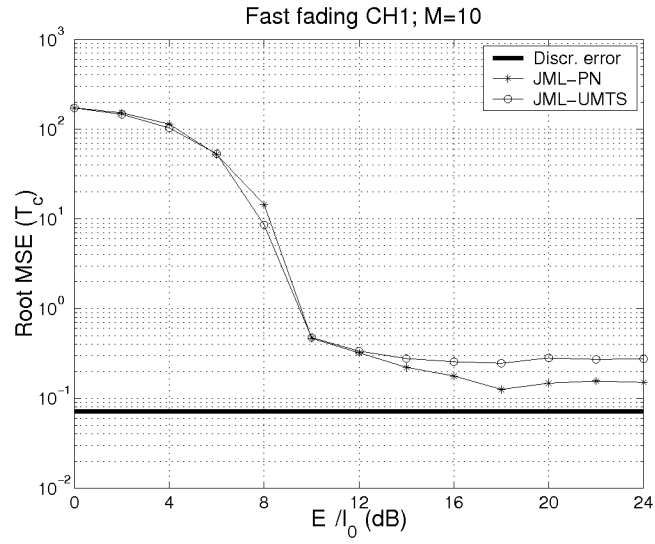
Figure 3.12: RMSE with fast fading CH1 vs. $\mathcal{E}/I_0$ for UMTS and PN sequences and $M = 10$ accumulated bursts
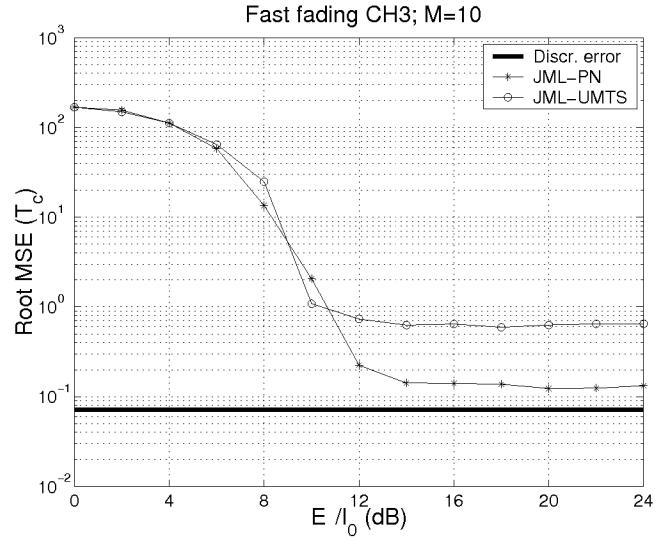

Figure 3.13: RMSE with fast fading CH3 vs. $\mathcal{E}/I_0$ for UMTS and PN sequences and $M = 10$ accumulated bursts

Table 3.1: Channel MIPs

MIP	Delays (T_c)	Variances (dB)
CH1	$(0, 1, 2, 3)$	$(0, -3, -6, -9)$
CH2	$(0, 7.5)$	$(0, 0)$
CH3	$(0, 1.12, 1.34, 4.85, 5.35, 5.62)$	$(-3, 0, -3, -5, -7, -8)$
CH4	$(0, 7.5, 15)$	$(0, 0, 0)$

more delays to the sequence $\tau_0, \ldots, \tau_{D-1}$ with received energy $X_p \leq \beta_D$ is not going to affect neither the value of β_D nor the value of the maximum $\overline{\mathcal{L}}(\boldsymbol{y}|\theta, \tau_1, \ldots, \tau_p)$.

Therefore, the only situation that must be taken into account is when, for given p, $\beta_p < X_{p-1}$ and we add a delay τ_p with received energy $X_p > \beta_p$. From the proof of Proposition 1 we have that

$$X_p > \beta_p \Rightarrow X_p > \beta_{p+1}$$

i.e., $\mathcal{L}(\boldsymbol{y}|\xi_0, \ldots, \xi_p, \tau_0, \ldots, \tau_p, I_0)$ is actually maximized by all $\xi_i > 0$, implying that $\overline{\mathcal{L}}(\boldsymbol{y}|\theta, \tau_0, \ldots, \tau_{p-1}) \neq \overline{\mathcal{L}}(\boldsymbol{y}|\theta, \tau_0, \ldots, \tau_p)$. Proposition 2 is proved by showing that

$$\overline{\mathcal{L}}(\boldsymbol{y}|\theta, \tau_0, \ldots, \tau_{p-1}) \leq \overline{\mathcal{L}}(\boldsymbol{y}|\theta, \tau_0, \ldots, \tau_p)$$

By using the fact that

$$\beta_{p+1} = \frac{Q-p}{Q-p-1}\left(\beta_p - \frac{X_p}{Q-p}\right)$$

and by letting $Q - p = k$ we have

$$\overline{\mathcal{L}}(\boldsymbol{y}|\theta, \tau_0, \ldots, \tau_p) - \overline{\mathcal{L}}(\boldsymbol{y}|\theta, \tau_0, \ldots, \tau_{p-1}) =$$

$$= -(k-1)\log\beta_{p+1} - \log\prod_{i=0}^{p} X_i + k\log\beta_p + \log\prod_{i=0}^{p-1} X_i$$

$$= -k\log\left[\frac{k}{k-1}\left(1 - \frac{X_p}{k\beta_p}\right)\right] + \log\left[\frac{k}{k-1}\left(\frac{\beta_p}{X_p} - \frac{1}{k}\right)\right]$$

$$= (k-1)\log\frac{1-1/k}{\beta_p/X_p - 1/k} + k\log\frac{X_p}{\beta_p}$$

$$> 0$$

since the arguments of both logarithms in the third line above are larger than 1. This concludes the proof.

Chapter 4

Iterative multiuser detection

We propose a low complexity multiuser joint Parallel Interference Cancellation (PIC) decoder and Turbo Decision Feedback Equalizer for CDMA. In our scheme, an estimate of the interference signal (both MAI and ISI) is formed by weighting the hard decisions produced by conventional (i.e., hard-output) Viterbi decoders. The estimated interference is subtracted from the received signal in order to improve decoding in the next iteration. By using asymptotic performance analysis of random-spreading CDMA, we optimize the feedback weights at each iteration. Then, we consider two (mutually related) performance limitation factors: the bias of residual interference and the ping-pong effect. We show that the performance of the proposed algorithm can be improved by compensating for the bias in the weight calculation, and we propose a modification of the basic PIC algorithm, which prevents the ping-pong effect and allows higher channel load and/or faster convergence to the single-user performance. The proposed algorithm is validated through computer simulation in an environment fully compliant with the specifications of the time-division duplex mode of 3rd generation systems, contemplating a combination of TDMA and CDMA and including frequency-selective fading channels, user asynchronism, and power control. The main conclusion of this work is that, for such application, Soft-Input Soft-Output (SISO) decoders (e.g., implemented by the forward-backward BCJR algorithm) are not needed to attain very high spectral efficiency, and simple conventional Viterbi decoding suffices for most practical settings.

4.1   Introduction and motivation

In both FDD and TDD modes of the UMTS standard, the basic receiver scheme contemplates the use of conventional Single-User Matched Filtering (SUMF). Since

39

Multiple-Access Interference is treated as additional background noise [1], powerful and high-complexity channel coding such as 256-states convolutional codes and turbo codes [29] are envisaged in order to attain low Bit Error Rates (BER) at low decoder input signal-to-interference plus noise ratio (SINR). In any case, channel loads larger than 1 user/chip are practically very difficult if not impossible to attain by the SUMF front-end and single-user decoding [9].

On the other hand, Information Theory shows that much larger channel loads can be achieved provided that a *non-linear* multiuser joint detector and decoder is employed [9, 10]. This may range from the impractically complex optimal joint decoder to practically appealing successive interference cancellation approaches [11, 12].

In practice, successive interference cancellation must cope with decision errors, which prevent perfect cancellation of already decoded users. Then, several *iterative* schemes have been proposed, which limit the deleterious effect of decision errors by feeding back soft-estimates of the detected symbols (see for example [30, 31, 32]). These schemes require Soft-Input Soft-Output (SISO) decoders, usually implemented by the forward-backward BCJR algorithm [33]. However, such SISO decoders represent a non-negligible factor in the complexity of whole receiver.

In real CDMA applications for either TDD and FDD modes, the maximum achievable channel load is often limited by synchronization and channel estimation issues, rather than by the ultimate capability of the decoder itself [34]. Hence, it makes sense to investigate simpler joint detection and decoding schemes, which outperform the conventional linear SUMF, MMSE and decorrelator, and non-linear Parallel Interference Cancellation (PIC) or Serial Interference Cancellation (SIC) receivers [35], and nevertheless yield performance similar to the SISO-based schemes at lower decoding complexity.

Driven by this consideration, this Chapter proposes a low complexity iterative multiuser receiver, where SISO decoders are replaced by simpler standard (i.e. hard-output) Viterbi decoders. The Viterbi hard decisions are weighted and fed back to the interference cancellation stage. By using large-system analysis of random CDMA [36] we optimize the feedback weights at each iteration such that the SINR at the decoders input of the next iteration is maximized.

We address the problem of bias of residual interference [37, 38] and of the *ping-pong* effect [35, 39] and we show that the performance of the proposed algorithm can be improved by compensating for the bias in the weight calculation and by modifying the basic PIC algorithm in order to prevent the ping-pong effect. These modifications allow higher channel load and/or faster convergence to the single-user performance at almost no additional computational cost.

We validate the proposed receiver algorithm in UMTS-TDD realistic scenarios, including asynchronous transmission, frequency selective fading channels and power control. In this regime, the proposed receiver performs very close to the single user (i.e., MAI-free) Matched Filter Bound (i.e., ISI-free) performance, even for large channel load.

The remainder of this Chapter is organized as follows: Section 4.2 gives a description of the system model. Section 4.3 describes the large system asymptotic analysis.

---

[1]Notice that the only difference between the SUMF and the linear MMSE fi lter is that the latter treats MAI as colored noise while the former treats it as white noise [8].

Based on the latter, the feedback optimal weights are derived in Section 4.4 for synchronous and flat channels, taking into account the bias on the residual interference and ping-pong effect for large channel load. Section 4.5 deals with asynchronous transmission and frequency selective fading channels. Finally in Section 4.6 conclusions are pointed out.

4.2 System model

We consider the uplink of a DS-CDMA system where U users send *encoded* information to a common receiver. The baseband transmission chain for the uth user is depicted in Figure 2.4. Source bits are channel-encoded and organized in codewords of length N bits. The codewords are then interleaved and modulated with transmitted energy per symbol $\mathcal{E}_u$. For simplicity we assume that all users make use of convolutional coding and BPSK modulation. Let $a_u[n]$, the nth symbol generated by the uth user, be in the set $\{-1, +1\}$, and

$$a_u = \left[a_u[0], a_u[1], \ldots, a_u[N-1] \right]^{\text{T}}$$

represent the code word of user u *after interleaving*. The symbols are then spread by the spreading sequence

$$s_u = \left[s_u[0], s_u[1], \ldots, s_u[L-1] \right]^{\text{T}}$$

We assume all the users have the same spreading factor (number of chips per symbol) L and unitary energy sequences, that is,

$$s_u^{\text{H}} s_u = 1$$

$\forall u = 1, \ldots, U$. If the chip pulse-shaping filter is $\psi(t)$ and is common to all the users, then the uth baseband continuous-time transmitted signal is

$$x_u(t) = \sqrt{\mathcal{E}_u} \sum_{n=0}^{N-1} a_u[n] \sum_{l=0}^{L-1} s_u[l] \psi(t - lT_c - nT) \tag{4.1}$$

where T_c is the chip period and $T = LT_c$ is the symbol period.

We focus on UMTS-TDD, where users are synchronous at the slot level but asynchronous at the chip level. The channels are considered random but slowly varying and constant over one slot. Moreover, for the sake of simplicity, we assume that the convolutional codewords span a single slot.

Thus, the uth user signal is sent through the channel $h_u(t)$ with impulse response given by

$$h_u(t) = \sum_{p=0}^{P_u-1} c_{u,p} \delta(t - \tau_{u,p}) \tag{4.2}$$

where P_u is the number of resolvable paths, $\tau_{u,p}$ is the pth path delay, and $c_{u,p}$ is the pth path coefficient assumed a Gaussian complex circularly symmetric random variable
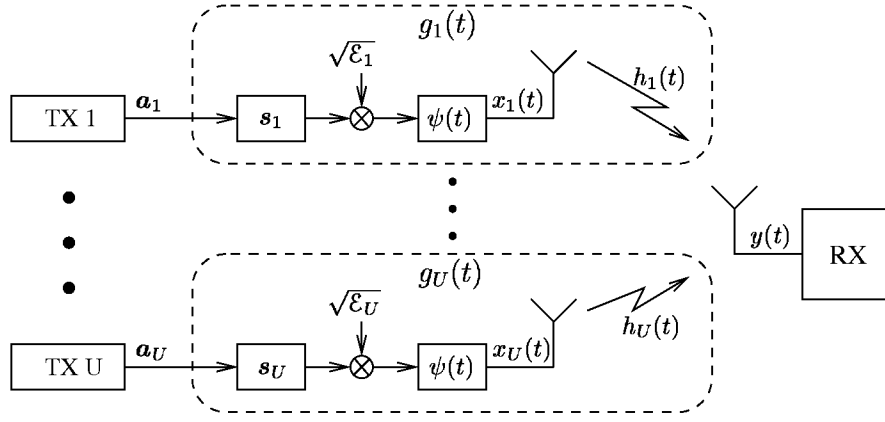
Figure 4.1: Transmission channel

with distribution $\mathcal{N}_\mathbb{C}(0, \sigma_{u,p}^2)$ where $\sigma_p^2 = \mathrm{E}[|c_{u,p}|^2]$. This model takes into account also users' asynchronous transmission, where the relative delays between users are included into the channel path delays.

The signal at the receiver is given by

$$y(t) \;=\; \sum_{u=1}^{U} \int_{-\infty}^{+\infty} x_u(\tau) h_u(t - \tau)\, \mathrm{d}\tau + \nu(t) \tag{4.3}$$

$$=\; \sum_{u=1}^{U} \sum_{n=0}^{N-1} a_u[n]\, g_u(t - nT) + \nu(t) \tag{4.4}$$

where $\nu(t)$ is the Gaussian noise and $g_u(t)$ is defined by

$$g_u(t) = \sqrt{\mathcal{E}_u} \sum_{l=0}^{L-1} s_u[l] \sum_{p=0}^{P_u-1} h_{u,p}\, \psi(t - lT_c - \tau_{u,p}) \tag{4.5}$$

and represents the overall channel impulse response for the uth user as depicted in Figure 4.1.

The signal $y(t)$ is sampled by the receiver at rate N_c/T_c, an integer multiple of the chip-rate, where N_c is a suitable integer chosen in order to satisfy the Nyquist criterion.

The discrete time version of $g_u(t)$, sampled at rate N_c/T_c, may have an infinite support but most of its energy is concentrated in a finite interval. This interval depends on the channel maximum delay spread, on the pulse-shaping filter $\psi(t)$, and on the spreading factor L. After a suitable truncation we can represent the discrete-time channel impulse response as a vector

$$\boldsymbol{g}_u = \Big[g_u[0], \ldots, g_u[N_g - 1] \Big]^{\mathrm{T}}$$

$\forall u = 1, \ldots, U$ where N_g is the maximum discrete-time channel length of all user channels. Subject to these assumptions, the received discrete-time baseband signal
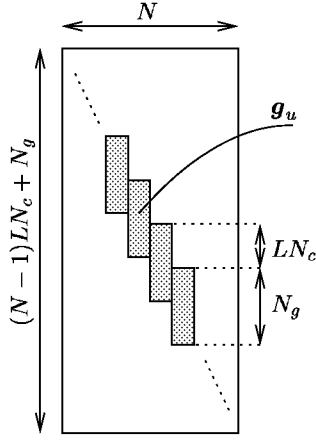
Figure 4.2: Structure of the matrix G_u

can be written as follows

$$y = \sum_{u=1}^{U} G_u a_u + \nu = Ga + \nu \tag{4.6}$$

where

- $y = \left[y[0], \ldots, y[(N-1)LN_c + N_g]\right]^{\mathrm{T}}$ is the vector of the received signal samples.

- G is a $((N-1)LN_c + N_g) \times UN$ matrix given by $G = [G_1, \ldots, G_U]$ where the $((N-1)LN_c + N_g) \times N$ matrices G_u contain, in each column, a shift of the vector g_u as shown in Figure 4.2.

- $a = \left[a_1^{\mathrm{T}}, \ldots, a_U^{\mathrm{T}}\right]^{\mathrm{T}}$ is the concatenation of the U user codewords.

- $\nu = \left[\nu[0], \ldots, \nu[(N-1)LN_c + N_g]\right]^{\mathrm{T}}$ contains the noise samples where the $\nu[i]$'s are i.i.d. circularly symmetric complex Gaussian random variables with distribution $\nu \sim \mathcal{N}_{\mathbb{C}}(0, I_0 I)$.

For the sake of simplicity, the receiver front-end is constrained to be the conventional Single User Matched Filter (SUMF) [8] given by the matrix G^{H}.[2] The matched filter performs at the same time pulse-shape matched filtering, channel matched filtering, and despreading. The output of the bank of SUMFs is given by [8]

$$
\begin{aligned}
z &= \mathrm{Re}\left\{G^{\mathrm{H}} y\right\} \\
&= \mathrm{Re}\left\{G^{\mathrm{H}} Ga + G^{\mathrm{H}} \nu\right\} \\
&= Ra + v \tag{4.7}
\end{aligned}
$$

where

---

[2]Some works as for example [31] and [32] consider linear MMSE front-end.

- $z = \left[z_1^{\mathrm{T}}, \ldots, z_U^{\mathrm{T}}\right]^{\mathrm{T}}$ and $z_u = \left[z_u[0], \ldots, z_u[N-1]\right]^{\mathrm{T}}$ for $u = 1, \ldots, U$ is the concatenation of the U matched filter outputs.

- R is the $UN \times UN$ cross-correlation matrix given by $R = \mathrm{Re}\left\{G^{\mathrm{H}}G\right\}$ where $(\cdot)^{\mathrm{H}}$ denotes the Hermitian operator.

- the noise term, $v = \left[v_1^{\mathrm{T}}, \ldots, v_U^{\mathrm{T}}\right]^{\mathrm{T}}$ is given by $v = \mathrm{Re}\left\{G^{\mathrm{H}}\nu\right\}$ and has distribution $v \sim \mathcal{N}(0, \frac{I_0}{2}R)$. The vector

$$v_u = \mathrm{Re}\left\{G_u^{\mathrm{H}}\nu\right\} = \left[v_u[0], \ldots, v_u[N-1]\right]^{\mathrm{T}}$$

represents the additive colored noise contribution after the uth matched filtering.

In particular, the SUMF output for the nth symbol of the uth user is given by

$$z_u[n] = z[uN + n] = \sum_{k=0}^{UN-1} R[uN + n, k]a[k] + v[UN + n] \qquad (4.8)$$

The matrix R is Hermitian and contains U^2 blocks of size $N \times N$ each. In the following, $R_{u,v}$ indicates the $(u, v)^{\mathrm{th}}$ block given by

$$R_{u,v} = \mathrm{Re}\left\{G_u^{\mathrm{H}}G_v\right\} \qquad (4.9)$$

The $[i, j]$ entry of $R_{u,v}$ is given by

$$R_{u,v}[i, j] = R[uN + i, vN + j] = \sum_{k=0}^{N_g} \mathrm{Re}\left\{g_u^*[k]g_v[k + (j - i)LN_c]\right\} \qquad (4.10)$$

From the structure of G_u, depicted in Figure 4.2, and from (4.10) it is clear that the matrices $R_{u,v}$ are banded with $2D + 1$ non-zero diagonals where

$$D = \left\lfloor \frac{N_g}{LN_c} \right\rfloor \qquad (4.11)$$

Notice that since $R_{u,v}[i, j]$ depends only on the difference $(j - i)$, $R_{u,v}$ is uniquely defined by the vector $r_{u,v} = \left[r_{u,v}[-D], \ldots, r_{u,v}[0], \ldots, r_{u,v}[+D]\right]^{\mathrm{T}}$ where
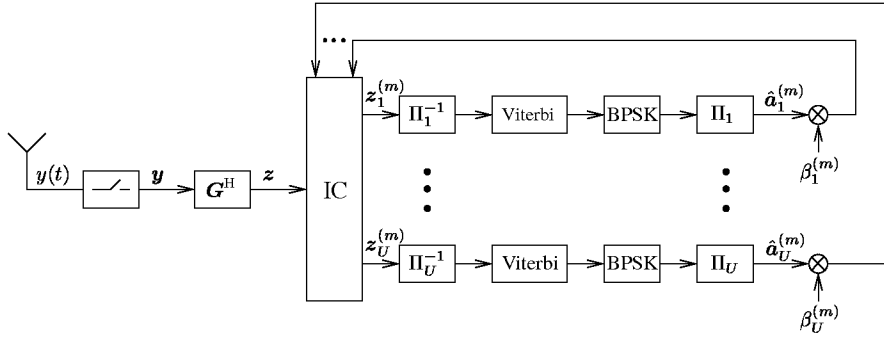
$$r_{u,v}[j - i] = R_{u,v}[i, j]$$

Figure 4.3: Scheme of the proposed turbo multiuser receiver

Hence, using (4.7) and the above considerations it is possible to rewrite (4.8) as

$$
\begin{aligned}
z_u[n] &= \sum_{v=0}^{U-1} \sum_{k=0}^{N-1} \boldsymbol{R}_{u,v}[n,k] a_v[k] + v_u[n] \\
&= \sum_{v=0}^{U-1} \sum_{d=-D}^{D} \boldsymbol{R}_{u,v}[n, n+d] a_v[n+d] + v_u[n] \\
&= \sum_{v=0}^{U-1} \sum_{d=-D}^{D} r_{u,v}[d] a_v[n+d] + v_u[n] \\
&= |\boldsymbol{g}_u|^2 a_u[n] + \underbrace{\sum_{\substack{d=-D \\ d\neq 0}}^{D} r_{u,u}[d] a_u[n+d]}_{\text{ISI}} + \underbrace{\sum_{\substack{v=0 \\ v\neq u}}^{U-1} \sum_{d=-D}^{D} r_{u,v}[d] a_v[n+d]}_{\text{MAI}} + v_u[n]
\end{aligned}
$$

(4.12)

where the first term is the useful symbol, the second term denotes the Inter Symbol Interference (ISI), the third term is the MAI, and the last term is the colored noise.

The SUMF output feeds the proposed iterative multiuser detector-decoder depicted in Figure 4.3. After SUMF, the signal z passes through an Interference Cancellation (IC) stage that uses the estimates $\hat{a}_u^{(m)}[n]$ of the symbols $a_u[n]$ to remove ISI and MAI (the superscript (m) denotes m^{th} iteration). The hard decisions $\hat{a}_u^{(m)}[n] \in \{\pm 1\}$ are provided by a bank of Viterbi decoders, whose outputs are weighted by a factor $\beta_u^{(m)} \in [0,1]$. Thus, the signal at the output of the IC stage in the mth iteration is given by

$$
\begin{aligned}
z_u^{(m)}[n] &= z_u[n] \\
&\quad - \left(\sum_{\substack{d=-D \\ d\neq 0}}^{D} r_{u,u}[d] \beta_u^{(m)} \hat{a}_u^{(m)}[n+d] + \sum_{\substack{v=0 \\ v\neq u}}^{U-1} \sum_{d=-D}^{D} r_{u,v}[d] \beta_v^{(m)} \hat{a}_v^{(m)}[n+d] \right) \\
&= |\boldsymbol{g}_u|^2 a_u[n] + \zeta_u^{(m)}[n] + v_u[n]
\end{aligned}
$$

(4.13)

where

$$
\begin{aligned}
\zeta_u^{(m)}[n] = &\sum_{\substack{d=-D \\ d\neq 0}}^{D} r_{u,u}[d] \left(a_u[n+d] - \beta_u^{(m)}\hat{a}_u^{(m)}[n+d] \right) \\
&+ \sum_{\substack{v=0 \\ v\neq u}}^{U-1} \sum_{d=-D}^{D} r_{u,v}[d] \left(a_v[n+d] - \beta_v^{(m)}\hat{a}_v^{(m)}[n+d] \right)
\end{aligned}
\tag{4.14}
$$

is the residual MAI+ISI at iteration m, and $v_u[n] \sim \mathcal{N}\left(0, \frac{I_0|\boldsymbol{g}_u|^2}{2} \right)$.

Equation (4.13) shows that the IC stage performs at the same time MAI suppression and also non-causal Decision Feedback Equalization (DFE) by removing from the nth symbol the contributions due to the past and future symbols of the same user.

At the first iteration, the initial estimated symbols are set to zero, $\hat{a}_u^{(0)}[n] = 0$, $u = 0, 1, \ldots, U-1$ and $n = 0, \ldots, N-1$ so that $z_u^{(0)}[n] = z_u[n]$. In the case of perfect symbol estimates and $\beta_u^{(m)} = 1$, equation (4.13) reduces to

$$
z_u^{(m)}[n] = |\boldsymbol{g}_u|^2 \, a_u[n] + v_u[n]
\tag{4.15}
$$

where the MAI and ISI are completely removed and the single-user Matched Filter Bound (MFB) performance for user u is attained. For later use, we define the normalized received instantaneous channel energy for user u as $\gamma_u = \frac{|\boldsymbol{g}_u|^2}{\mathcal{E}_u}$, such that $E[\gamma_u] = 1$, and the single-user MFB instantaneous SNR for user u as

$$
\text{SNR}_u^{\text{MFB}} = \frac{2\mathcal{E}_u}{I_0}\gamma_u
\tag{4.16}
$$

Intuitively, the weighting factors $\beta_u^{(m)}$ should depend on the reliability of the estimated symbols $\hat{a}_u^{(m)}[n]$ and be equal to 1 or to 0 in the case of completely reliable or completely unreliable symbol estimates, respectively. In the next Section we make this statement precise by studying the performance of an idealized synchronous system in the large-system limit.

4.3   Large system asymptotic analysis

Rigorous asymptotic analysis of this iterative scheme in the large-system limit (i.e., for $N, U, L \to \infty$ with finite ratio $U/L = \alpha$ and $U/N \to 0$), for single-path channels and synchronous users is proposed in [37]. This analysis is based on the general approach of density evolution over graphs: a standard analysis tool for evaluating the asymptotic performance of message-passing iterative decoders [40], and makes use of results from the theory of large random matrices developed in [36] for the analysis of linear receivers with randomly spread CDMA in the large-system limit. In [37] it is also shown that this analysis holds only if the symbol estimates $\hat{a}_u^{(m)}[n]$ are functions of the decoder *extrinsic information* [41]. The decoder extrinsic information is defined for a SISO decoder based on the sum-product algorithm [42], such as the BCJR algorithm, but it is not defined for an ML decoder such as the Viterbi algorithm. Hence,

we shall optimize the weights $\beta_u^{(m)}$ for a *fictitious* receiver where the Viterbi decoders are replaced by BCJR decoders and the hard decisions $\hat{a}_u^{(m)}[n]$ are obtained by one-bit quantization of the extrinsic likelihood ratios produced by the latter.

We hasten to say that the fictitious receiver is used as a reference but has no practical relevance, for the obvious reason that if BCJR decoders are used, then much more efficient soft-estimation of the interfering symbols as in [30, 31, 32] is possible. However, as it will be clear from the rest of this section, the weight optimization based on the asymptotic analysis of the fictitious receiver allows us to derive a very simple expression for the optimal weights, independent of the user sequences and their mutual correlations, and a very simple practical algorithm for calculating these weights.

We make the following assumptions:

- complex random spreading sequences formed by i.i.d. chips uniformly distributed over the QPSK constellation;

- users are slot and chip synchronous;

- equal received expected energy per symbol $\mathcal{E}$ for each user;

- frequency-flat identically distributed propagation channels;

- we let $N, U, L \to \infty$ with $U/L = \alpha$ (α denotes the *channel load*);

- the empirical distribution of the user received normalized powers, defined by [36]

$$F_\gamma^{(U)}(z) = \frac{1}{U} \sum_{u=1}^{U} 1\{\gamma_u \leq z\} \tag{4.17}$$

converges weakly to a given non-random cumulative distribution function $F_\gamma(z)$, for $U \to \infty$.

With the above assumptions, for a user u randomly selected with uniform probability in the user population, we have $\text{SNR}_u^{\text{MFB}} = \frac{2\mathcal{E}}{I_0}\gamma_u$ where γ_u is a random variable distributed (in the limit of large U) according to $F_\gamma(z)$.

Under these conditions, the SINR at the decoders input in the mth iteration for the fictitious receiver can be written as follows [37]

$$\text{SINR}_u^{(m)} = \eta^{(m)}\text{SNR}_u^{\text{MFB}} = \eta^{(m)}\frac{2\mathcal{E}}{I_0}\gamma_u \tag{4.18}$$

where

$$\eta^{(m)} = \frac{1}{1 + \alpha\frac{\mathcal{E}}{I_0}\mu^{(m)}} \tag{4.19}$$

is the degradation factor paid by any user with respect to its single-user MFB performance, and where

$$\mu^{(m)} = \text{E}\left[\gamma\left|a - \beta^{(m)}\hat{a}^{(m)}\right|^2\right] \tag{4.20}$$

is the average variance of the residual interfering symbols. In (4.20), a denotes a coded symbol of a generic user received at instantaneous power γ, and $\hat{a}^{(m)}$ denotes the hard decision relative to a at the decoder output. Expectation in (4.20) is with

respect to $a \sim$ uniform over $\{\pm 1\}$, $\hat{a}^{(m)}$ distributed as the hard decision about a at the decoder output, and $\gamma \sim F_\gamma(z)$. We refer to $\eta^{(m)}$ as the Multiuser Efficiency (ME) [8] at iteration m. Clearly, the single-user MFB performance is achieved for all users if $\lim_{m \to \infty} \eta^{(m)} = 1$.

We can optimize the weighting factor $\beta^{(m)}$ as a function of the channel energy γ in order to minimize the expected interference variance $\mu^{(m)}$ at every iteration. Therefore, for each iteration m we seek the solution of the simple optimization problem

$$\min_{\beta=\beta(\gamma)} \quad \mathrm{E}\left[\left| a - \beta \hat{a}^{(m)} \right|^2 \Big| \gamma \right] \tag{4.21}$$

By expanding the above conditional expectation, we get

$$1 + \beta^2 - 2\beta \mathrm{E}[a\hat{a}^{(m)}|\gamma]$$
$$1 + \beta^2 - 2\beta \left[(+1)(1 - \epsilon^{(m)}(\gamma)) + (-1)\epsilon^{(m)}(\gamma) \right]$$
$$1 + \beta^2 - 2\beta \left(1 - 2\epsilon^{(m)}(\gamma) \right) \tag{4.22}$$

where $\epsilon^{(m)}(\gamma)$ is the Symbol Error Rate (SER) of a decoder with an input signal-to-noise ratio $\mathrm{SINR}^{(m-1)} = \eta^{(m-1)}\frac{2\mathcal{E}}{I_0}\gamma$. The solution of (4.21) is easily obtained as

$$\beta^\star(\gamma) = 1 - 2\epsilon^{(m)}(\gamma) \tag{4.23}$$

Assuming that the residual interference plus noise at iteration m is Gaussian [3] the SER is a known function $f(\cdot)$ of the decoder input SINR. We shall refer to $f(\cdot)$ as the *SER characteristic* of the user code (see Appendix 4.A). Thus, for user u at iteration m the optimal weighting factor is given by

$$\beta_u^{(m)} = \beta^\star(\gamma_u) = 1 - 2f\left(\eta^{(m-1)}\frac{2\mathcal{E}}{I_0}\gamma_u \right) \tag{4.24}$$

The resulting minimized average interference variance is given by

$$\mu^{(m)} = 4\mathrm{E}\left[\gamma f\left(\eta^{(m-1)}\frac{2\mathcal{E}}{I_0}\gamma \right)\left(1 - f\left(\eta^{(m-1)}\frac{2\mathcal{E}}{I_0}\gamma \right) \right) \right] \tag{4.25}$$

where expectation is with respect to $\gamma \sim F_\gamma(z)$.

The behavior of the asymptotic system is described by the evolution of the ME and it can be represented by the one-dimensional non-linear dynamical system $\eta^{(m)} = \Psi(\eta^{(m-1)})$ with initial condition $\eta^{(0)} = \frac{1}{1+\alpha\mathcal{E}/I_0}$, and where mapping function $\Psi(\cdot)$ is defined by

$$\Psi(\eta) = \frac{1}{1 + 4\alpha\frac{\mathcal{E}}{I_0}\mathrm{E}\left[\gamma f\left(\eta\frac{2\mathcal{E}}{I_0}\gamma \right)\left(1 - f\left(\eta\frac{2\mathcal{E}}{I_0}\gamma \right) \right) \right]} \tag{4.26}$$

It can be easily checked that, since $f(\cdot)$ has range $[0, 1/2]$ and it is non-increasing, then $\Psi(\eta)$ has range $[\eta^{(0)}, 1]$ and it is non-decreasing. Therefore, the dynamical system

---

[3]In the large-system limit and under mild technical conditions this assumption is valid, as shown rigorously in [43].
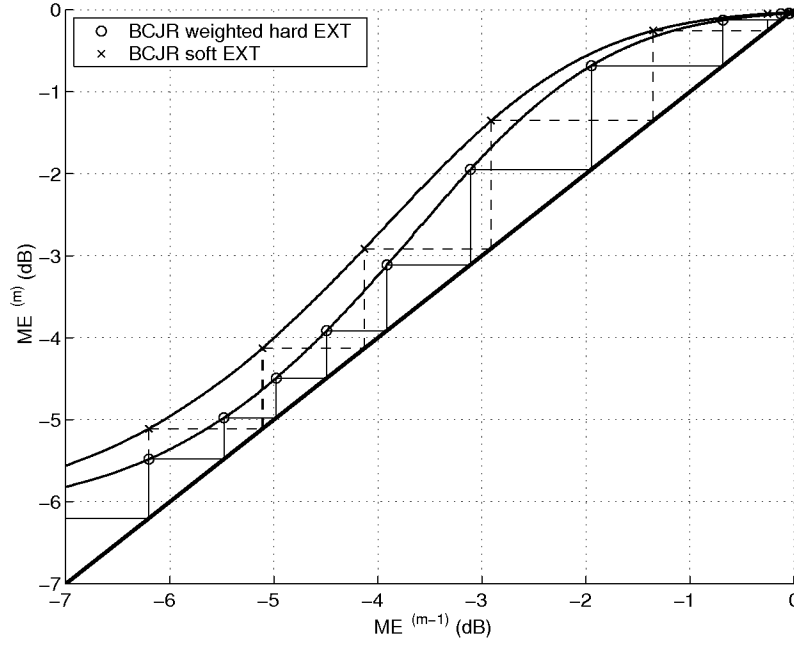
Figure 4.4: Evolution of the ME given by asymptotic analysis for $CC(5,7)$, $\alpha = 2$, and $E_b/I_0 = 5$dB

defined by $\Psi(\eta)$ with initial condition $\eta^{(0)}$ has at least one stable fixed point in the interval $[\eta^{(0)}, 1]$, and the sequence $\{\eta^{(m)}\}_{m=0}^{\infty}$ is non-decreasing and upper bounded by 1. The limit $\eta^* = \lim_{m\to\infty} \eta^{(m)} \leq 1$ exists and is equal to the left-most stable fixed point of the system in the interval $[\eta^{(0)}, 1]$.

As an example, Figure 4.4 shows the function $\Psi(\eta)$ for channel load $\alpha = 2$, $E_b/I_0 = 5$dB, constant instantaneous received power (i.e. $\gamma_u = 1$ for all users), and the 4-states convolutional code of rate $1/2$ and octal generators $\{5,7\}$ (denoted in the following by $CC(5,7)$). For the sake of comparison, we show also the evolution of the same system when the BCJR decoder provides soft extrinsic estimates as proposed in [30]. The $\Psi(\eta)$ function in this case is derived in [37]. The limit η^* in this case is very close to 1, meaning that all users attain near-single-user performance. Notice that soft feedback assures a faster decoder convergence to the single-user performance.

When the channel load is increased, the Ψ curves are modified so that for a certain threshold channel load α, the curve corresponding to weighted hard decisions is tangent to the diagonal, as shown in Figure 4.5. This means that the system has reached its maximum load and is not able to converge to near-single-user performance. On the contrary, the system using soft decisions still converges to single user performance. This shows that SISO decoding and soft feedback also provides a higher threshold channel load, i.e., a larger overall maximum achievable spectral efficiency of the system.
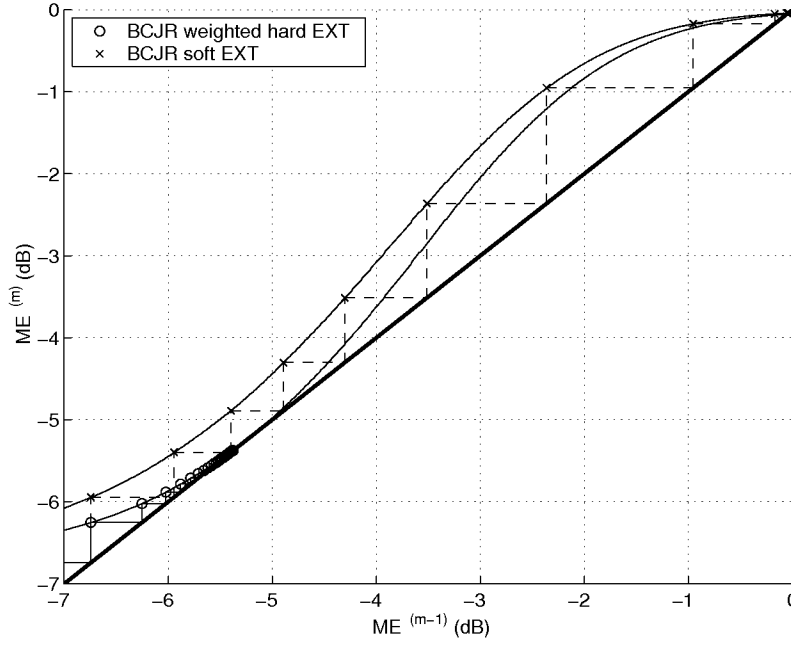
Figure 4.5: Evolution of the ME given by asymptotic analysis for $CC(5,7)$, $\alpha = 2.35$, and $E_b/I_0 = 5$dB

4.4   Implementation of the proposed receiver

4.4.1   The basic algorithm

The performance of the proposed receiver depends on the computation of the weighting factors $\beta_u^{(m)}$ which do depend on a reliable SINR estimation. Driven by the asymptotic analysis of the previous section, we propose to compute the weighting factor for the uth user at iteration m as

$$\beta_u^{(m)} = 1 - 2f\left(\widehat{\text{SINR}}_u^{(m-1)}\right) \tag{4.27}$$

where $f(\cdot)$ is the (known) SER code characteristics, and $\widehat{\text{SINR}}_u^{(m)}$ is the estimated SINR at the uth decoder input of the mth iteration. In order to estimate the input SINR, we can use the estimator proposed in [44], given by

$$\widehat{\text{SINR}}_u^{(m)} = \frac{1}{\frac{1}{N}\sum_{n=0}^{N}\left|\tilde{z}_u^{(m)}[n]\right|^2 - 1} \tag{4.28}$$

where $\tilde{z}_u^{(m)} = \frac{z_u^{(m)}}{|g_u|^2}$.

In [44] it is shown that

$$\xi_u^{(m)} = \frac{1}{N}\sum_{n=0}^{N}\left|z_u^{(m)}[n]\right|^2 - |g_u|^2$$

is an unbiased estimator of the residual MAI plus ISI plus noise variance at the decoder input if $\zeta_u^{(m)}[n]$ is uncorrelated with the desired variable $a_u[n]$. Remarkably, in this case, the MSE of this estimator is very close to that of the ML estimator assuming known useful symbols, given by $\frac{1}{N}\sum_{n=0}^{N}\left|z_u^{(m)}[n]-|\boldsymbol{g}_u|^2 a_u[n]\right|^2$ (which is not applicable here, since the symbols $a_u[n]$ are unknown).

When the symbol estimates $\hat{a}_u^{(m)}[n]$ are provided by a decision statistics *containing* the current observation interval, such as in the Viterbi decoder, then the residual interference term given by (4.14) is conditionally biased given $a_u[n]$, that is,

$$\mathrm{E}\left[\zeta_u^{(m)}[n]\,|\,a_u[n]\right]=\delta_u^{(m)}a_u[n] \tag{4.29}$$

where the bias coefficient $\delta_u^{(m)}$ is non-positive and depends on the system parameters and on the user and iteration indexes as shown in [37, 38]. The bias is not negligible especially for high channel load α even in the absence of ISI and the bias reduces the energy of the useful signal at iteration m by a factor $\left(1+\frac{\delta_u^{(m)}}{|\boldsymbol{g}_u|^2}\right)^2$.

On the contrary, if the symbol estimates $\hat{a}_u^{(m)}[n]$ are provided by estimates *not containing* the current observation interval, i.e., they are based on the decoder *extrinsic information* [37, 45], then in the limit for large block length (i.e., $N\to\infty$) and random interleaving, the residual interference is conditionally unbiased, i.e.

$$\mathrm{E}\left[\zeta_u^{(m)}[n]\,|\,a_u[n]\right]=0$$

We can rewrite the input of the uth decoder at iteration m given in (4.13) as

$$z_u^{(m)}[n]=\left(|\boldsymbol{g}_u|^2+\delta_u^{(m)}\right)a_u[n]+\widetilde{\zeta}_u^{(m)}[n]+v_u[n] \tag{4.30}$$

where $\widetilde{\zeta}_u^{(m)}[n]$ is uncorrelated with $a_u[n]$.

Hence, the true SINR in the presence of bias is given by

$$\mathrm{SINR}_u^{(m)}=\frac{\left(|\boldsymbol{g}_u|^2+\delta_u^{(m)}\right)^2}{\mathrm{E}\left[\left|\widetilde{\zeta}_u^{(m)}[n]+v_u[n]\right|^2\right]}=\frac{\left(|\boldsymbol{g}_u|^2+\delta_u^{(m)}\right)^2}{\sigma_\zeta^2} \tag{4.31}$$

where we define $\sigma_\zeta^2=\mathrm{E}\left[\left|\widetilde{\zeta}_u^{(m)}[n]+v_u[n]\right|^2\right]$. Now, the SINR estimator proposed in (4.28), in the presence of bias and for large N, converges in probability to

$$\widehat{\mathrm{SINR}}_u^{(m)}\to\frac{1}{\mathrm{E}\left[\left|\frac{\widetilde{\zeta}_u^{(m)}[n]+v_u[n]}{|\boldsymbol{g}_u|^2}\right|^2\right]+\left(1+\frac{\delta_u^{(m)}}{|\boldsymbol{g}_u|^2}\right)^2-1}$$

Since $\delta_u^{(m)}\le 0$ (i.e., the bias tends to decrease the useful signal term), we conclude that the estimator (4.28) tends to overestimate the SINR at the decoder input. As a consequence, the weights $\beta_u^{(m)}$ computed according to (4.27) are mismatched in the presence of bias.

4.4.2 Estimation of the bias

In order to overcome this problem, a better SINR estimation taking into account the bias of residual interference is required. The term σ_ζ^2 in (4.31) appears also in the variance of the decoder input signal, given by

$$\sigma_{z_u}^{(m)\,2} = \mathrm{E}\left[\left|z_u^{(m)}[n]\right|^2\right] = \left(|g_u|^2 + \delta_u^{(m)}\right)^2 + \sigma_\zeta^2 \qquad (4.32)$$

and the bias term $\delta_u^{(m)}$ is contained in the expression of the correlation between the symbol estimates and the decoder input, that, recalling (4.30), is given by

$$
\begin{aligned}
\phi_u^{(m)} &= \mathrm{E}\left[z_u^{(m)}[n]\hat{a}_u[n]\right] \\
&= \left(1 - 2f\left(\mathrm{SINR_u}^{(m-1)}\right) + \Gamma\left(\mathrm{SINR_u}^{(m-1)}\right)\right)\left(|g_u|^2 + \delta_u^{(m)}\right)
\end{aligned}
$$
$$(4.33)$$

where $\Gamma(\cdot)$ is a known characteristic function of the convolutional code, proportional to the correlation between the symbol estimates and the interference (see Appendix 4.A).

Using (4.31) and (4.32) the correlation in equation (4.33) can be rewritten as

$$
\begin{aligned}
\phi_u^{(m)} &= \left(|g_u|^2 + \delta_u^{(m)}\right) \cdot \\
&\quad \cdot \left[1 - 2f\left(\frac{\left(|g_u|^2 + \delta_u^{(m)}\right)^2}{\sigma_{z_u}^{(m)\,2} - \left(|g_u|^2 + \delta_u^{(m)}\right)^2}\right) + \Gamma\left(\frac{\left(|g_u|^2 + \delta_u^{(m)}\right)^2}{\sigma_{z_u}^{(m)\,2} - \left(|g_u|^2 + \delta_u^{(m)}\right)^2}\right)\right]
\end{aligned}
$$
$$(4.34)$$

In practice, an approximation of $\sigma_{z_u}^{(m)\,2}$ and $\phi_u^{(m)}$ can be computed as follows

$$\sigma_{z_u}^{(m)\,2} \approx \frac{1}{N}\sum_{n=0}^{N-1}\left(z_u^{(m)}[n]\right)^2$$

$$\phi_u^{(m)} \approx \frac{1}{N}\sum_{n=0}^{N-1} z_u^{(m)}[n]\hat{a}_u[n]$$

and (4.34) can be solved numerically for $\delta_u^{(m)}$. Let $\hat{\delta}_u^{(m)}$ be the estimated bias, solution of (4.34). Then the estimated SINR is given by

$$\widehat{\mathrm{SINR}}_u^{(m)} = \frac{\left(|g_u|^2 + \hat{\delta}_u^{(m)}\right)^2}{\sigma_{z_u}^{(m)\,2} - \left(|g_u|^2 + \hat{\delta}_u^{(m)}\right)^2} \qquad (4.35)$$

Figure 4.6 refers to a flat non-fading system, (i.e. $\gamma_u = 1$ for all users), with $U = 32$ users and spreading factor $L = 16$ (corresponding to the channel load $\alpha = 2$), $E_b/I_0 = 5\mathrm{dB}$ using the convolutional code $\mathrm{CC}(5, 7)$. Users are chip-asynchronous and their relative delays are uniformly distributed over an interval spanning one symbol. The true and estimated SINR vs. the iterations for a given user are shown. The curve
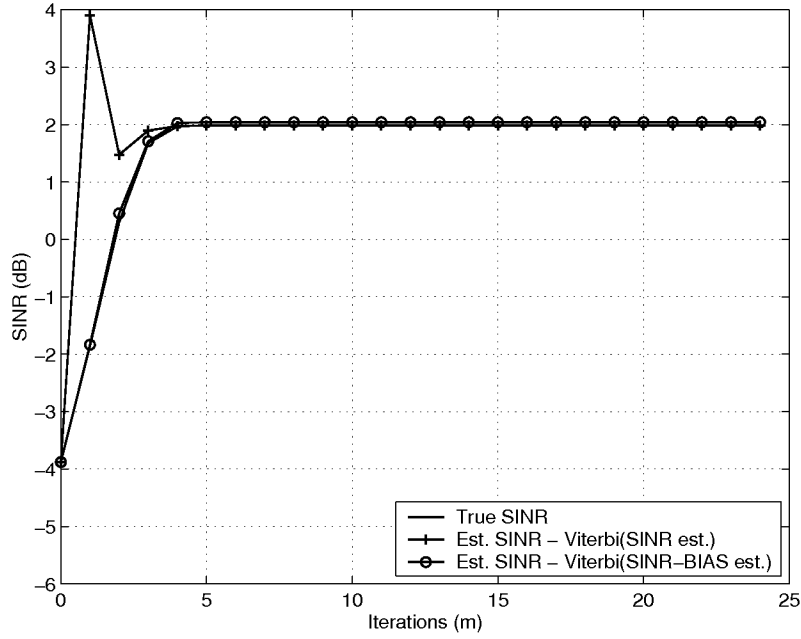
Figure 4.6: True and estimated SINR for "Viterbi (SINR est.)" and "Viterbi (SINR-BIAS est.)" decoders, using $CC(5,7)$, $U = 32$, $L = 16$, and $E_b/I_0 = 5\text{dB}$

labeled "Viterbi (SINR est.)" refers to the proposed iterative receiver that estimates the SINR using equation (4.28) while the curve labeled "Viterbi (SINR-BIAS est.)" refers to the system that estimates both the bias and the SINR, using (4.35). Notice that in the first few iterations the SINR estimator given by (4.28) overestimates the true SINR up to several dBs. Instead, the SINR estimation given by (4.35) is very close to the true SINR.

4.4.3 The ping-pong effect and its compensation

As it has been shown in the previous Sections, the proposed receiver allows system loads up to a certain threshold above which the system cannot approach the single user performance. In such high load situations, the system parameters as BER, SER, ME, and bias tend to oscillate between two convergence patterns [35]. This phenomenon is called *ping-pong* and it is related to the bias in the residual interference term. In fact, it does not appear when feedback is obtained from a SISO decoder extrinsic information [37]. [4]

A further investigation reported in [39] showed that such a bistable situation is due to a fixed subset of the estimated symbols that flip when passing from one iteration to the next, while the estimated symbols in the complementary subset do not change. A countermeasure to this problem proposed in [39] consists of introducing a perturbation into the bistable situation, by feeding back to the IC stage the average of the estimates

---

[4]For the extrinsic-based schemes, there obviously exists a threshold load above which single-user performance cannot be achieved, but no oscillatory behavior appears.
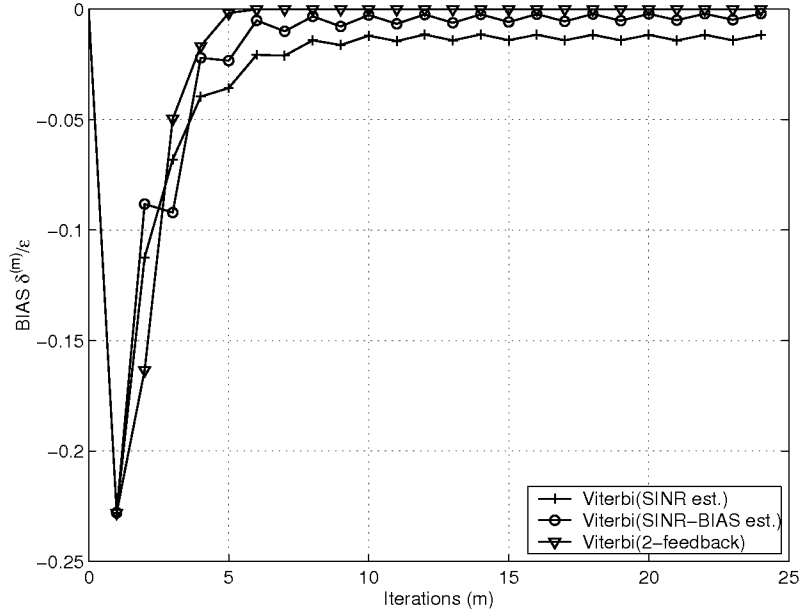
Figure 4.7: Bias in the statistic of $z_u^{(m)}$ using $CC(5,7)$, $U = 40$, $L = 16$, and $E_b/I_0 = 5\text{dB}$. The figure shows the oscillations due to the ping-pong effect

obtained from the two previous iterations. Thus, the contribution of the flipping symbols (considered as not reliable) is mitigated.

By considering this idea, (4.20) is modified as

$$\mu^{(m)} = E\left[\gamma \left|a - \beta_1^{(m)}\hat{a}^{(m)} - \beta_2^{(m)}\hat{a}^{(m-1)}\right|^2\right] \qquad (4.36)$$

where the two previous estimates are now weighted with the coefficients $\beta_1^{(m)}$ and $\beta_2^{(m)}$. Now, we can optimize the weighting factors $\beta_1^{(m)}$ and $\beta_2^{(m)}$ as functions of the channel energy γ in order to minimize the expected interference variance $\mu^{(m)}$ at every iteration. In analogy with what done before, we seek the solution of the optimization problem

$$\min_{\beta_1=\beta_1(\gamma),\beta_2=\beta_2(\gamma)} E\left[\left|a - \beta_1\hat{a}^{(m)} - \beta_2\hat{a}^{(m-1)}\right|^2 \bigg| \gamma\right] \qquad (4.37)$$

After straightforward algebra (we skip the details for the sake of space limitations), we obtain the solution

$$\beta_1^\star(\gamma) = \frac{A - BC}{1 - C^2} \qquad (4.38)$$

$$\beta_2^\star(\gamma) = \frac{B - AC}{1 - C^2} \qquad (4.39)$$

where

$$A = \mathrm{E}\left[a\hat{a}^{(m)}\right] = 1 - 2\epsilon^{(m)}(\gamma)$$

$$B = \mathrm{E}\left[a\hat{a}^{(m-1)}\right] = 1 - 2\epsilon^{(m-1)}(\gamma)$$

$$C = \mathrm{E}\left[\hat{a}^{(m)}\hat{a}^{(m-1)}\right]$$

In practice, the weights $\beta_{1,u}^{(m)}$ and $\beta_{2,u}^{(m)}$ of user u at iteration m are computed as follows:

- for $m = 1$, $\beta_{2,u}^{(1)}$ is irrelevant (since $\hat{a}^{(0)} = 0$) and $\beta_{1,u}^{(1)} = 1 - 2f(\widehat{\mathrm{SINR}}_u^{(1)})$ where $\widehat{\mathrm{SINR}}_u^{(1)}$ is computed according to (4.35).

- for $m = 2, 3, \ldots$, we let $C = \frac{1}{N}\sum_{n=0}^{N-1}\hat{a}_u^{(m)}[n]\hat{a}_u^{(m-1)}[n]$, $A = 1 - 2f(\widehat{\mathrm{SINR}}_u^{(m)})$, and $B = 1 - 2f(\widehat{\mathrm{SINR}}_u^{(m-1)})$. Thus, $\beta_{1,u}^{(m)}$ and $\beta_{2,u}^{(m)}$ are given by (4.38) and (4.39), respectively.

Figures 4.7 and 4.8 illustrate the bias and the true SINR plotted versus the iterations for a system using Viterbi decoding, with unfaded chip asynchronous flat channel, (i.e. $\gamma_u = 1 \; \forall u$) $U = 40$, $\alpha = 2.5$ and in the same conditions of Figure 4.6. The "Viterbi (SINR est.)" and the "Viterbi (SINR-BIAS est.)" decoders do not converge to near-single-user performance and show the ping-pong effect in the bias and in the SINR. The receiver that weights the two previous iterations, denoted in the Figures by "Viterbi (2-feedback)", converges faster to near-single-user performance and does not show oscillations.

This behavior can also be seen in Figure 4.9 where the BER provided by the proposed receivers is shown, for an unfaded chip asynchronous flat channel, and the same conditions of Figure 4.8. The curve labeled "Viterbi ($\beta = 1$)" denotes the receiver that feeds-back hard decisions (i.e. assuming $\beta_u^{(m)} = 1$ for $u = 1, \ldots, U$ and $m = 0, 1, \ldots$) and the bold horizontal line represents the single user performance. The receiver "Viterbi (2-feedback)" converges to single user performance in 6 iterations. In these conditions, it converges even faster than employing BCJR decoders providing soft extrinsic output, denoted by "BCJR (soft EXT)".

Finally, Figure 4.10 compares the performance of several receivers in terms of speed of convergence to near-single-user performance for $E_b/I_0 = 5\mathrm{dB}$, $L = 16$, and for $\gamma_u = 1 \; \forall u$. As test of convergence, we consider the number of iterations required to reach an average ME larger than $-0.1\mathrm{dB}$. The basic hard feedback Viterbi receiver has maximum channel load $\alpha = 1.5$. The weighted hard feedback Viterbi with SINR and bias estimation improves this limit to $\alpha = 2.4$. Eventually, the receiver "Viterbi (2-feedback)" outperforms any other considered receiver and has limit load $\alpha = 3.7$ (corresponding to a spectral efficiency of 1.85 bit/s/Hz). The dashed curves refer to the receivers employing BCJR decoders and extrinsic information feedback and are shown as a reference.

We should remark that higher spectral efficiency could be achieved by employing more powerful codes (e.g. turbo codes) in the proposed iterative decoder. However, since our aim was to find a low complexity solution, we only considered very simple convolutional codes as the CC(5,7). So, despite of the good performance shown in
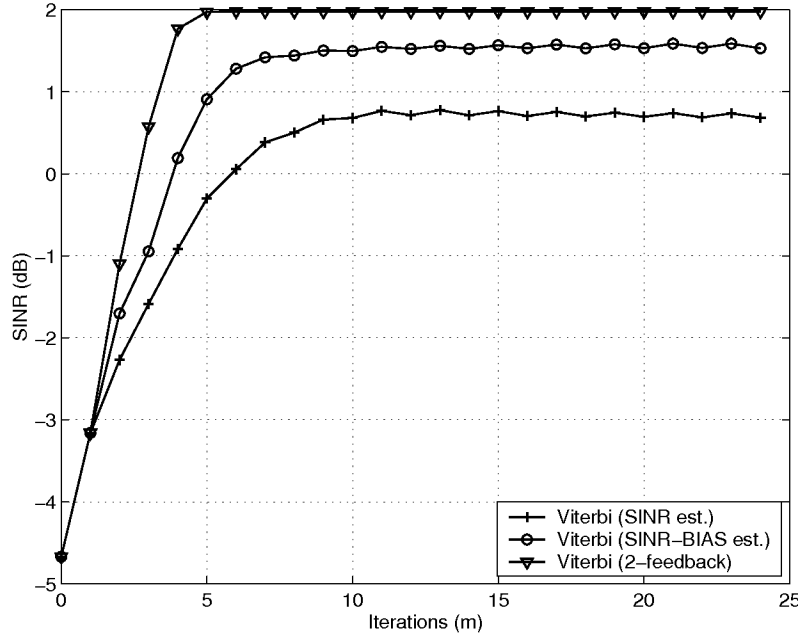
Figure 4.8: True SINR of several multiuser receivers using $CC(5,7)$, $U = 40$, $L = 16$, and $E_b/I_0 = 5\text{dB}$

terms of spectral efficiency, the proposed receiver works very far from capacity. For this reason it makes sense to compare the performance of our receiver to the "single-user performance", the performance that the system could achieve if no interference were present.

4.5   Performance in frequency selective fading channels

In this Section we consider frequency selective channels and asynchronous users. Thus, the ISI term appears in (4.12). In presence of ISI, the system converges to near single-user Matched Filter Bound (MFB) performance [10] for a channel load α generally lower than the limit for flat synchronous channels. Indeed, the presence of ISI slows down the convergence to single user performance and allows lower channel loads. Two different cases are considered:

- constant instantaneous power for all users;

- constant average power for all users.

4.5.1   Constant instantaneous power

This case is representative of perfect fast power control that fully compensates for the instantaneous (slot-by-slot) effect of fading, so that $\gamma_u = 1$. Thus,

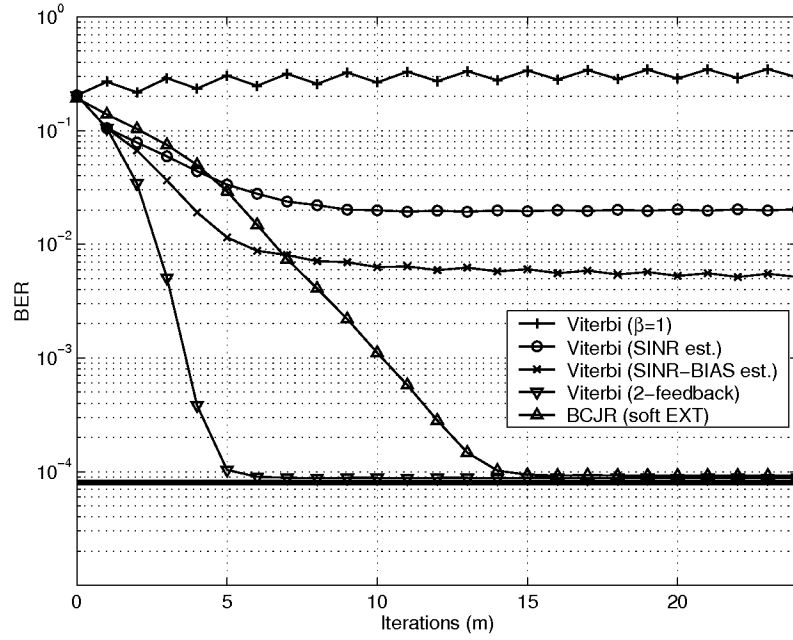$$|g_u|^2 = \mathcal{E}, \quad \forall u = 1,...,U \tag{4.40}$$

Figure 4.9: BER of several multiuser receivers using $CC(5,7)$, $U = 40$, $L = 16$, and $E_b/I_0 = 5\text{dB}$
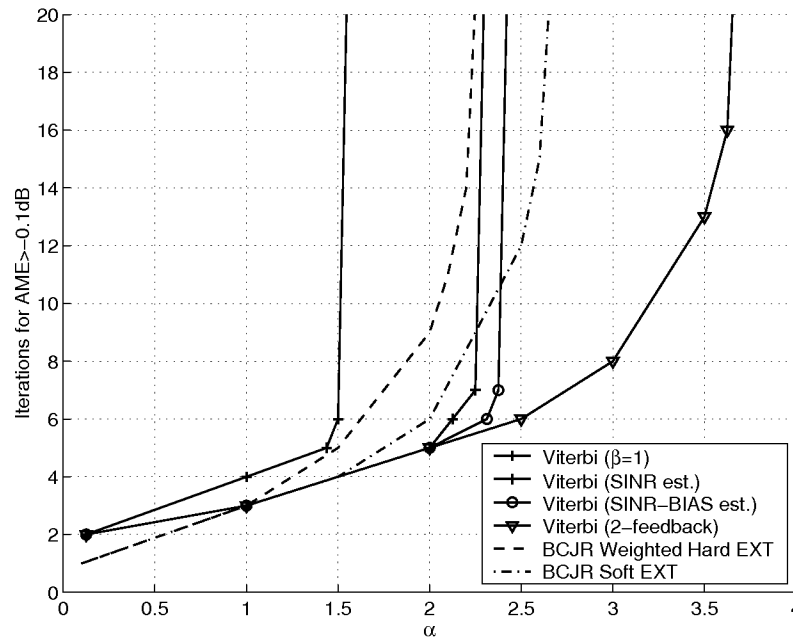

Figure 4.10: Number of iterations required to attain an $\text{ME} > -0.1\text{dB}$ for several multiuser decoders using $CC(5,7)$, $L = 16$, and $E_b/I_0 = 5\text{dB}$

Table 4.1: MIP of the considered channels

MIP	Delays (T_c)	Variances (dB)
CH1	(0, 1.2, 34.2, 49.5, 65.7, 76.8)	(-2.5, 0, -12.8, -10.0, -25.2, -16.0
CH2	(0, 16)	(0, 0)
CH3	(0, 16, 32)	(0, 0, 0)

Under these conditions, we evaluated by simulation the degradation due to the ISI with respect to the results shown in the previous Section. Figure 4.11 shows the number of iterations needed to reach ME larger than −0.1dB, as a function of the channel load, for $E_b/I_0 = 5$dB, $L = 16$, the "Viterbi (2-feedback)" receiver, and for three different channels whose Multipath Intensity Profile (MIP) [16] is shown in Table 4.1. CH1 is specified as a standard UMTS test channel in [21] while CH2 and CH3 were created "ad hoc" in order to test the system in severe ISI conditions.

CH1 shows a negligible degradation with respect to the single-path case while, for the channels CH2 and CH3, the maximum achievable channel load is decreased to $\alpha = 3.3$ and $\alpha = 2.9$, respectively. Notice also that, in the case of strong ISI and low channel loads, more iterations are required for the convergence with respect to the single-path case.

4.5.2   Constant average power

This case is representative of a slow power control system that cannot compensate for the instantaneous fading, but maintains a fixed *average* received power for each user. The average received power is assumed to be the same for all users, that is

$$\mathrm{E}\left[|g_u|^2\right] = \mathcal{E} \ \ ; \ \ \forall u = 1, ...U \tag{4.41}$$

Figure 4.11 shows the number of iterations needed to reach ME larger than −0.1dB as a function of the channel load and for the channels given in Table 4.1. In this case, two contrasting phenomena characterize the convergence to single-user MFB performance. On one hand, faded users have little impact onto unfaded users, since they are received at much lower power. On the other hand, even if unfaded users can be reliably estimated and subtracted from the received signal, faded users have an instantaneous SINR that is too low for achieving a small SER, therefore, their contribution cannot be perfectly eliminated even in the absence of MAI. The fact that the performance for slow power-control are worse than their fast power-control counterparts (see Figure 4.11) indicates that the effect of uncanceled faded users dominates the performance of the receiver. Moreover, Figure 4.11 shows also another interesting fact. Namely, the degradation of the receiver performance due to uncompensated fading is larger for channels with little multipath diversity (e.g., single-path, CH2 and CH3), while it is smaller for channels with rich multipath diversity (e.g., the UMTS test channel CH1). This is intuitively clear, since when the multipath diversity is rich, then the random

fluctuations of the instantaneous received power $|g_u|^2$ are reduced, and the fraction of users that can be reliably estimated and subtracted is larger.

In general, the average bit error rate (BER) for a finite-dimensional system can be computed by Monte Carlo simulation, by averaging over a large number of frames and channel realizations. In order to reduce the complexity of BER computation, we propose a semi-analytic approach. Assuming symmetric users, with the same channel statistics and average received power, the average BER (averaged with respect to both the channel statistics and over the user population) can be bounded by

$$
\begin{aligned}
\mathrm{BER}^{(m)} &= \mathrm{E}\left[f_b\left(\eta^{(m)}\gamma\,\mathrm{SNR}^{\mathrm{MFB}} \right) \right] \\
&= \frac{1}{U}\sum_{u=1}^{U} \mathrm{E}\left[f_b\left(\eta_u^{(m)}\gamma_u\,\mathrm{SNR}^{\mathrm{MFB}} \right) \right] \\
&\overset{a}{\geq} \mathrm{E}\left[f_b\left(\gamma\mathrm{SNR}^{\mathrm{MFB}}\frac{1}{U}\sum_{u=1}^{U}\eta_u^{(m)} \right) \right] \\
&= \mathrm{E}\left[f_b\left(\gamma\mathrm{SNR}^{\mathrm{MFB}}\eta^{(m)} \right) \right]
\end{aligned}
\tag{4.42}
$$

where $f_b(\cdot)$ is the bit error probability vs. decoder input SNR function of the employed convolutional code, where (a) follows from Jensen's inequality applied to the convex function $f_b(\cdot)$ and where we define the average ME $\eta^{(m)}$ as the arithmetic mean of the ME of all users. Notice that, under mild conditions, for randomly spread CDMA in the large-system limit the ME converges to a constant independent of the user index, and inequality in (4.42) holds with equality. However, for a finite-dimensional system and given spreading sequences the above provides only a lower bound.

The expectation in the last line of (4.42) is with respect to the normalized channel energy γ (assumed identically distributed for all users). The evaluation of the above lower bound is much less computationally intensive than full Monte Carlo simulation of the whole system. In fact, the average ME $\eta^{(m)}$ can be obtained by running short simulations, since it requires a much smaller statistical sample to converge than the average BER. Then, the expectation with respect to γ can be obtained by either another Monte Carlo simulation or, if the distribution of γ is known, by numerical integration.

Figure 4.12 shows the comparison between the full Monte Carlo simulation and the semi-analytic approach for a system with $U = 32$, $L = 16$, and channel CH3. Solid lines show the BER obtained by Monte Carlo simulation for $m = 1, 2, 3, 6$ iterations respectively, plotted versus E_b/I_0. The dashed lines show the results obtained using the semi-analytic approach. The thick solid line corresponds to the single-user MFB. For low SNR the system does not converge to the single user MFB even for a large number of iterations while for high SNR the convergence is obtained in a few iterations. We notice that the semi-analytic approach yields fairly accurate results already for such a small system.

4.6   Conclusions

We proposed a low complexity iterative turbo equalizer and multiuser decoder/detector for TD-CDMA systems, characterized by convolutional coding, hard-output Viterbi
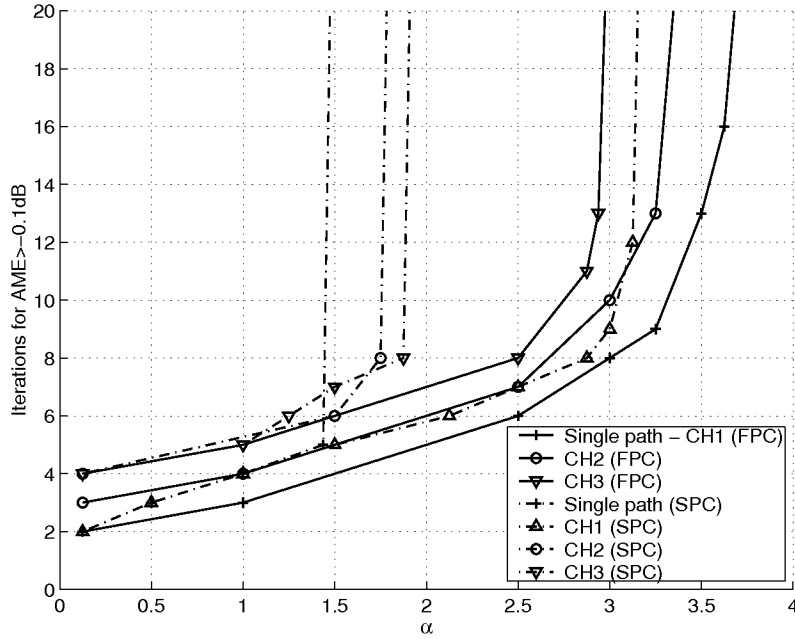
Figure 4.11: Performance of the "Viterbi (2-feedbacks)" multiuser decoder in the presence of multipath fading channels using $CC(5,7)$, $L = 16$, and $E_b/I_0 = 5$dB. FPC and SPC denote fast and slow power control conditions, respectively

decoding and weighted feedback. From a rigorous large-system analysis of synchronous users and flat channels we gained the rationale for the optimization of the feedback weights. In the proposed iterative scheme, however, the presence of Viterbi decoders (not providing extrinsic information) produces biased statistics after the IC stage. Hence, we proposed a method for estimating the bias and improving the performance of the basic iterative decoder. Moreover, in order to cope with the ping-pong effect, we proposed a modified algorithm where a weighted sum of the decisions made in the two previous iterations is used for interference cancellation. The modified algorithm outperforms the the basic PIC receiver and even the receiver based on SISO decoding and soft feedback, with lower complexity.

The proposed receiver was validated in a realistic scenario, including asynchronous users, frequency selective fading channels and power control. Simulation results show that the receiver is robust to severe ISI conditions, even though its performance is degraded by uncompensated fading. However, this degradation is not very evident in the presence of sufficient multipath diversity. Eventually, a simple and fast semi-analytic approach to compute the BER was proposed and its behavior has been compared with the results obtained via Monte Carlo simulation.

As a concluding remark, we would like to point out that the proposed receiver structure is fully suited to be implemented in a UMTS-TDD base station, as an alternative to conventional single user decoding and high-complexity convolutional or turbo codes proposed in the current standard.
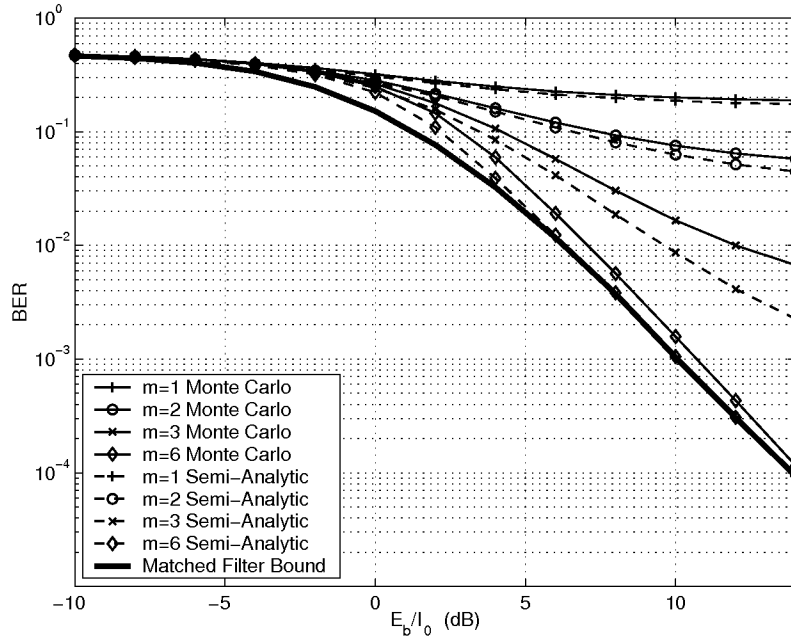
Figure 4.12: BER provided by the "Viterbi (2-feedbacks)" multiuser decoder for channel CH3 using $\mathrm{CC}(5,7)$, $U = 32$, and $L = 16$

4.A   Definition of $f(\cdot)$, $f_b(\cdot)$ and $\Gamma(\cdot)$

Consider a transmitter that maps the information bit sequence $\{b[j]\}$ onto a sequence of coded binary BPSK symbols $\{a[n]\}$ and sends over the AWGN channel defined by

$$y[n] = a[n] + \nu[n]$$

where $\nu[n]$ is Gaussian noise with distribution $\mathcal{N}(0, \sigma^2)$. The signal-to-noise ratio is SNR $= \frac{1}{\sigma^2}$. The receiver decodes the signal $y[n]$ providing hard decisions $\hat{a}[n]$ on the transmitted symbols $a[n]$ and hard decisions $\hat{b}[j]$ on the information bits $b[j]$. We define

1. The SER vs. SNR characteristic

$$f(\mathrm{SNR}) = \frac{1 - \mathrm{E}\left[\hat{a}[n]a[n]\right]}{2} \tag{4.43}$$

2. The BER vs. SNR characteristic

$$f_b(\mathrm{SNR}) = \frac{1 - \mathrm{E}\left[\hat{b}[j]b[j]\right]}{2} \tag{4.44}$$

3. The correlation characteristic between decisions and noise

$$\Gamma(\mathrm{SNR}) = \mathrm{E}[\hat{a}[n]\nu[n]] \tag{4.45}$$

The above functions depend uniquely on the code considered (i.e., they are "charac-teristics" of the code) and, although generally unknown in closed form, they can be pre-computed by Monte Carlo simulation and stored as look-up tables in the receiver memory. Therefore, the impact of real-time evaluation of these functions on the overall receiver complexity is negligible.

Chapter 5

Front-end signal processing

We present low-complexity algorithms for transmitter and receiver front-end suited to the implementation of software defined radio (SDR) terminals. The proposed algorithms make the processing sampling frequency independent of the symbol rate of the digitally modulated signal and use the "IF-sampling" technique for D/A and A/D conversion. As a case-study, we consider a training-based joint multiuser channel estimation and we show that our front-end algorithms work nicely when coupled with an efficient FFT-based joint channel estimator.

5.1 Introduction and motivations

Because of the proliferation of mobile communication systems, the implementation of Software Defined Radio terminals able to reconfigure themselves to handle several different standards is a key issue in order to provide universal connection to the users. At the physical layer, the careful design of algorithms for the transceiver front-end signal processing seems to provide the required flexibility. The basic idea is to make the standard-dependent base-band signal processing independent on the Intermediate Frequency which is characterized by the hardware. Moreover these algorithms must be suited to the implementation on a programmable CPU. The goal is to perform operations like *channel selection* [5, 6], *up- and down-conversion* [7], synchronization and detection in the all-digital domain, by using high performance Digital Signal Processors (DSPs) while, traditionally, these operations are performed by dedicated hardware.

In this Chapter, we propose some front-end algorithms for the class of linearly-modulated digital signals, including most today's and future mobile communications standards, like GSM, IS-54, IS-136, IS-95, and DECT (see e.g. [1] and references

therein), UMTS (both FDD and TDD modes) [13], CDMA2000 (see e.g. [22], [46]) and EDGE (see e.g. [47] and references therein) [1].

We assume that a multi-band RF section takes care of translating the desired signal from a fixed Intermediate Frequency carrier to the required Radio Frequency carrier, and vice-versa. Then, on the transmitter side we are concerned with the efficient generation of an IF analog signal from the base-band digital signal while on the receiver side we are concerned with the efficient generation of a digital signal from the IF analog signal.

Different options are compared in terms of their complexity and performance. Complexity is measured in real operations per sample. This can be translated into actual processing speed limits once the DSP number of instructions per second is known. Performance is given in terms of the Signal-to-Interference plus Noise Ratio (SINR) at the output of the receiving filter matched to the modulation elementary pulse, assuming that the transmission channel is pure additive white (not necessarily Gaussian) noise. In this case the interference should be intended as the result of the whole signal distortion generated through the transmitter and receiver chain. The SINR is expressed as a function of $\mathcal{E}/I_0$, where $\mathcal{E}$ is the average symbol energy and I_0 denotes the (frequency-flat) noise power spectral density, in the complex base-band equivalent model. By modeling interference plus noise at the output of the receiver matched filter as Gaussian, the output SINR can be easily translated into actual error probabilities for different modulation schemes with and without channel coding. In this way, both complexity and performance measures are independent of the considered particular modulation scheme and the comparison between different solutions is consistent.

In order to validate the proposed algorithms on an actual system, we consider the training-based multiuser joint channel estimation scheme of UMTS-TDD (see e.g. [18], [19], and [20]). We recall briefly an efficient Fast Fourier Transform (FFT)-based implementation for this scheme and we apply it to the signal generated by our transmit/receive front-end. Performance for a particular multipath test channel are given in terms of the actual measured Matched Filter Bound (MFB) at the output of the estimated channel matched filter versus the MFB of an ideal system.

5.2   Transmitter front-end

5.2.1   Linearly modulated signals

The continuous-time complex envelope of a linearly modulated signal is given by

$$x(t) = \sum_{k} d[k]\psi(t - kT_s) \tag{5.1}$$

where $d[k]$ is a sequence of modulation symbols belonging to some complex alphabet (e.g., PSK, QAM [16]), T_s is the symbol interval, and $\psi(t)$ is the symbol-shaping

---

[1]GSM and DECT make use of GMSK modulation, which is non-linear [1]. However, in several current implementations a linear approximation of GMSK is used.

pulse, bandlimited over $[-W_\psi/2, W_\psi/2]$. Despite its simplicity, several cases of interest can be expressed by (5.1):

- In a Direct-Sequence CDMA system [16], T_s should be interpreted as the chip interval and $d[k] = a[\lfloor k/L \rfloor]s[k]$, where $a[m]$ is the mth modulation symbol, $s[k]$ is the kth chip and L is the spreading gain (this generalizes trivially to systems with several spreading layers, like IS-95).

- In a multi-antenna multi-user system (e.g., downlink with beamforming) with Q antennas and U users the signal sent to the qth antenna is

$$x^{(q)}(t) = \sum_k d^{(q)}[k]\psi(t - kT_s)$$

where

$$d^{(q)}[k] = \sum_{u=1}^{U} W_u^{(q)} d_u[k]$$

$W_u^{(q)}$ is the qth antenna weight coefficient for the uth user and $d_u[k]$ is the uth user symbol (or chip).

In a digital transmitter, the signal $x(t)$ is the output of a D/A converter which takes as input the discrete-time signal

$$x[n] = x(n/f_s)$$

with sampling frequency $f_s \geq W_\psi$. In classical I-Q modulators, the continuous baseband components $x_I(t) = \text{Re}\{x(t)\}$ and $x_Q(t) = \text{Im}\{x(t)\}$ are generated by low-pass filtering the output of two separate D/A converters, and the IF signal

$$x_{\text{IF}}(t) = \text{Re}\left\{x(t)e^{j2\pi f_{\text{IF}}t}\right\} \tag{5.2}$$

is produced by mixing $x_I(t)$ and $x_Q(t)$ with in-phase and quadrature IF carrier signals, and by summing the modulated real signals [16]. This approach requires two D/A converters, two low-pass filters, two analog mixers and one adder.

Another approach consists of producing a sampled version of the IF modulated signal $x_{\text{IF}}(t)$ by using a sampling rate f_s greater than $2f_{\text{IF}}$. The continuous-time signal is obtained by band-pass filtering the output of a single D/A converter. This solution (for the receiver front-end) is described in [7] and [48]. However, since intermediate frequencies usually range between tens of MHz up to 100 MHz, this approach is extremely computationally intensive as it requires the generation of signal samples and the multiplication by the carrier signal at extremely large sampling frequency.

In the following, we propose a transmit front-end algorithm allowing a sampling frequency of the order of the base-band signal bandwidth (and not of the order of the IF carrier), no explicit multiplication by the carrier signal and a single D/A converter and analog filter centered at f_{IF}.

5.2.2   IF-sampling and up-conversion

We need to generate the IF modulated discrete-time real signal

$$x'[n] = \text{Re}\left\{ x[n]e^{j2\pi(f_{\text{IF}}/f_s)n} \right\} \tag{5.3}$$

from the base-band signal $x[n]$. We choose throughout this Chapter the sampling rate f_s according to the expression

$$f_s = \frac{f_{\text{IF}}}{\ell \pm 1/4} \qquad \text{for a positive integer } \ell \tag{5.4}$$

With this choice (5.3) reduces to modulating the base-band signal by $f_s/4$ and taking the real part that in turn corresponds to

$$x'[n] = \text{Re}\left\{ j^{\pm n}x[n] \right\} \tag{5.5}$$

In this way, the periodic spectrum of $x'[n]$ has a spectrum replica centered at f_{IF}. After ideal D/A conversion, a pass-band filter centered at f_{IF} removes the other replicas, generating the desired IF modulated analog signal. The discrete-time modulation by $f_s/4$ in (5.5) has a negligible computational cost since it corresponds to alternately changing the signs of the real and imaginary part of $x[n]$. Finally, in order to avoid aliasing the sampling rate must satisfy the condition $f_s \geq 2W_\psi$.

5.2.3   D/A conversion

In the above description we assumed an ideal D/A converter with flat frequency response. Unfortunately, actual D/A converters show a low pass behavior that can be approximated with a frequency response of the form $\text{sinc}(f/f_s)$. The spectrum of the continuous-time signal at the D/A converter output corresponding to the discrete-time input signal $x'[n]$ takes the form

$$X_{\text{IF}}(f) \propto \sum_i X' \left(e^{j2\pi(f/f_s - i)} \right) \text{sinc}(f/f_s) \tag{5.6}$$

where

$$X'(e^{j2\pi f/f_s}) = \sum_n x'[n]e^{j2\pi n f/f_s}$$

is the Discrete-time Fourier Transform (DFT) of $x'[n]$. Hence, the spectrum replica located at frequency f_{IF} is attenuated and distorted by the D/A impulse response as shown in figure 5.1(a).

A way to reduce the attenuation consists of using a D/A converter working at rate $f_d = L_{\text{D/A}}f_s$, where $L_{\text{D/A}}$ is a suitable integer, and up-sampling $x'[n]$ by the factor $L_{\text{D/A}}$. By choosing $L_{\text{D/A}}$ such that $f_d \gg f_{\text{IF}}$, the spectrum replica around f_{IF} falls inside the first lobe of the D/A frequency response since its first zero is located at f_d (see figure 5.1(b)). Unfortunately this approach reduces the average signal energy per sample by a factor $L_{\text{D/A}}$. Thus, in order to compensate the signal attenuation resulting from high values of $L_{\text{D/A}}$, high amplification gains may become necessary in the
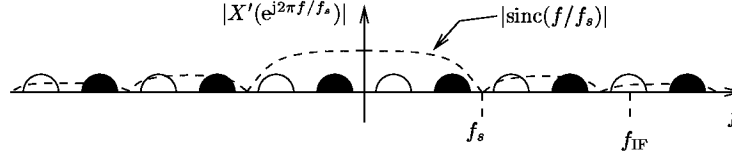
(a) D/A frequency response without up-sampling
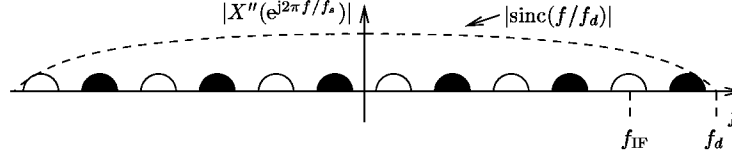
(b) D/A frequency response with up-sampling

Figure 5.1: D/A frequency response and IF signal spectrum

IF/RF conversion stage which can lead to significant non-linear distortion. To overcome this problem one may pre-compensate the linear response of the D/A converter by introducing a pass-band FIR filter between the up-sampler and the D/A converter. The filter must be designed in order to enhance the spectrum replica at IF while attenuating the other replicas. This would avoid high amplification gains in the IF/RF stage yielding less signal distortion. In the following we address a low complexity implementation of such a filter.

Low Complexity Implementation. Denote by $x''[n]$ the up-sampled version of $x'[n]$, given by

$$x''[n] = \begin{cases} x'[k] & \text{for } n = L_{\mathrm{D/A}}k \\ 0 & \text{otherwise} \end{cases} \tag{5.7}$$

and by $h_{\mathrm{D/A}}[n]$ the pass-band FIR filter impulse response. The filter output is given by

$$x'''[n] = \sum_m h_{\mathrm{D/A}}[m]x''[n-m] \tag{5.8}$$

If the filter impulse response has length $L_{\mathrm{D/A}}$, there is only a single non-zero term in the sum in the RHS of (5.8). Then, $x'''[n] = h_{\mathrm{D/A}}[m]x'[k]$ where $k = \lfloor n/L_{\mathrm{D/A}} \rfloor$ and $m = n$ modulo $L_{\mathrm{D/A}}$. Therefore, the computational cost of the filtering operation consists of one real product per output sample at rate f_d. Since f_d is large, this might still be too complex for practical applications. Then, the filter coefficients can be constrained to be in the set $\{0, \pm 1\}$. In this way products are avoided (change of sign comes basically at no cost). The problem of optimizing the FIR filter reduces to exhaustive search for the best frequency response over all possible filter vectors of length $L_{\mathrm{D/A}}$ with ternary elements $\{0, \pm 1\}$ (a total of $3^{L_{\mathrm{D/A}}}$ possibilities).

5.2.4 Signal resampling

In the scheme described above, the sampling frequency f_s depends on f_{IF} and on the signal bandwidth W_ψ. In a SDR system, we can think of W_ψ as the maximum signal bandwidth over all handled signal formats, while f_{IF} is fixed and depends on the analog hardware. In any case, f_s should be independent of the symbol rate $R_s = 1/T_s$ of the particular signal format. When $f_s \neq R_s$, the transmitter must produce the signal $x[n]$ at rate f_s from the discrete-time symbol sequence $d[n]$ at rate R_s. We refer to this general problem as "resampling".

In [49, 50, 51, 52] resampling by rational factors is discussed. A general sampling rate conversion scheme by a rational factor L_u/L_d consists of an up-sampler by a factor L_u, a low-pass filter and a down-sampler by a factor L_d. The low-pass filter can be efficiently implemented by a polyphase filter bank [49] composed by L_u phases, where each filter phase is sampled at rate R_s. Unfortunately, in general the ratio f_s/R_s is not a rational number, therefore f_s can be only approximated by $\frac{L_u}{L_d} R_s$ by a careful choice of the integers L_u and L_d.

Since the shaping filter $\psi(t)$ of the modulation scheme is bandlimited, it can be used as low-pass filter in the resampler. In this way, shaping and resampling are integrated in a single step with considerable saving in computational complexity. Assume that $\psi(t)$ is approximated by a finite-support impulse response spanning N_ψ symbol intervals (e.g., by windowing [51]) and let $\psi_\ell[i] = \psi((iL_u + \ell)/(L_u R_s))$ with $\ell = 0, \ldots, L_u - 1$ and $i = 0, \ldots, N_\psi - 1$, denote the ith sample of the ℓth phase of the polyphase filter bank implementation of the shaping discrete-time filter. Then, the output at rate $L_u R_s$ of the polyphase pulse-shaping filter bank is given by

$$v[k] = \sum_{i=0}^{N_\psi - 1} \psi_\ell[i] d[m - i] \qquad (5.9)$$

where $m = \lfloor k/L_u \rfloor$ and $\ell = k$ modulo L_u.

A low cost approach for achieving the desired non-rational sampling rate conversion consists of using a suboptimal interpolation method (e.g., nearest neighbor, linear, cubic or cubic spline interpolation) at the output of the polyphase filter bank. In general, the interpolator computes the time epoch t_n of the desired n^{th} output sample and compares it to the input-sample time-instants. The cost of this operation does not depend on the interpolator type and can be assumed to be (roughly) 1 addition per output sample. On the contrary, the computation of the output sample value depends on the interpolation method. Therefore, when comparing the complexity of the interpolation schemes, we shall always refer to this cost, neglecting the part common to all methods. Notice that the polyphase filter-bank coefficients can be pre-computed thus the up-sampling factor L_u only affects the memory occupancy and not the complexity of the interpolation algorithm. In general the higher L_u the higher the interpolation accuracy will be. In particular the more the complexity of the interpolation algorithm the lower values for L_u are required to achieve the same interpolation accuracy.

Nearest neighbor (NN) interpolation is the simplest technique, since it approximates the desired output sample to the time-nearest input sample. In fact using nearest neighbor interpolation the overall cost of the resampler reduces to storing in memory the shaping filter bank. The nearest neighbor interpolator produces the output sequence

$x[n]$ at sampling rate f_s as

$$x[n] = v[k]$$

where

$$|t_n R_s - k/L_u| \leq \frac{1}{2} \qquad (5.10)$$

and where $t_n = t_0 + n/f_s$ is the desired sampling epoch (t_0 is a fixed time-offset). The computational complexity is then the cost of the inner product given by (5.9) per output sample. Normally the shaping filter coefficients are real while, in general, the symbols $d[k]$ are complex. Then, the resulting computational complexity is $2N_\psi$ multiplications and $2(N_\psi - 1)$ additions per output complex sample. However, as indicated in (5.3), only the real signal $x'[n]$ is needed in our transmit front-end. This is equivalent to computing alternately $x_I[n]$ and $x_Q[n]$. Therefore, the actual computational complexity per output sample reduces to N_ψ multiplications and $N_\psi - 1$ additions.

It is clear from (5.10) that the accuracy of nearest neighbor interpolation critically depends on L_u. However, since memory is a very cost-effective resource, in the transmitter it is advisable to choose L_u large enough and insist on nearest neighbor interpolation rather than consider a lower L_u and implement a more complex interpolation method (e.g., linear, cubic, etc.). We shall see in next section that this conclusion does not apply to the receiver front-end.

5.3 Receiver front-end

5.3.1 IF-sampling and down-conversion

The IF received analog signal $y_{\text{IF}}(t)$ is sampled by an A/D converter at rate f_s. If $f_s \geq 2W_\psi$ is chosen according to (5.4), because of the periodicity of the discrete-time signal spectrum, the resulting real sampled signal $r[n] = y_{\text{IF}}(n/f_s)$ is pass-band with a spectrum replica centered at $f_s/4$ (although f_{IF} and f_s at the receiver can be different from f_{IF} and f_s at the transmitter, for simplicity we use the same notation).

5.3.2 Resampling

To simplify synchronization and data detection, the received signal should be sampled at rate R_s', integer multiple of the symbol rate (or chip rate, in the case of CDMA). As in the transmitter, the system should be able to choose R_s' independently of f_s (within a certain range of supported signal formats). In addition, R_s'/f_s is non-rational in general and resampling is needed. A general approach to have a perfect transparent resampling system consists of resampling the I and Q components of the real pass-band signal $r[n]$. Once the I and Q components sampled at rate R_s' are generated, we can remodulate the signal at frequency $R_s'/4$ by simple sign change (as done in (5.5)) in order to have a real pass-band signal sampled at the desired rate R_s'. We consider the following two resampling approaches.
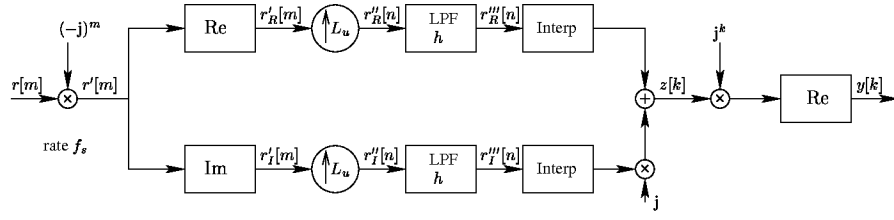
Figure 5.2: Receive resampling approach 1

Approach 1

This is a fairly similar resampling scheme to the one proposed for the transmitter (see section 5.2.4). Notation refer to the scheme of figure 5.2. The low-pass real interpolation filter h is implemented as a polyphase FIR filter bank with L_u phases ($h_\ell[i]$ denotes the ℓth phase i^{th} coefficient, for $\ell = 0, \ldots, L_u - 1$ and $i = 0, \ldots, N_h - 1$).

Let $r'''[n] = r'''_{\mathrm{R}}[n] + \mathrm{j} r'''_{\mathrm{I}}[n]$ denote the output of the polyphase filter bank, given by

$$r'''[n] = \sum_{i=0}^{N_h-1} h_\ell[i](-\mathrm{j})^{m-i} r[m - i] \tag{5.11}$$

where $m = \lfloor n/L_u \rfloor$ and $\ell = n$ modulo L_u. Using nearest neighbor interpolation produces the output sequence $z[k]$ at sampling rate R'_s as $z[k] = r'''[n]$ where

$$\left| t_k f_s - n/L_u \right| \leq \frac{1}{2} \tag{5.12}$$

and where $t_k = t_0 + k/R'_s$ is the desired sampling epoch (t_0 is a fixed time-offset). Finally, the resampled pass-band signal modulated at frequency $R'_s/4$ is given by $y[k] = \mathrm{Re}\{\mathrm{j}^k r'''[n]\}$. Since the interpolation filter is used to remove the high frequency noise components it can be chosen to be real. In this case $y[k]$ can be directly written as

$$y[k] = \begin{cases} + \displaystyle\sum_{i=0}^{N_h-1} h_\ell[i]\mathrm{Re}\{(-\mathrm{j})^{m-i} r[m-i]\} & \text{for } k = 4l \\[2mm] - \displaystyle\sum_{i=0}^{N_h-1} h_\ell[i]\mathrm{Im}\{(-\mathrm{j})^{m-i} r[m-i]\} & \text{for } k = 4l + 1 \\[2mm] - \displaystyle\sum_{i=0}^{N_h-1} h_\ell[i]\mathrm{Re}\{(-\mathrm{j})^{m-i} r[m-i]\} & \text{for } k = 4l + 2 \\[2mm] + \displaystyle\sum_{i=0}^{N_h-1} h_\ell[i]\mathrm{Im}\{(-\mathrm{j})^{m-i} r[m-i]\} & \text{for } k = 4l + 3 \end{cases} \qquad \text{for integer } l \tag{5.13}$$

where m and ℓ depend on n, which is a function of k through the resampling epoch relation (5.12).

After some algebra it is possible to show that the computation of $y[k]$ reduces to
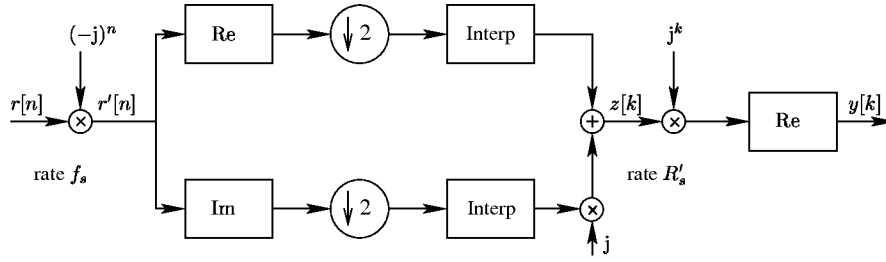
Figure 5.3: Receive resampling approach 2

computing alternately the values

$$y_0[k] \quad = \quad \sum_{i=0}^{N_h/2-1} \tilde{h}_{\ell,0}[i] r[m - 2i] \tag{5.14}$$

$$y_1[k] \quad = \quad \sum_{i=0}^{N_h/2-1} \tilde{h}_{\ell,1}[i] r[m - 2i - 1] \tag{5.15}$$

where the modified (real) filter coefficients

$$\tilde{h}_{\ell,0}[i] \quad = \quad (-1)^i h_\ell[2i]$$
$$\tilde{h}_{\ell,1}[i] \quad = \quad (-1)^i h_\ell[2i + 1]$$

can be precomputed.[2]

The overall complexity of this resampling approach amounts to an inner product of length $N_h/2$ (i.e., $N_h/2$ multiplications and $N_h/2 - 1$ additions) per output sample at rate R'_s.

One may notice that we could use as interpolation filter the same shaping filter ψ used in the transmitter. In this way, resampling and pulse shaping matched filtering could be implemented jointly. However, while this approach gives a complexity saving in the transmitter, it is not suited to the receiver because better low-pass FIR responses h, with the same number of taps, can be synthesized by using appropriate filter design methods (see e.g. [49]). Moreover, after filtering by $\psi(t)$ (which is normally a real Nyquist pulse) and sampling at $R'_s > R_s$ the resulting interference plus noise sequence is correlated even if the interference plus noise process at the receiver input is white. Correlation in the noise sequence might prevent some blind channel estimation techniques based on second-order statistics to work [53, 54] (or they might require the correlated noise to be whitened, with added complexity), and should be avoided. Then, we conclude that the interpolation filter h must be as close as possible to an ideal low-pass filter.

Moreover, when the received signal is affected by linear distortion caused by a multipath propagation channel $h(t)$, a channel estimation scheme applied to the discrete-time resampled signal $y[k]$ directly provides an estimate of the whole convolution $g(t) = \psi(t) \star h(t)$. In this way the pulse-shaping matched filter is included in the channel matched filter.

---

[2]The actual value of $y[k]$ is given either by $\pm y_0[k]$ or by $\pm y_1[k]$, where the sign depends on the parity of k and m.

Approach 2

An alternative approach consists of exploiting the fact that in our system the base-band signal $r'[n]$ is already oversampled with respect to the Nyquist rate. Thus the interpolation filter h can be avoided with a significant reduction of complexity for the same type of interpolation. Figure 5.3 shows the block diagram of this re-sampling system.

The received signal is first converted to base-band, then the real and imaginary parts of $r'[n]$ are treated separately and eventually recombined. Since $r[n]$ is real, the real and imaginary parts of $r'[n] = (-\mathrm{j})^n r[n]$ have zeros in every other sample. This can be seen as the effect of high-frequency components in the spectrum of $r'[n]$ originated by the spectrum replicas around $\pm f_s/2$. Hence, interpolation is obtained by eliminating the zero samples (by downsampling by a factor 2) and by applying some interpolation algorithm to the non-zero samples. After recombination, the complex signal $z[k]$ is remodulated and the real part is taken, thus obtaining $y[k]$. Notice that the whole processing of remodulating $z[k]$ at frequency $R'_s/4$ and taking the real part reduces to computing alternately the real and the imaginary part of $z[k]$ and alternately changing the sign to obtain $y[k]$. Therefore, the overall complexity amounts to one interpolated real value per output sample at rate R'_s. In this work we consider nearest-neighbor, linear, cubic and cubic spline interpolators (the details are given in [55] and references therein) whose computational cost is given by [55]:

- 0 for nearest neighbor interpolation.

- 2 additions and 1 multiplication per output sample for linear interpolation.

- 11 additions and 8 multiplications per output sample for cubic interpolation.

- 5 additions and 9 multiplications per output sample plus 4 additions and 3 multiplications per input sample for cubic spline interpolation. When the ratio between the interpolator input and output rates is approximately 1 the overall complexity can be considered roughly 9 additions and 12 multiplications per output sample.

We shall show in the next section that approach 2 yields significantly better performance with respect to approach 1 even with lower complexity.

5.4   Performance over additive white noise channel

In this section we illustrate the impact of the various system parameters on the performance of the proposed front-end algorithms over an additive white noise channel. As performance measure we use the SINR measured at the output of receiver front-end versus the nominal $\mathcal{E}/I_0$ ratio, where the interference should be intended as the consequence of the signal distortion. In practice the SINR is defined in this case as the ratio between the mean square and the variance of the received signal at the output of the pulse-shaping matched filter. The SINR loss with respect to the nominal $\mathcal{E}/I_0$ is due to two effects: Inter-Symbol Interference and energy decrease of the useful samples. ISI
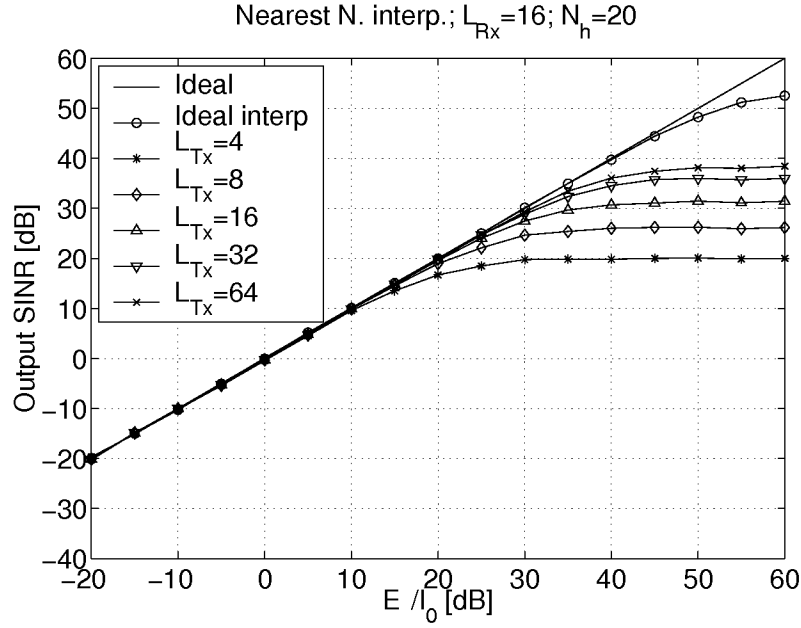
Figure 5.4: Receive resampling approach 1, $N_h = 20$, $L_{Rx} = 16$, and nearest neighbor interpolation

is due to the shaping filter truncation and to the distortion introduced by resampling, while the useful samples energy decrease is only due to resampling distortion.

We consider

- the QPSK modulation

- the root-raised cosine shaping filter proposed by the UMTS norm with roll-off factor $r_{off} = 0.22$, approximated by a FIR spanning 10 symbol intervals

- an IF carrier of 70 MHz

- the symbol rate (chip rate) proposed by the UMTS-TDD norm, that is $R_s = 3.84$ Mchips/s

The transmitter and receiver sampling frequency is $f_s = f_{IF}/(5 + 1/4) = 13.33$ MHz, yielding $f_s/R_s \approx 3.4722$ according to (5.4). In approach 1 the low-pass filter h is a linear phase FIR filter designed by using the Remez algorithm [51] in order to minimize the distortion in the signal bandwidth. For the sake of notation we denote as L_{Tx} and L_{Rx} the upsampling factors for the transmitter and receiver resampling system respectively, instead of using L_u as done in the previous sections.

Figures 5.8–5.11 show the performance of the receiver front-end with resampling approach 2 using nearest neighbor, linear, cubic, and cubic spline interpolation at the receiver, respectively. Each figure shows the performance for transmitter up-sampling factors $L_{Tx} = 4, 8, 16, 32, 64$. With large L_{Tx} and cubic spline interpolation at the receiver the system yields negligible SINR degradation over the range $[-20, 30]$ dB of nominal $\mathcal{E}/I_0$.
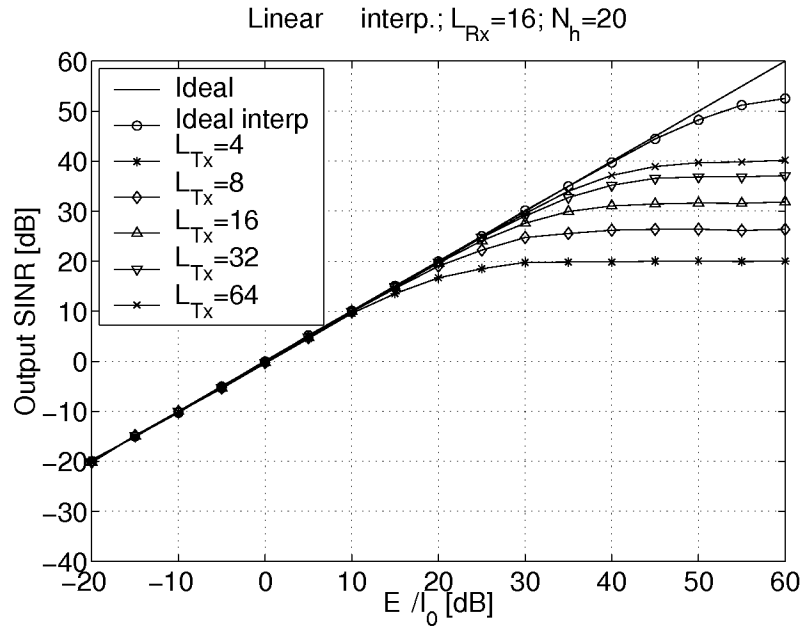
Figure 5.5: Receive resampling approach 1, $N_h = 20$, $L_{Rx} = 16$, and linear interpolation

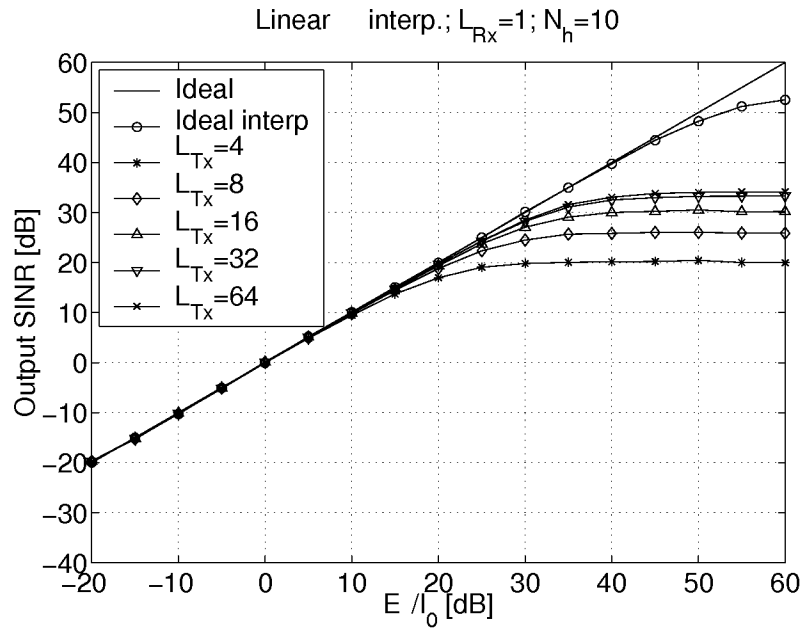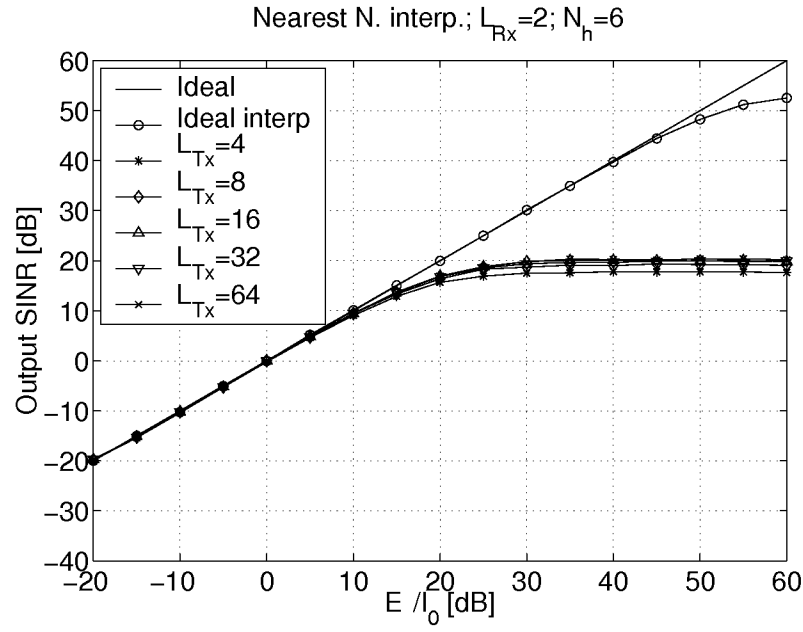Figure 5.6: Receive resampling approach 1, $N_h = 10$, $L_{Rx} = 1$, and linear interpolation

Figure 5.7: Receive resampling approach 1, $N_h = 6$, $L_{Rx} = 2$, and nearest neighbor interpolation
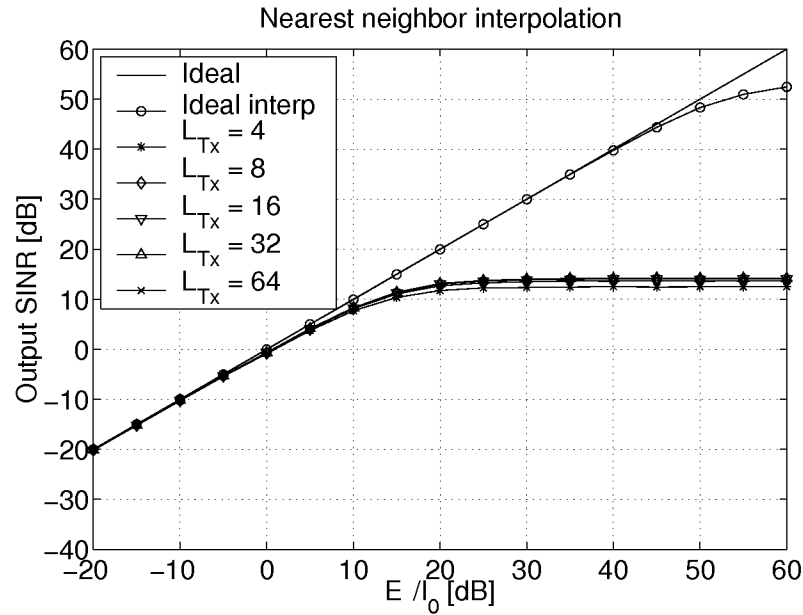

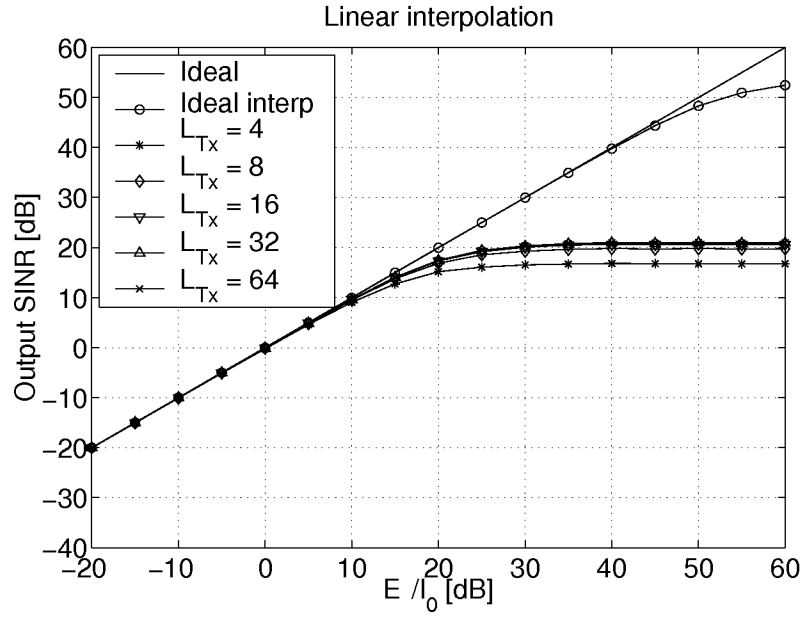Figure 5.8: Receive resampling approach 2 and nearest neighbor interpolation

Figure 5.9: Receive resampling approach 2 and linear interpolation
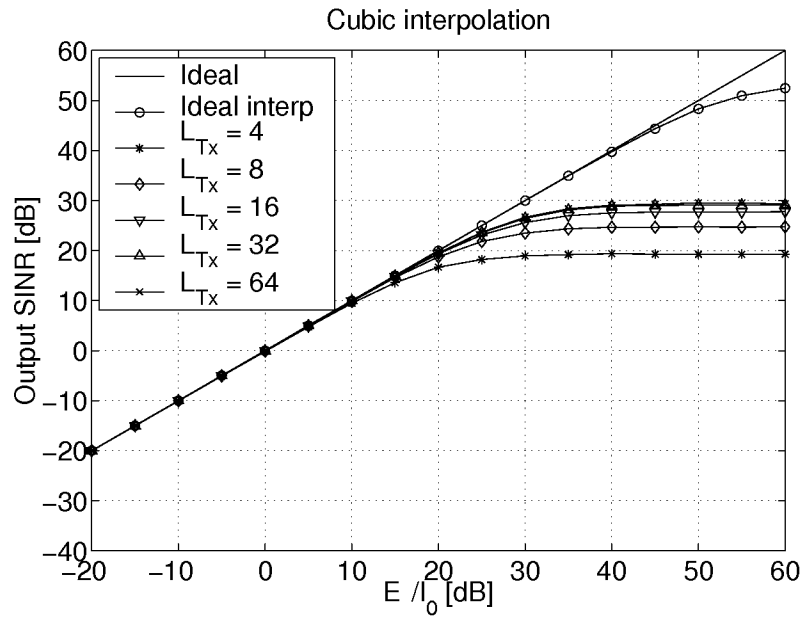

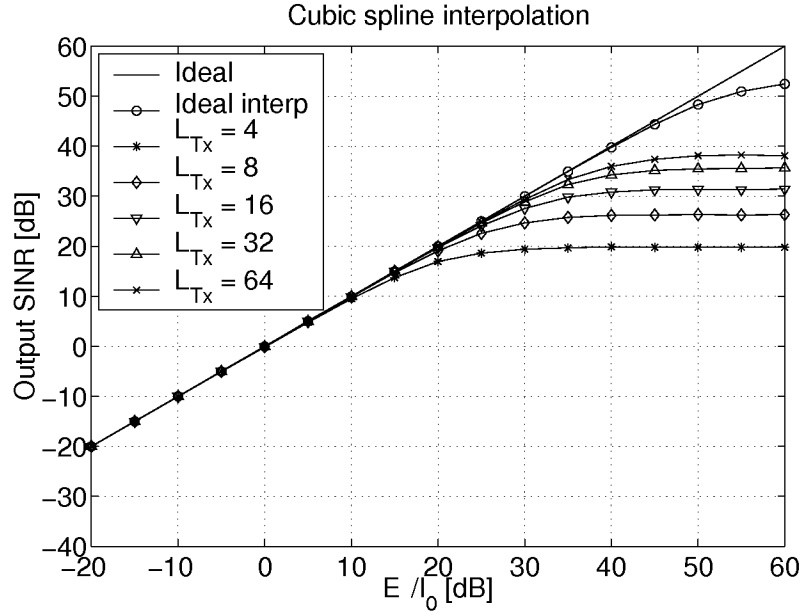Figure 5.10: Receive resampling approach 2 and cubic interpolation

Figure 5.11: Receive resampling approach 2 and cubic spline interpolation

The best performance with approach 2 are achieved by cubic spline interpolation whose complexity is approximately equivalent to that of approach 1 when a filter with $N_h = 20$ coefficients per phase, $L_{Rx} = 16$, and nearest neighbor interpolation are employed at the receiver (see figure 5.4). Although the complexity of the two approaches is almost the same in this case, we remark that with approach 1 up to 320 coefficients need to be stored in and loaded from memory. Moreover when the number of filter coefficients becomes high because of large values of L_{Rx}, the DSP has to handle memory accesses and loading data while doing computations and this fact can significantly reduce the actual computation speed.

Approach 1 can achieve better performance than approach 2 at the cost of an increased complexity, e.g. by using the same $L_{Rx} = 16$ but employing linear interpolation instead. As shown in Figure 5.5 the performance gain is about 3 dB in the high $\mathcal{E}/I_0$ region while the complexity is doubled with respect to the nearest neighbor interpolation and to approach 2 with cubic spline interpolation.

We may also try to keep the same complexity as approach 2 with cubic spline interpolation by using a filter of length $N_h = 10$ samples per phase and linear interpolation. However this solution yields worse performance as shown in figure 5.6.

In general, a way to reduce the complexity in approach 1 consists of reducing the length of the filter h. Anyway a shorter filter rejects less noise and introduces larger signal distortion. So when increasing L_{Rx} this corresponds to increasing the temporal resolution of the interpolation and can result in poor performance. Indeed, high temporal resolution makes the interpolation follow the signal variations due to the high frequency components associated with noise and distortion. For instance, in the case of $N_h = 10$ and linear interpolation we have seen that for $L_{Rx} > 1$ the performance monotonically decreases as L_{Rx} increases. For the same value of N_h nearest neighbor interpolation yields the maximum performance for $L_{Rx} = 4$. This

leads to conclude that for a given filter length there exists an optimal trade-off between the type of interpolation and the number of filter phases L_{Rx}.

Another example of this behavior is given in figure 5.7 where the performance is shown for $L_{\text{Rx}} = 2$, $N_h = 6$, and nearest neighbor interpolation. Larger values for L_{Rx} worsen the performance for the reasons explained above. The complexity of this system is about the double of the one of approach 2 with linear interpolation (see figure 5.9), but yields worse performance.

We can conclude that approach 2 is actually an attractive solution for many practical scenarios in terms of performance and complexity.

5.5   Example: training-sequence based channel estimation

The receiver front-end output signal, sampled at rate multiple integer of the symbol rate is suitable to be further processed by the receiver. In this section we test the effectiveness of the proposed front-end algorithms on a training-sequence based multiuser channel estimation procedure for block-synchronous CDMA (e.g., UMTS in TDD mode).

In this scheme users are roughly synchronized to a common time-reference and transmit their training sequences at the same time (user timing errors are included as effect of the channel and accounted for in the estimation procedure). The maximum channel length (including possible timing errors) is C_{off} chips (see Section 2.1.4) and the training sequence sent by each user is built from the same common base sequence $s_{\text{t}} = \left[s_{\text{t}}[0], s_{\text{t}}[1], \ldots, s_{\text{t}}[P_{\text{tr}} - 1] \right]^{\text{T}}$ of length P_{tr} chips, by adding a cyclic extension of C_{off} chips. This solution allows a joint estimation of all users' channels if $P_{\text{tr}} \geq C_{\text{off}} U$, where U is the number of interfering users (see [18, 19], and with some modifications [20], and references therein for more details).

Under these assumptions we can write the received signal sampled at frequency $R'_s = N_c R_s$ during the P_{tr} symbols spanned by the training sequence as

$$y \;=\; \bar{S}_{\text{t}} g + \nu \tag{5.16}$$

where

$$y = \left[y[0], \; y[1], \ldots, \; y[P_{\text{tr}} N_c - 1] \right]^{\text{T}}$$

is the received signal,

$$g = \left[g_1^{\text{T}}, \; \ldots, \; g_u^{\text{T}} \ldots, \; g_U^{\text{T}} \right]^{\text{T}} \tag{5.17}$$

is a vector containing the channel impulse responses of all U users,

$$g_u = \left[g_u[0], \; g_u[1], \; \ldots, \; g_u[C_{\text{off}} N_c - 1] \right]^{\text{T}}$$

is the uth user channel impulse response, and ν is a vector of interference plus noise samples, assumed white. The $P_{\text{tr}} N_c \times P_{\text{tr}} N_c$ matrix $\bar{S}_{\text{t}}$ is defined as

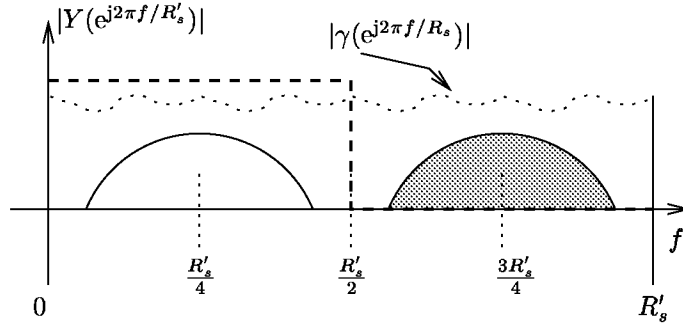$$\bar{S}_{\text{t}} = S_{\text{t}} \otimes \mathbf{I}_{N_c} \tag{5.18}$$

Figure 5.12: Estimation of the complex pass-band channel response

where S_t is a circulant matrix containing all the possible cyclic shifts (by columns) of the base sequence s_t. The matrix $\bar{S}_t$ is also circulant and it is unitary similar [56] to the diagonal matrix $\mathrm{diag}(\bar{\gamma})$, where

$$\bar{\gamma} = \left[\underbrace{\gamma^T, \ldots, \gamma^T}_{N_c \text{ times}} \right]^T$$

and where γ is the discrete Fourier transform of s_t. After some algebra, it is possible to show that the least squares estimation of the overall channel impulse response g is given by [20]

$$\hat{g} = \mathrm{IDFT}\left\{ \frac{\mathrm{DFT}\{y\}}{\bar{\gamma}} \right\} \tag{5.19}$$

where DFT and IDFT denote direct and inverse discrete Fourier transforms and the ratio of two vectors should be interpreted as the element-by-element division.

In the case of pass-band signals considered here, figure 5.12 shows qualitatively the spectrum $Y(e^{j2\pi f/R'_s})$ of y, and the spectrum corresponding to $\bar{\gamma}$ for $N_c = 4$. Since the transmitted signal is (approximately) bandlimited and centered around $R'_s/4$, the pass-band one-sided (i.e., complex) channel impulse response of all users can be estimated by setting to zero all coefficients of DFT$\{y\}$ but those in the frequency range $[R'_s/4 - W_\psi/2, R'_s/4 + W_\psi/2]$. In this way, the computation of (5.19) is further simplified.

The method applies to pass-band signals as well as to base-band signals, without complexity increase. Furthermore, pass-band signals do not need explicit demodulation. Demodulation can be automatically achieved by down-sampling the output of the pass-band symbol matched filter at symbol rate.

5.5.1 Performance with channel estimation

We used the training sequence defined in the 3GPP proposal for the UMTS-TDD mode [13] and the "Midamble type 2" defined in the Table 2.1. The sequence length is $P_{tr} = 192$ chips and the assumed channel length is $C_{off} = 64$ chips, allowing the simultaneous estimation of $U = 3$ users. Due to the oversampling factor $N_c = 4$ we need to perform an FFT over $192 \times 4 = 256 \times 3$ (real) samples, which can be efficiently

implemented as a mixed radix FFT, (i.e., one radix 4 and one radix 3). We considered a channel with MIP given by the set of delays

$$\tau = [0,\ 0.9,\ 2.8,\ 4.7]$$

normalized with respect to the chip interval, and by the relative path strengths

$$\sigma^2 = [0,\ -2,\ -7,\ -8.5]\ \mathrm{dB}$$

(the sum of the path gains is normalized to 1). The output SINR is not useful here since this would be dominated by the ISI introduced by the multipath channel. Then, as performance measure we use the Matched Filter Bound (MFB) [16], that is, the SINR at the output of the matched filter for the transmission of an isolated symbol (i.e., without ISI). This can be regarded as an upper bound to the performance of the optimal ML sequence estimator.

Figures 5.13, 5.14, 5.15, and 5.16 show the MFB resulting from the estimated matched filter versus the MFB of an ideally matched filter, equal to the nominal $\mathcal{E}/I_0$, the total channel gain being normalized to one. Since in this case we are dealing with a CDMA system $\mathcal{E}$ corresponds to the average chip energy. In the light of the previous results we consider the transmitter to employ nearest neighbor interpolation while the receiver resampling system adopts one of the methods of approach 2. The curves denoted by "Ideal interp." refer to the performance when ideal interpolation is used at both transmitter and receiver. Notice that in this case this curve does not have a horizontal asymptote since ISI is not present. Here, the degradation is due to the channel estimation errors (dominating the low $\mathcal{E}/I_0$ region) and to resampling distortion (dominating the high $\mathcal{E}/I_0$ region).

With linear interpolation and $L_{\mathrm{Tx}} = 32$ phases at the transmitter an operating range between 0 and 35 dB is achieved. This shows that the degradation of linear interpolation with respect to cubic and cubic spline interpolators evidenced in figures 5.8–5.11 is mainly due to ISI, namely inter-chip interference for a CDMA system. The effect of the inter-chip interference is negligible when the processing gain is large. Because of the presence of the processing gain a CDMA system typically operates in the low $\mathcal{E}/I_0$ region, therefore linear interpolation can be chosen in this case. In fact there is no need to insist on more complicated interpolation techniques to increase the performance in the high $\mathcal{E}/I_0$ region (namely higher than 10–20 dB). On the contrary, more advanced interpolation might be needed for non-spread spectrum system, especially employing modulation scheme with large spectral efficiency (e.g., 16, 64, 256 QAM modulations) which require to operate in the high $\mathcal{E}/I_0$ region to achieve the desired performance.

5.6   Conclusions

We presented simple and effective algorithms suited for a flexible implementation of transmit and receive front-ends based on programmable DSPs, for SDR applications. We compared various solutions in terms of complexity and performance. The resulting architectures for transmitter and receiver are both based on the concept of IF sampling and resampling. At the transmitter, we can generate directly the IF analog signal via

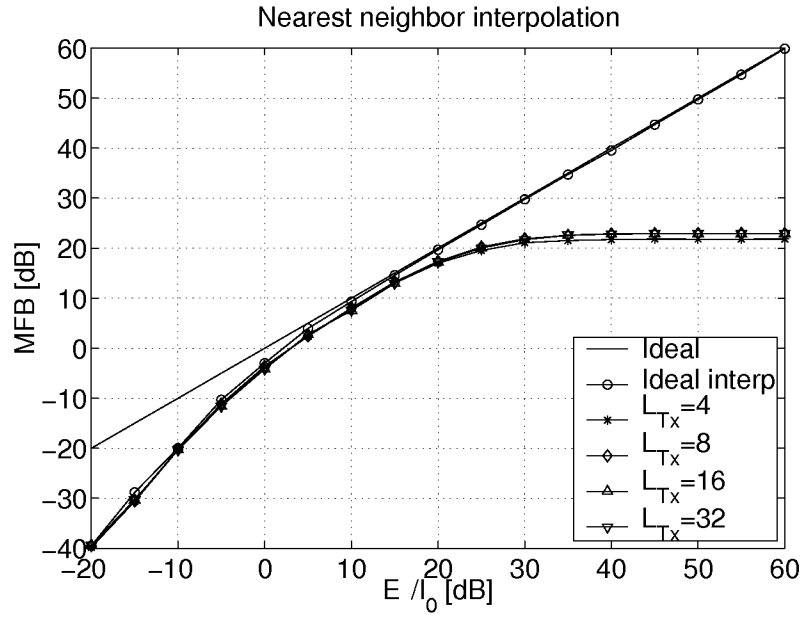Figure 5.13: Channel estimation with multipath channel and nearest neighbor interpolation at the receiver
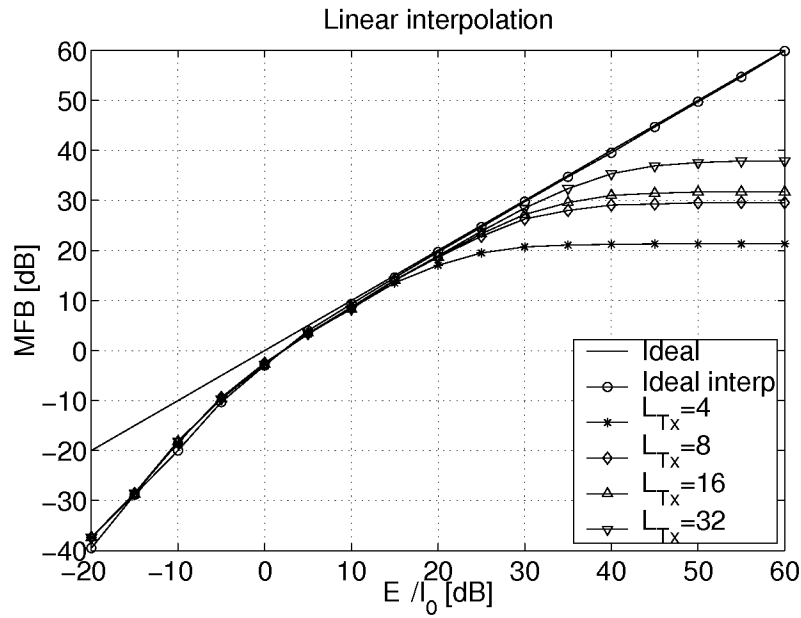

Figure 5.14: Channel estimation with multipath channel and linear interpolation at the receiver
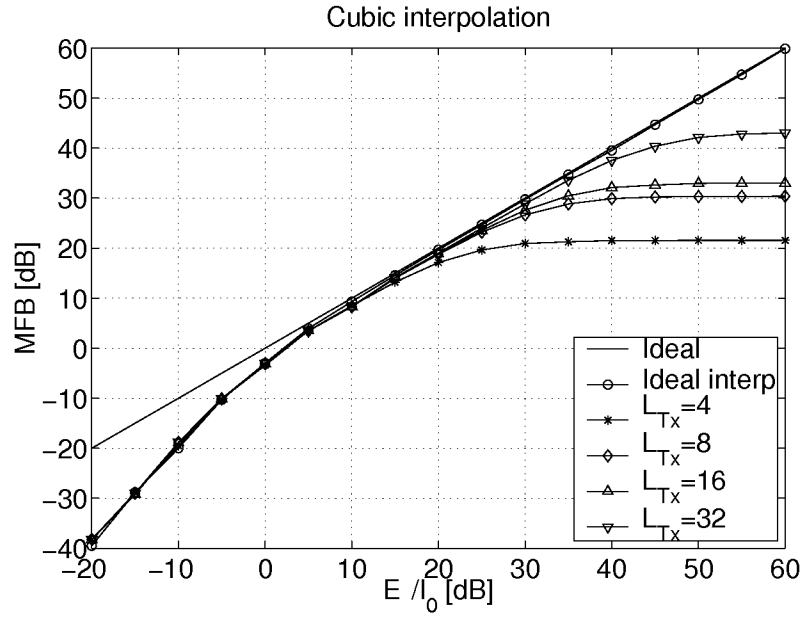
Figure 5.15: Channel estimation with multipath channel and cubic interpolation at the receiver
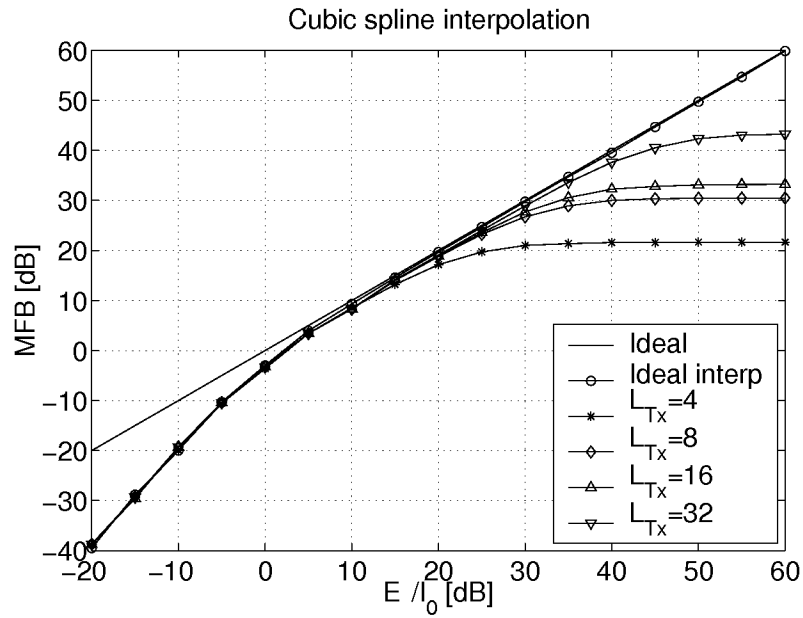
Figure 5.16: Channel estimation with multipath channel and cubic spline interpolation at the receiver

the D/A converter, without using mixers, filters and I-Q adders. At the receiver, the IF analog signal is downsampled at a much lower rate than the Nyquist rate in order to generate a pass-band digital signal with low carrier frequency, suited to further processing. Resampling at both transmitter and receiver is needed to support several different symbol (or chip) rates. At the transmitter resampling can be integrated with pulse-shaping and can be efficiently implemented by a polyphase filter-bank followed by nearest-neighbor interpolation. At the receiver more accurate interpolation techniques are needed while the pulse-shaping matched filter can be more efficiently integrated with the channel matched filter, provided by a channel estimator. Our simulation results show that cubic-spline interpolation with approach 2 provide very small SINR degradation over a wide range of nominal $\mathcal{E}/I_0$. Finally, we tested our front-end algorithms with an actual channel estimation technique. In terms of MFB, results are very good also for linear interpolation. In the case of CDMA with sufficient processing gain, the inter-chip interference due to resampling distortion might have a negligible effect and linear interpolation in the receiver might be a good low-complexity solution.

Chapter 6

Architecture of the Software Radio Platform

We describe a software radio architecture developed for providing real-time wide-band radio communication capabilities in a form attractive for advanced 3G system research. It is currently being used to implement signaling methods and protocol similar, but not limited to, evolving 3G radio standards (e.g. UMTS, CDMA2000). An overview of the hardware system is provided along with example software implementation on both high performance DSP systems and conventional microprocessors.

6.1 Introduction and Motivation

Motivated by the worldwide activity around third generation mobile communication systems, Eurécom and EPFL have launched a joint project whose objective is to design and implement a real-time software radio communication platform to validate advanced mobile communication signal processing algorithms. The right to transmit has been granted for one 5 MHz UMTS channel in both France and Switzerland for experimental purposes.

The platform is characterized by the following major features:

- Flexibility, achievable by a software driven system.

- Duplex communication.

- Multiple antennas transmit and receive signal processing (i.e. joint spatio temporal signal processing).

Flexibility remains a key word for a software-defined system. In our case it serves several purposes. For instance one may perform propagation channel measurements and transmitter characterization, evaluate the performance of different signal processing algorithms for both single user and multi-user systems under different operating conditions. *Duplex communication* is also necessary to allow higher-layer protocol testing and services, and to analyze more complex system aspects, such as multiple-access, power control, and optimize down-link signal processing from up-link measurements. In a second phase, the platform will allow *multiple-antenna signal processing*, or more generally, spatio-temporal signal processing (also known as array processing) since this a very promising ensemble of techniques able to significantly increase the capacity of wireless communication systems.

The main focus of this Chapter is on the description of the basic platform architecture and signal processing to implement the essential physical layer level procedures of the UMTS-TDD mode.

We have previously learned that one of the keys to the flexibility is to move the digital processing toward the antenna. We then choose to extend the digital signal processing to the Intermediate Frequency, implementing the required algorithms on a general purpose programmable processor. In our case a multi-band Radio Frequency section takes care of translating the desired signal from a fixed IF carrier to the required RF carrier in the transmitter, and vice-versa in the receiver.

We are then concerned with the efficient generation of an IF analog signal from a base-band digital signal (transmitter front-end) and with the reverse operation (receiver front-end). Once the end-to-end transmitter and receiver architectures is defined the next step consists of synchronizing the receiver, estimating the channels associated with the users, and eventually detecting the transmitted symbols. All these operations are performed in real-time on our platform.

The adopted modulation scheme (BPSK and QPSK), the spread signal bandwidth ($W_\psi \approx 5\,\text{MHz}$), the spreading gain (DS-CDMA with allowed spreading gain of $L = 1, 2, 4, 8, 16$) and the frequency band (around 2.1 GHz) are the same as those defined in the UMTS/TDD specifications [15]. The TDD mode has been chosen because under certain circumstances it allows the exploitation of the channel reciprocity between up-link and down-link in duplex communication, and also reduces the DSP computational load for a given bandwidth.

6.2   System architecture

In a first phase, the development of the platform has been based on a single antenna architecture for the Mobile Terminal as well as for the Base Station. The retained architecture permits to easily enhance the capabilities of the platform without redesigning the essential hardware and software parts.

The BS and the MT are based on the same hardware platform and differ only in the software implementation. The different hardware parts of the platform are highly partitioned in order to enable the use as many standard cards and components as possible.

The hardware portion of the test-bed consists of 4 elements which are under software control, namely

Software-Controllable Hardware Components
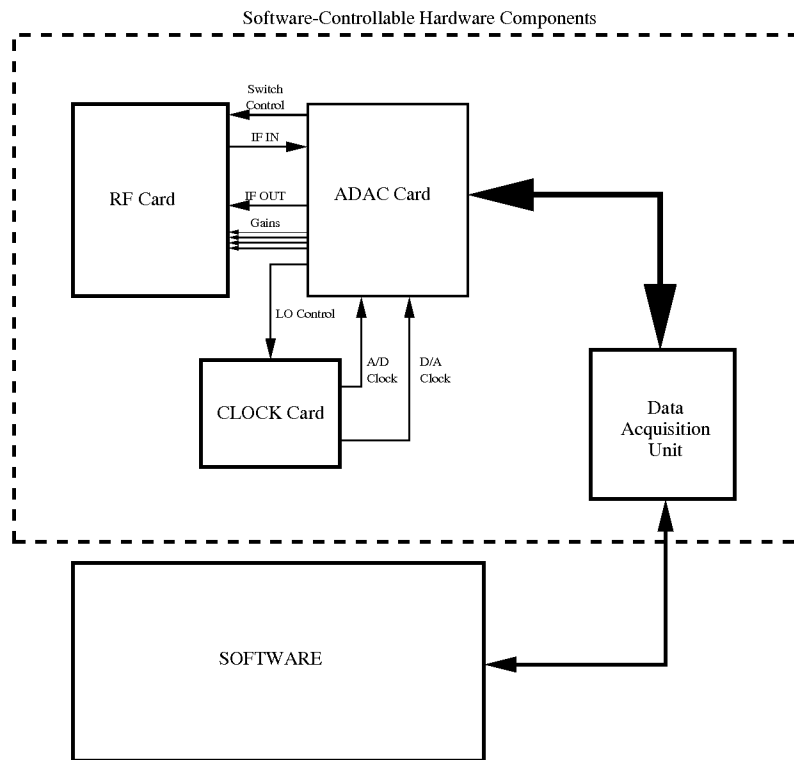
Figure 6.1: System Architecture

1. a PCI bus based reconfigurable Data Acquisition Card (DAQ) based on a Field Programmable Gate Array (FPGA)

2. an RF front-end

   - a single stage up/down-conversion from/to a 70 MHz IF carrier with Time-Division-Duplex multiplexing

   - 1 high-speed 12-bit pass-band sampling A/D converter working at rate f_{ADC}.

   - 1 high-speed 12-bit up-sampling D/A converter working at rate f_{DAC}.

   - 8 slow D/A converters for controlling various amplifier gains on the RF card

   - control for various switches on RF card

3. a clock card for generating sampling clocks (fixed frequency) and local oscillators (programmable frequency)

We show a simplified block diagram of the entire system for a single antenna in Figure 6.1.

We have considered two software implementations, the first using a combination of commercially available embedded DSP cards and a common PC and the second using the DSP units (e.g. MMX) of a standard PC under an operating system proving

hard real-time support (e.g. RTLinux). Both run in real-time and are compatible over the air.

6.2.1   RF front-end

A simplified block diagram of our RF front-end is shown in Figure 6.2. It was designed in conjunction with STMicroelectronics in Geneva, Switzerland.

On reception (Rx), the RF signal is filtered, amplified and down-converted to a 70 MHz IF. The Local Oscillator (LO) frequency is digitally tunable in steps of 500 Hz. The IF signal is amplified by a digitally tunable gain control and directly sampled at rate f_{ADC}. The samples are transferred via a ribbon cable using high-speed line drivers to the Data Acquisition Card.

On the transmission end (Tx), samples from the DAQ drive a hardware up-sampling circuit and a high-speed D/A converter, working at rate f_{DAC}, to directly synthesize the 70 MHz IF signal. The IF signal is then amplified, up-converted to RF, filtered and amplified by a variable-gain power amplifier.

The mode of the transceiver (i.e. transmission, reception, calibration) is fully controllable from the software portion of the platform.

Special low-speed lines control the gains of the Rx variable-gain amplifier and Tx Power Amplifier, LO frequency, as well as the antenna switch. Although not included in Figure 6.2, automatic wide-band calibration capabilities (for both Tx and Rx) are included in the design, which are required for multi-antenna systems (see e.g. [57]). These will be used in a later stage of the project where the architecture will be extended to implement multiple antenna transceivers. The basic characteristics of the RF front-end are summarized in Table 6.1.

Pass-band A/D conversion

The main difference of the current implementation with respect to the UMTS-TDD 3GPP standard is that we choose a chip rate $f_c = 3.6864$ Mchips/s (CDMA2000 chip rate) and not 3.84 Mchips/s. Moreover, in order to avoid signal re-sampling [1] we suppose the rate f_{ADC} to be a multiple integer of the chip rate (i.e. $f_{\text{ADC}} = N_c f_c$). In our implementation we set $N_c = 4$ that yields

$$f_{\text{ADC}} = 4f_c = 14.7456 \, \text{Msamples/s}$$

So, once the RF signal at the antenna has been down-converted to IF, it is sampled by the A/D converter at rate f_{ADC} (see Figure 6.4). Because of the periodicity of the discrete-time signal spectrum, the resulting real sampled signal is given by [2]

$$y[n] = y_{\text{IF}}\left(n/f_{\text{ADC}}\right)$$

---

[1]The re-sampling techniques studied in Chapter 5 will be implemented in the next version of the software

[2]Notice that, by using the notation of Chapter 5 (see for example Figures 5.2 and 5.3), and avoiding interpolation at the receiver, we have $y[n] = r[n] = y_{\text{IF}}(n/f_{\text{ADC}})$
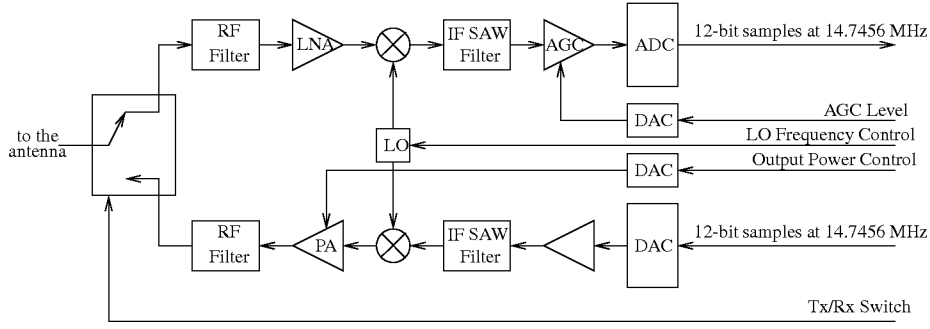
Figure 6.2: RF Front-end

The signal $y[n]$ is pass-band with a spectrum replica centered at $f_{\mathrm{ADC}}/4$ as shown in Figure 6.4. In practice we applied (5.4) using $\ell = 5$ and choosing the sign $(-)$ in the denominator. The sampling frequency f_{ADC} also satisfies the condition

$$f_{\mathrm{ADC}} \geq 2W_\psi \approx 10\,\mathrm{MHz}$$

required by the theory in Section 5.2.2.

Although a base-band version of the received signal can be obtained by multiplying $y[n]$ by $(-j)^n$ and then by low pass filtering, we will show further how the channel estimation and the data detection processes can be performed at pass-band.

Pass-band D/A conversion

At the transmitter side we send to the D/A converter the pass-band signal $x'[n]$, obtained by the base-band signal $x[n]$ using (5.5). The signal $x'[n]$ shows a replica of the spectrum in f_{IF} and is sampled at rate

$$f_s = N_c f_c = 14.7456\,\mathrm{Msamples/s}$$

where we set $N_c = 4$ as for the receiver. Also in this case the sampling rate satisfies the inequality $f_s \geq 2W_\psi$.

In Section 5.2.3 it is shown that, in order to reduce the attenuation introduced by the D/A impulse response up-sampling is required. In our implementation we chose

$$f_{\mathrm{DAC}} = 8f_s = 117.9648\,\mathrm{Msamples/s}$$

so that the spectrum replica of $x'[n]$ at f_{IF} falls inside the main lobe of the D/A frequency response (see Figure 5.1(b)).

6.2.2 Data Acquisition Card (DAQ)

The data acquisition card is a PCI bus-mastering device permitting high-speed full duplex parallel transfer of digital data from an external device. It contains the necessary glue logic which connects the input (A/D) and output (D/A) sample streams as well as some control signals to the main CPU/DSP. A PCI architecture was adopted since

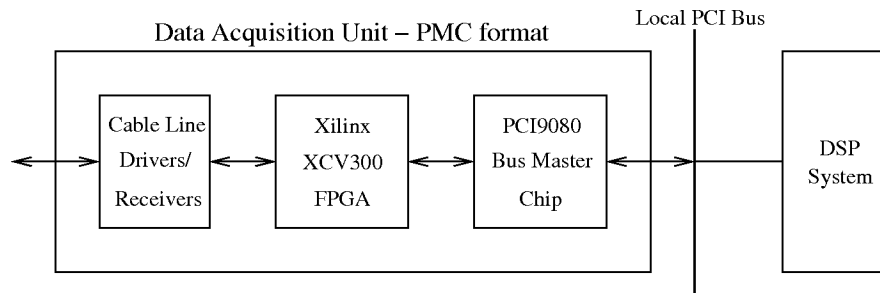Data Acquisition Unit – PMC format   Local PCI Bus

Figure 6.3: Data Acquisition Unit

it is the most general purpose bus architecture and is used on most standard PCs, as well as DSP systems. It consists of two components, namely a powerful Xilinx Field Programmable Gate Array (FPGA) XCV300 [58] and a bus-mastering PCI controller PLX9080 [59]. The format is a *PCI Mezzanine Card* (PMC) to allow for integration into both embedded DSP architectures and ordinary PCs. A simplified overview of the DAQ is shown in Figure 6.3.

Firmware on the FPGA for formatting and transferring data via the DMA engines of the PLX9080 to the host (DSP, CPU) memory has been developed in VHDL (Very High Speed Integrated Circuit Hardware Description Language). After an initial configuration phase, transfers are continuous and completely transparent to the host, who just "sees" a circular buffer containing samples acquired from or to be transferred to the external RF front-end.

The basic components of the DAQ are the following

1. Line Drivers/Receivers for transfer from external devices via ribbon-cables

2. A reconfigurable FPGA-based 16-bit bi-directional interface external device (up to 30 Msamples/s full-duplex)

3. A PCI bus-mastering controller for direct transfer of samples to/from memory (DMA) on PCI-based signal processing units (e.g. DSP cards, high-performance PCs, workstations (SPARC, PowerPC, Alpha), embedded processor cards, etc.)

4. A *Processor Mezzanine Card (PMC)* form-factor for maximum flexibility

The FPGA is programmed via the PCI bus by serial download.

6.2.3   Texas Instruments TMSC6201 implementation

The embedded DSP architecture is based on a commercially available dual-DSP card (Spectrum Signal Processing Daytona [60]). The basic architecture is shown in Figure 6.7 and is centered around 2 Texas Instruments TMSC6201 fixed-point DSPs. These DSPs are capable of providing a maximum of 1600 MIPS each. Our DAQ is placed on the local PCI bus of the DSP board and transfers samples to/from both of the memory buffers on the DSPs busses. These buffers are used as temporary storage as the internal (fast) memory of the DSP is rather small. The DSP DMA engines take care of automatically transferring data to their internal memory concurrently with the
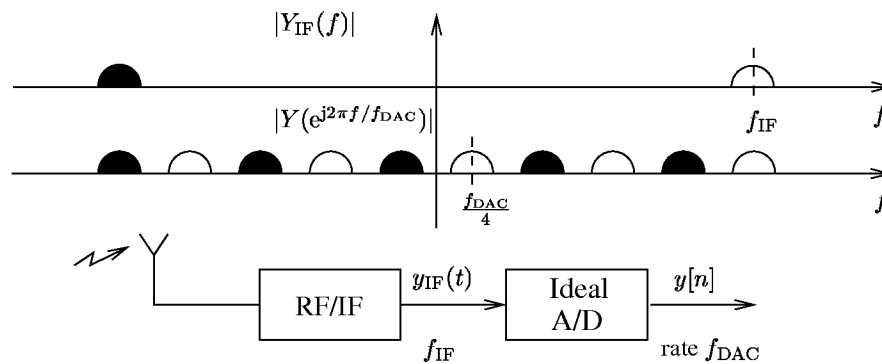
Figure 6.4: Receiver front-end

signal processing functions. One DSP is used exclusively for transmission functions and the other for reception.

The DSPs are used for the front-end processing as described in the previous sections. Symbol rate data is transferred via the PCI bus to the PC which hosts the DSP card. This data is processed by the Pentium and handles tasks such as Viterbi decoding, carrier frequency offset compensation, higher layer protocol stacks, etc..

6.2.4 RTLinux-based PC implementation

The second implementation does not rely on embedded DSPs. Here the DAQ is placed on the master PCI bus of a workstation, possibly multiprocessor, running the hard real-time extension to the Linux operating system, RTLinux[61]. The software radio runs in kernel space and is integrated into the IPv4 (Internet Protocol) subsystem of Linux as a network device.

This x86 implementation makes use of the MMX (multimedia extensions) SIMD (single instruction multiple data) instructions for obtaining maximum processor efficiency for intensive DSP computations. All DSP routines use fixed-point arithmetic and are written in C with embedded assembly macros for time-critical code sections. We typically make use of

1. MMX packed 16-bit arithmetic (multiply, add, MAC, interleaving, etc.)

2. loop unrolling

3. software pipelining

Because of the high-level software structure, this should be portable to other processor architectures (e.g. PowerPC, Alpha, etc.). For the same reason, it is easily portable to large-scale SMP (symmetric multi-processing) platforms which could be useful for advanced base-station implementations.

6.3   Physical layer digital signal processing

This section gives an overview of some theoretical principles on which the platform software has been implemented. We have implemented variant of the UMTS-TDD 3GPP standard and are now implementing a complete subset of layers 1 and 2 of the true standard (including 1.28 Mchips/s version). After D/A conversion, a pass-band filter centered at f_{IF} removes the other replicas, generating the desired IF modulated signal. The discrete-time modulation by $f_{\mathrm{DAC}}/4$ requires a negligible computational cost since it corresponds to change alternatively the signs of $x[n]$ as can be noticed by (5.3).

6.3.1   Receiver

In this section we give a description of the receiver front-end architecture. Then we focus on channel estimation, matched filter synthesis and symbol detection.

Frame synchronization

In order to minimize the computational cost, the frame synchronization is achieved using a simplified version of the "MAX" timing estimator defined in Section 3.5. In our implementation we correlate the input signal $y[n]$ with a filter matched to the primary synchronization sequence s_{tr} but not to the chip pulse $\psi(t)$. The timing estimation is achieved by filtering the pass-band received signal $y[n]$ as

$$y_{\mathrm{ps}}[n] = \left[\sum_{k=0}^{255} s_{\mathrm{ps}}[k]\delta[n + 4k] \right] \star y[n] = \sum_{k=0}^{255} s_{\mathrm{ps}}[k]y[n + 4k] \qquad (6.1)$$

and averaging the $y_{\mathrm{ps}}[n]^2$ over several frames. This is typically the most computationally intensive part of the receiver front-end since it requires a fairly long filter operating at the sampling rate. The 3GPP standard uses a hierarchical structure for the primary synchronization sequence (see Section 2.1.3) which allows the filter to be implemented as a concatenation of 2 FIR filters of length 16. The filter output $y_{\mathrm{ps}}[n]$ can then be obtained by

$$\begin{aligned} y_{\mathrm{ps}}[n] &= \left[\sum_{k=0}^{15} s_{\mathrm{ps2}}[k]\delta[n + 64k] \right] \star \left[\sum_{k=0}^{15} s_{\mathrm{ps1}}[k]\delta[n + 4k] \right] \star y[n] \\ &= \left[\sum_{k=0}^{15} s_{\mathrm{ps2}}[k]\delta[n + 64k] \right] \star \left[\sum_{k=0}^{15} s_{\mathrm{ps1}}[k]y[n + 4k] \right] \end{aligned} \qquad (6.2)$$

reducing the computational cost by a factor 8. The maximum output of this filter is used to adjust the receive signal strength (via a variable gain IF amplifier) and synchronization is achieved when the maximum is greater than a pre-defined threshold. Note that this filtering operation involves purely real quantities. A block diagram of the primary synchronization signal processing is shown in Figure 6.5.
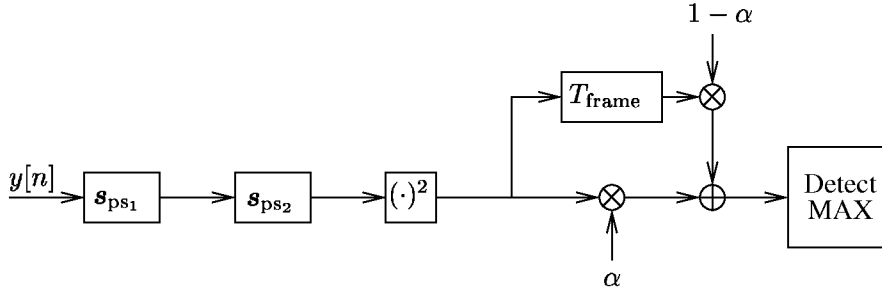
$$1 - \alpha$$

$$y[n] \rightarrow \boxed{s_{\mathrm{ps}_1}} \rightarrow \boxed{s_{\mathrm{ps}_2}} \rightarrow \boxed{(\cdot)^2} \rightarrow \boxed{T_{\mathrm{frame}}} \rightarrow \otimes$$

$$\alpha$$

$$\boxed{\begin{array}{c}\text{Detect}\\\text{MAX}\end{array}}$$

Figure 6.5: Scheme of the implemented primary synchronization signal processing

Channel estimation

The training-sequence based multiuser channel estimation procedure for block synchronous CDMA described in the UMTS/TDD standard has been implemented following the FFT approach given in Section 5.5. The algorithm provides the estimates $\hat{g}$ of the channel g. A block scheme of the channel estimation procedure is summarized in Figure 6.6.

Matched filter synthesis and data detection

Given the channel estimates, we are then interested in synthesizing the Matched Filters f_u, for $u = 1, \ldots, U$, matched to the cascade formed by the user data spreading sequence, the chip pulse shape filter and the user channel. This is also shown in Figure 6.6. The overall impulse response for the uth user is given by

$$f_u(t) = \sum_{k=0}^{L_u-1} s_u[k] g_u(t - k/f_c) \tag{6.3}$$

where L_u is the uth user spreading gain. Using the sampled channel estimate $\hat{g}$ we synthesize the discrete-time filters

$$f_u[k] = f_u(t)|_{t=k/f_{\mathrm{ADC}}}$$

matched to the overall response as follows

$$\hat{f}_u[k] = s_u[k] \star \hat{g}_u[k] \tag{6.4}$$

In order to extract the data symbols we filter the received signal with the MF obtaining

$$v_u[k] = y[k] \star \hat{f}_u^*[-k] \tag{6.5}$$

In a pass-band approach $y[k]$ is real while $\hat{f}_u[k]$ is complex so the product requires two real multiplications. In the base-band case, instead, the samples of $y[k]$ would be at half the sampling rate but would be complex. So the two complexities are identical.

Notice that the signal after matched filtering is still pass-band and the symbol estimates after sub-sampling are given by
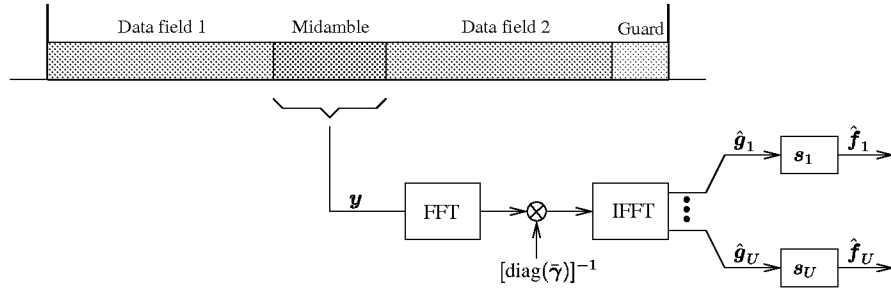
$$\hat{a}_u[k] = v_u'[N N_c k] \tag{6.6}$$

Figure 6.6: Channel Estimation and Matched Filter Synthesis

where $v'_u[k]$ is the complex envelope of the MF output. But since

$$v'_u[k] = (-\text{j})^k v_u[k] \tag{6.7}$$

substituting into (6.6) and for $N_c = 4$ we get

$$\hat{a}_u[k] = (-\text{j})^{L_u N_c k} v_u[L_u N_c k] = v_u[4 L_u k] \tag{6.8}$$

Then the symbol estimates are given by sub-sampling the MF output at symbol rate without taking care of the demodulation.

Carrier synchronization and decoding

The carrier synchronization is done at symbol rate with a classical decision directed algorithm [16]. The algorithm then takes a decision on the symbols and recovers the data.

6.4   Validation of the existing platform

The described platform has been validated by the transmission and the reception of two user full-duplex real-time video flows in an indoor environment. Two H263 video streams are transmitted in parallel and decoded in real time. For this we use the following parameters:

- spreading factor 16

- bit rate 397 kbit/s (peak) per user

- TDD configuration: 1 Tx slot followed by 1 Rx slot (transmission is done every 2 slots).

- two synchronous full-duplex streams per slot

- RF band: 5 MHz at 2.1 GHz
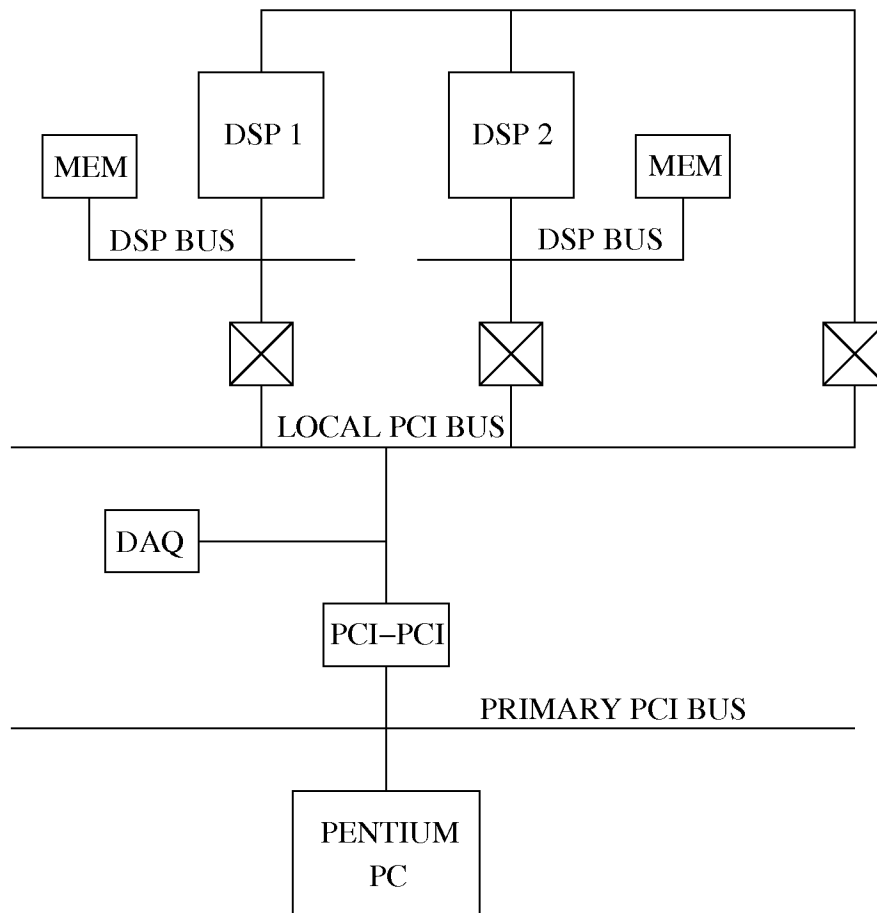
Figure 6.7: Embebbed DSP Architecture

6.5 Conclusion

This first demonstration shows that the architecture of the platform is capable of sustaining real-time communications and is thus promising for future developments. The platform is currently being enhanced and opened to both industrial and academic collaboration.

The enhancements will consist of

- support for multiple antenna transceivers

- more sophisticated signal processing algorithms

- multi user detection

- layer 2 (RLC,MAC) functionality

Collaboration has already begun under the label of the RNRT (*Réseau National de la Recherche en Télécommunications*) financing program organized by the French Ministry of Industry and Finance. Three projects have been initiated covering the following topics:

Frequency Band	2100-2170 MHz
Bandwidth	5 MHz (initially)
Transmit Power (per antenna)	1 W
Receiver Sensitivity	-100 dBm
Noise Figure	< 5 dB
Input IP3	> -7 dBm
Duplex mode	Time Division
Rx Gain Control	Digital tuning, 1dB steps over 40 dB
Tx Power Control	Digital tuning, 1dB steps over 80 dB range
Local Oscillator	Digital tuning, step: few kHz in each band
RF Calibration	Digital control, Tx and Rx
Direct IF sampling (70 MHz) on Rx	12-bit A/D @ 14.7456 Msamples/s
Direct IF synthesis (70 MHz) on Tx	12-bit D/A @ 117.9648 Msamples/s
Digital Interface	High speed: LVDS
	Low speed: 3.3V CMOS line drivers

Table 6.1: RF Front-end characteristics

- radio subsystem improvement (flexibility and sensitivity)

- compliance with the 3GPP UMTS/TDD specification

- higher-level protocol stacks

- integration to an IPv6 experimental backbone

Chapter 7

General conclusions

In this thesis we addressed the problem of improving the physical layer reliability of W-CDMA third generation transceivers by designing simple and low complexity algorithms suited to be implemented on a real system. The work was developed in a framework of a joint project between Eurécom and EPFL whose objective is to design a real-time Software Defined Radio platform able to validate advanced signal processing algorithms. The UMTS-TDD 3GPP standard, on which the platform has been initially targeted, was used throughout this work as a reference system for comparisons. These algorithms, suited to SDR, cover some major issues of the physical layer signal processing such as synchronization, and multiuser detection. Since the aim was to propose solutions for a practical implementation, particular care has been devoted to the algorithm complexity evaluation. Finally, the proposed algorithms have been tested in a realistic scenario, including frequency selective channels, fast and slow fading conditions, power control, and timing estimation errors.

The initial synchronization between a Mobile Terminal and a Base Station has been covered by Chapter 3 where we derived a Joint Maximum Likelihood slot timing estimator for bursty pilot signals in the presence of multipath fading channels, with the following conclusions:

- While the traditional "MAX" slot timing estimator provides good performance for short channels it performs very poorly in the presence of sparse channels

- The proposed "JML" estimator shows good performance in all the considered conditions, and is very robust to mismatch. Moreover, at the same time, it provides an estimate of the multipath intensity profile and of the interference plus noise power spectral density.

- With respect to a PN sequence, the primary synchronization sequence proposed

97

by the UMTS-TDD standard reduces the performance of the slot timing estimators because of its less peaky aperiodic autocorrelation function.

Future research in this area may consider the exploitation of the additional informations provided by the JML algorithm for improving the communication reliability immediately after the primary synchronization process (e.g. demodulation of the UMTS-TDD secondary synchronization signal and detection of the scrambling sequence).

In order to increase the system capacity, in Chapter 4 we designed an iterative turbo equalizer and multiuser decoder/detector for TD-CDMA systems. Simulation results showed that:

- Simple and low-complexity multiuser detection techniques outperforms the powerful and high complexity channel coding envisaged by the UMTS-TDD norm.

- High channel loads can be obtained by using simple convolutional codes and Viterbi decoding instead of using the more computationally intensive SISO decoding.

- Since the proposed algorithm is very simple and it is robust to severe ISI conditions it is well suited to be implemented on a UMTS-TDD base station.

The problem of designing a SDR architecture able to support different standards with the same hardware has been investigated in Chapter 5 where we proposed some resampling techniques for the transceiver front-end. These techniques have been tested in realistic scenarios, evaluating the SINR degradation with respect to the ideal interpolation. From the results of this Chapter the following conclusions can be pointed out:

- Resampling techniques are an efficient way to make the baseband signal processing independent on the Intermediate Frequency.

- Resampling techniques at both transmitter and receiver have a complexity affordable by the technology available on the market.

- In general, most part of the computational complexity required by the interpolation techniques stays in the receiver.

- With a negligible computational cost the transmitter front-end can directly generate the IF signal at the output of the D/A converter.

- Even if interpolation distorts the signal, a careful choice of the interpolation technique allows a wide SINR operating range at the receiver.

- In the case of CDMA with sufficient processing gain, the inter-chip interference due to resampling distortion might have a negligible effect.

Moreover we have shown that with a common PC, equipped with conventional microprocessor and/or with high performance DSPs it is possible to implement real-time UMTS-TDD Base Stations and Mobile Terminals, compliant to the 3GPP standard. The theoretical research developed throughout this thesis has been of main relevance for the platform physical layer implementation and, in some cases, addressed solutions to improve the UMTS-TDD standard.

Bibliography

[1] T. Rappaport, *Wireless Communications*. Englewood Cliffs, NJ: Prentice-Hall, 1996.

[2] S. Srikanteswara, J. H. Reed, P. Athanas, and R. Boyle, "A soft radio architecture for reconfigurable platforms," *IEEE Communications Magazine*, February 2000.

[3] "Special issue on software radio," *IEEE JSAC*, vol. 4, April 1999.

[4] "Software radio," *IEEE Personal Communications*, vol. 4, August 1999.

[5] H. Tsurumi and Y. Suzuki, "Broadband RF stage architecture for software-defined radio in handheld terminal applications," *IEEE Communications Magazine*, February 1999.

[6] K. Zangi and R. Koilpillai, "Software radio issues in cellular base stations," *IEEE JSAC*, vol. 17, pp. 561–573, April 1999.

[7] J. Razavilar, F. Rashid-Farrokhi, and K. J. R. Liu, "Software radio architecture with smart antennas: A tutorial on algorithms and complexity," *IEEE JSAC*, vol. 17, pp. 662–676, April 1999.

[8] S. Verdu, *Multiuser detection*. Cambridge, UK: Cambridge University Press, 1998.

[9] S. Verdu and S. Shamai, "Spectral efficiency of CDMA with random spreading," *IEEE Trans. on Inform. Theory*, vol. 45, pp. 622–640, March 1999.

[10] S. Shamai and S. Verdu, "The impact of frequency-flat fading on the spectral efficiency of CDMA," *IEEE Trans. on Inform. Theory*, vol. 47, pp. 1302–1327, May 2001.

[11] M. Varanasi and T. Guess, "Optimum decision feedback multiuser equalization with successive decoding achieves the total capacity of the Gaussian multiple access channel," in *Proc. Asilomar Conference*, (Pacific Groove, CA), November 1997.

[12] R. R. Müller and S. Verdu, "Design and analysis of low-complexity interference mitigation on vector channels," *IEEE Journal on Selected Areas in Communications*, vol. 19, pp. 1429–1441, August 2001.

[13] 3GPP-TSG-RAN-WG1, "TS-25.2xx series," tech. rep., January 2000.

[14] 3GPP-TSG-RAN-WG1, "TS-25.214 v3.1.0: Physical Layer Procedures (FDD)," tech. rep., January 2000.

[15] 3GPP-TSG-RAN-WG1, "TS-25.224 v3.1.0: Physical Layer Procedures (TDD)," tech. rep., January 2000.

[16] J. G. Proakis, *Digital Communications*. NY: McGraw Hill, 4th ed., 2000.

[17] R. A. Horn and C. R. Johnson, *Topics in Matrix analysis*. Cambridge University Press, 1991.

[18] B. Steiner and P. Jung, "Optimum and suboptimum channel estimation for the uplink of cdma mobile radio systems with joint detection," *European Transaction on Communications*, vol. 5, pp. 39–49, Jan.-Feb. 1994.

[19] 3GPP-TSG-RAN-WG1, "TS-25.221 v3.1.0; physical channels and mapping of transport channels onto physical channels (TDD)," tech. rep., January 2000.

[20] G. Caire and U. Mitra, "Structured multiuser channel estimation for block-synchronous DS/CDMA." Submitted to IEEE Transaction on Communications., July 1999.

[21] 3GPP-TSG-RAN-WG4, "TS-25.105v3.1.0 UTRA (BS) TDD Radio transmission and Reception," tech. rep., January 2000.

[22] E. Dahlman, B. Gudmundson, M. Nilsson, J. Sköld, and E. R. S. AB, "UMTS/IMT-2000 based wideband CDMA," *IEEE Communications Magazine*, vol. 36, pp. 70–80, September 1998.

[23] R. R. Rick and L. B. Milstein, "Optimal decision strategies for acquisition of spread-spectrum signals in frequency-selective fading channels," *IEEE Trans. on Comm.*, vol. 46, pp. 686–694, May 1998.

[24] U. Lambrette, J. Horstmannshoff, and H. Meyr, "Techniques for frame synchronization on unknown frequency selective channels," in *Proc. VTC'97 Spring*, pp. 1059–1063, 1997.

[25] H. Meyr, M. Moeneclaey, , and S. Fechtel, *Digital communication receivers*. J. Wiley series in telecommunications and signal processing, New York: John Wiley and Sons, 1998.

[26] E. K. Chong and S. H. Zak, *An Introduction to Optimization*. John Wiley & Sons, 1996.

[27] S. M. Kay, *Fundamentals of statistical signal processing: Estimation theory*. Englewood Cliffs, NY: Prentice-Hall, 1993.

[28] T. Östman, S. Parkwall, and B.Ottersten, "An improved music algorithm for estimation of time delays in asynchronous DS-CDMA systems," *IEEE Transactions on Communications*, vol. 47, pp. 1628–1631, November 1999.

[29] 3GPP, "ETSI TS 125 222, Multiplexing and channel coding TDD 3GPP TS 25.222 Version 4.0.0 Release 4," tech. rep., March 2001.

[30] P. Alexander, A. Grant, and M. Reed, "Iterative detection in code-division multiple-access with error control coding," *European Trans. on Telecomm.*, vol. 9, pp. 419–425, September 1999.

[31] X. Wang and V. Poor, "Iterative (Turbo) soft interference cancellation and decoding for coded CDMA," *IEEE Trans. on Commun.*, vol. 47, pp. 1047–1061, July 1999.

[32] H. ElGamal and E. Geraniotis, "Iterative multiuser detection for coded CDMA signals in AWGN and fading channels," *IEEE J. Select. Areas Commun.*, vol. 18, pp. 30–41, January 2000.

[33] L. Bahl, J. Cocke, F. Jelinek, and J. Raviv, "Optimal decoding of linear codes for minimizing symbol error rate," *IEEE Trans. on Inform. Theory*, vol. 20, pp. 284–287, March 1974.

[34] R. Prasad, W. Mohr, and E. W. Konhäuser, *Third Generation Mobile Communication Systems*. Boston: Artech House, 2000.

[35] L. K. Rasmussen, "On ping-pong effects in linear interference cancellation for CDMA," *IEEE 6th int. Symp. on Spread-Spectrum Tech. & Appli.*, September 2000.

[36] D. Tse and S. Hanly, "Linear multiuser receivers: Effective interference, effective bandwidth and capacity," *IEEE Trans. on Inform. Theory*, vol. 45, pp. 641–675, March 1999.

[37] J. Boutros and G. Caire, "Iterative multiuser decoding: unified framework and asymptotic performance analysis." submitted to IEEE Trans. on Inform. Theory, August 2000.

[38] S. Marinkovic, B. Vucetic, and J. Evans, "Improved iterative parallel interference cancellation," in *Proc. ISIT 2001*, (Washington DC, USA), p. 34, June 2001.

[39] E. G. Ström and S. L. Miller, "Iterative demodulation of othogonal signaling formats in asynchronous DS-CDMA systems," *Proceedings of the ISSSE*, pp. 184–187, July 2001.

[40] T. Richardson and R. Urbanke, "An introduction to the analysis of iterative coding systems." IMA Proceedings, 2000.

[41] S. Benedetto, D. Divsalar, G. Montorsi, and F. Pollara, "Soft-Input Soft-Output building blocks for the construction of distributed iterative decoding of code networks," *European Trans. on Commun.*, April 1998.

[42] F. Kschischang, B. Frey, and H. Loeliger, "Factor graphs and the sum-product algorithm," *IEEE Trans. on Inform. Theory*, vol. 47, pp. 498–519, February 2001.

[43] J. Zhang, E. Chong, and D. Tse, "Output MAI distribution of linear MMSE multiuser receivers in DS-CDMA systems." submitted to IEEE Trans. on Inform. Theory, May 2000.

[44] M. Kobayashi, J. Boutros, and G. Caire, "Successive interference cancellation with SISO decoding and EM channel estimation." to appear on JSAC (special issue on multiuser detection), 2001.

[45] C. Berrou and A. Glavieux, "Near optimum error-correcting coding and decoding: Turbo codes," *IEEE Trans. on Commun.*, vol. 44, October 1996.

[46] "http://www.itu.int/imt/2-rad-devt/index.html."

[47] A. Furuskär, S. Mazur, F. Müller, H. Olofsson, and E. R. Systems, "EDGE: Enhanced data rates for GSM and TDMA/136 evolution," *IEEE Personal Communications*, vol. 6, pp. 56–66, June 1999.

[48] J. Mitola, "The software radio architecture," *IEEE Communications Magazine*, pp. 26–38, May 1995.

[49] P. Pirsch, *Architectures for Digital Dignal Processing.* NY: John Wiley & Sons, 1998.

[50] M. Frerking and R. Schafer, *Digital Signal Processing in Communication Systems.* New York: Van Nostrand Reinhold, 1993.

[51] A. Oppenheim and R. Schafer, *Discrete-time signal processing.* Prentice-Hall, 1989.

[52] S. Mitra and J. Kaiser, *Digital Signal Processing.* New York: John Wiley & Sons, 1993.

[53] E. Moulines, P. Duhamel, J. Cardoso, and S. Mayrargue, "Subspace methods for the blind identification of multichannel FIR filters," *IEEE Trans. on Signal Processing*, vol. 43, pp. 516–525, February 1995.

[54] L. Tong, G. Xu, , and T. Kailath, "A new approach to blind identification and equalization of multipath channels," in *Proc. of the 25th Asilomar Conference on Signals, Systems, and Computers*, (Pacific Grove, CA), November 1991.

[55] R. Sedgewick, *Algorithms in C.* Addison-Wesley, 1990.

[56] G. H. Golub and C. F. V. Loan, *Matrix Computation.* The John Hopkins University Press, 3rd ed., 1996.

[57] P. Mogensen, F. Frederiksen, H. Dam, K. Olesen, and S. Larsen, "A Hardware Testbed for Evaluation of Adaptive Antennas in GSM/UMTS," vol. IEEE PIMRC'96, pp. 540–544, Oct. 1996.

[58] Xilinx, "Xilinx 2001 FPGA Databook." http://www.xilinx.com, 2001.

[59] PLXTechnologies, "PCI9080."

[60] "Spectrum Signal Processing." http://www.spectrumsignal.com, 2001.

[61] FSMLabs, "RTlinux." http://www.rtlinux.org, 2001.

Curriculum Vitae

Alessandro Nordio

Birthdate	January 3, 1974
Address	13 Rue des petits ponts
	06250 Mougins le Haut (France)
Nationality	Italian
Telephone	+33 (0)4 93 00 29 07
e-mail	alessandro.nordio@eurecom.fr

Professional profile

- Experience in wireless communications, signal processing, synchronization, channel estimation, coding, and multiuser detection in the UMTS, W-CDMA and TD-CDMA domains.

- Software Defined Radio engineering, algorithm design and implementation for DSP.

Education and working experiences

- **January 1999 - to date** Ph.D student in the Mobile Communications Department of *Institut Eurécom*, Sophia-Antipolis, France.

  - **Thesis title:** *Advanced signal processing algorithms for third generation wireless mobile systems.*

- **August 1998 - December 1998** Consulting in a collaboration between *Politecnico di Torino* and Omnitel for the UMTS physical layer standardization. (Physical layer and radio link simulation, link parameters optimization, power control for uplink and downlink radio channels)

- **July 1998** Laurea (M.Sc.) degree in Telecommunications engineering (with honors) from *Politecnico di Torino*, Torino, Italy.

  - **Thesis title** *Project of a reading meter system with code division multiple access techniques.*

Other experiences

- Taught undergraduate Lab sessions at Institut Eurécom for the courses of "Digital communication theory," "Introduction to communication Systems, "Wireless Communications," and "Radio transmission" given by Prof. Giuseppe Caire.

- Consulting in the development of undergraduate thesis.

- Seminar and conferences, on wireless systems.

- Attended a DSP training course at Texas Instruments, Paris, France.

Computers science skills

- **Programming Languages:** knowledge of C, C++, Pascal, Assembler for processors Intel 80x86 and Pentium III MMX, assembler for DSP TI-TMS320C6x, Matlab, Topsim, and Maple.

- **Operating Systems:** DOS, Windows, Linux and Unix.

- **Software:** Word, Excel, PowerPoint, LATEX, and HTML.

- **Communication protocols**: TCP/IP, Frame Relay, ATM.

Languages

- **Italian:** mother tongue

- **English:** fluent

- **French:** excellent